Physical volcanology of the Rooiberg Group near Loskop Dam, Mpumalanga, South Africa

By

SAMSON MOTLAGOMANG MASANGO

Submitted in partial fulfilment of the requirements for the degree

Masters of Science (MSc) Geology

In the Faculty of Natural and Agricultural Sciences

University of Pretoria,

Pretoria

4 December 2014

Physical volcanology, of the Rooiberg Group near Loskop Dam, Mpumalanga, South Africa

By Samson Motlagomang Masango

Supervisor: Dr. Nils Lenhardt

Department: Geology

University: University of Pretoria

Degree: Masters of Science (MSc) Geology

ABSTRACT

The 2.06 Ga Rooiberg Group of South Africa, related to the greater Bushveld Igneous Complex forming event, is one of the most unique silicic large igneous provinces (sLIPs) of the Precambrian rock record. Akin to the Gawler Range Volcanics (Australia), the Trans-Pecos volcanic field (USA), the Sierra Madre Occidental (Mexico), Whitsunday province (Australia) and other silicic dominated LIPs, the Rooiberg Group is subaerial, dominated by voluminous silicic lava flows and formed in an intracontinental setting. The original extent of the Rooiberg Group is thought to be as much as ~200,000 km^2, of which 50,000-67,000 km^2 are remaining after erosion. The inferred eruption volume is ~300 000 km^3. The Rooiberg Group, overlying the metasediments and metavolcanics of the Transvaal Supergroup on the Kaapvaal Craton, can be subdivided into four formations, which are in stratigraphical order: the Dullstroom, Damwal, Kwaggasnek and Schrikkloof Formation. The best outcrop conditions for the Rooiberg Group can be found in the Loskop Dam area in the Mpumalanga Province, ca. 120 km E of Pretoria and 52 km N of Middleburg, where three of the four formations can be encountered in the field. After extensive mapping in this area, a lithofacies analysis was initiated in order to provide for the first time a properly constrained and detailed set of the lithofacies types that can be encountered within the Rooiberg Group.

Within the scope of the study area (Loskop Dam), eight lithofacies types could be identified, ranging from coherent lava flows and massive tuffs to cross-bedded sandstones and conglomerates. The lithofacies types can be grouped into syn-, and inter-eruptive lithofacies associations, thus, illustrating changes in time and space, as shown by intercalated products

of effusive and explosive eruptions and clastic sediments characterising times of relative quiescence. The tectonic situation within the Kaapvaal Craton and the predominance of lava flows is seen as evidence for a majority of fissure eruptions in the Loskop Dam area. Thick pyroclastic units elsewhere within the extent of the Rooiberg Group, however, suggest the existence of larger volcanic features and related explosive eruptions, probably contemporaneous with the fissure eruptions.

The new information gained in the course of this study enables the reconstruction of the geodynamic setting in which the Rooiberg Group formed. The felsic (dacitic, rhyodacitic, and rhyolitic) Rooiberg Group has a geochemical character consistent with within – plate setting. The REE and trace elements suggest the magma with origin consistent with partial melting of the crust.

DECLARATIONS

I hereby declare that this thesis is my own unaided work except where referenced otherwise. It is being submitted for the degree Masters of Science (MSc) in Geology at the University of Pretoria, Pretoria. This thesis has not been submitted before for any degree or examination to any other University.

Date: _____

Signature of Author: _____

TABLE OF CONTENTS

UNIVERSITEIT VAN PRETORIA
UNIVERSITY OF PRETORIA
YUNIBESITHI YA PRETORIA
Faculty of Natural and Agricultural Sciences

LIST OF PUBLICATIONS AND CONFERENCES

PUBLICATIONS

1) Lenhardt, N., **Masango, S.M.,** Jolayemi, O.O., Lenhardt, S.Z. & Eriksson, P.G. (in review) First facies analysis of a Palaeoproterozoic (2.06 Ga) intracratonic, silicic Large Igneous Province – the Rooiberg Group, Kaapvaal Craton, South Africa. Bulletin of Volcanology.

2) Jolayemi, O.O., Lenhardt, N., Roberts, J., **Masango, S.M.** (in review). Chemical evolution of the Palaeoproterozoic Rooiberg Group, Kaapvaal Craton, South Africa: new insights into the formation of silicic large igneous provinces (SLIPs). Bulletin of Volcanology and Geothermal Research.

CONFERENCES

1) **Masango, S.M.,** Lenhardt, N., Jolayemi, O.O. (2013). First facies analysis on and the geodynamic setting of a Palaeoproterozoic silicic large igneous province: the Rooiberg Group, Kaapvaal Craton, South Africa. 24th Colloquium of African Geology. Addis Ababa, Ethiopia. 09-13.01.2013.

2) Jolayemi, O.O., Lenhardt, N., Roberts, J., **Masango, S.M.** (2013). Chemical evolution of the Paleoproterozoic Rooiberg Group, Kaapvaal Craton, South Africa: new insights into the formation of silicic large igneous provinces (SLIPs). 24th Colloquium of African Geology, Addis Ababa, Ethiopia. 09-13.01.2013.

ACKNOWLEDGEMENTS

I like to dedicate this work to (*Ntate*) Professor Pat Eriksson for his unconditional support during all the stages of my development in the field of Geology. Furthermore, I like to thank Mrs. Melinda de Swart and Mrs. Wiebke Grote for their support and motivation. Mrs. Sukanya Lenhardt is thanked for drafting some figures, GIS assistance and moral support during the field work and course of this study. My colleague Mr. Olutola Jolayemi who has been there from the first to the last step of this MSc study is also thanked. I also thank Kamal Mistry, Asivhothe Madzivhandila, Susan Serfontein, Walter Lukhele and Archibald Moses (Mokete) for their assistance during field work. I also like to thank the farm owners around the Loskop Dam for their special permission to map their private properties.

Many people were involved in this project, thus I really appreciate their contribution and support throughout the ups and downs of this project. Special acknowledgements to my family: Bokang, Lesedi, Boitshepo *le* Junior '*ke le rata nou'*.

Ke leboga Doreen Masemola le Mothushi Phahlamohlaka.

Ke leboga ntate Dikgang le mme Dodo Moshwela, Aubuti Monageng, Sunyboy, Mpho, Marriel le Mariam, Thabo le Thabang, Orapeleng, Malerato, Thabang Debozza, Nthabiseng le Mathome Komane ka thekgo le thotoetso.

Go Modimo o matlaotlhe, ke a leboga.

LIST OF FIGURES

LIST OF TABLES

1. Introduction

The ca. 2060 ± 2 Ma (Walraven, 1997), Rooiberg Group of the Bushveld Magmatic Province (BMP), South Africa, is one of the unique silicic large igneous provinces (sLIPs) of the Precambrian rock record. It is one of the few Proterozoic sLIPs [e.g. the ~2450 Woongarra Province rhyolites, North West Australia (Trendall 1995; Barley et al., 1997), the ~1592 Ma Gawler Range Volcanics of South Australia, (Creaser and White, 1991; Creaser, 1995; Allen and McPhie, 2002; Allen et al., 2008) and the ~1100 Ma Rhyolites of the North Shore Volcanic Group in Minnesota, (Green and Fitz, 1997)] which formed during supercontinent amalgamation (Allen et al., 2008; Allen and McPhie, 2002). Only few of these unique sLIPs are documented world-wide (Allen et al., 2008). The Rooiberg Group was formed during the time of amalgamation of the Eburnean Supercontinent (ca. 2.15-1.8 Ga; Eriksson et al., 1999), which included the Kaapvaal and Zimbabwe Cratons along the Limpopo Mobile Belt (Kamber et al., 1995).

Recently, the term Bushveld LIP is used to describe the BMP (c.f., Ernst and Bell, 2010; Kinnaird, 2005; Bryan and Ernst, 2007; Lenhardt and Eriksson, 2012). The Bushveld LIP comprises the silicic volcanic rocks of the Rooiberg Group and the three suites, namely: the layered mafic-ultramafic rocks of the Rustenburg Layered Suite (RLS) (2058.9 ± 0.8 Ma; Buick et al., 2001), the S1- or A-type granites of the Lebowa Granite Suite (LBS) (2054 ± 2 Ma; Walraven and Hattingh, 1993; Buchanan, 2004), and the Rashoop Granophyre Suite (RGS) (2053 ± 12; Coertze et al., 1978). These three suites have been coined Bushveld Complex *per se* (SACS, 1980). Nevertheless, the Rustenburg Layered Suite intrusion thermally metamorphosed and possibly remelted parts of the lower two formations (Dullstroom and Damwal) that are now recrystallized hornfelses, granophyres and microgranites as described by Wager and Brown (1968) and von Gruenewaldt (1972), and that now form part of the Rashoop Granophyre Suite (Walraven, 1985; Cawthorn, 2013). The Lebowa Granite Suite metasomatically altered later on (deposition of secondary cassiterite, tourmaline and carbonate) the entire Group, particularly in its northwestern part (Buchanan, 2006). Akin to the Gawler Range Volcanics of Australia (McPhie et al., 2008), the Trans-Pecos volcanic field of USA (Parker and White, 2008), the Whitsunday Volcanic Province of Australia (Bryan et al., 2000) and other silicic dominated LIPs, the Rooiberg Group is subaerial, dominated by voluminous silicic lava flows and formed in an intracontinental setting. The presumed volume of magma produced by the Bushveld LIP is between 0.7 x 10^6 km^3 and 1 x 10^6 km^3 with individual igneous pulses occurring at periods of 1-3 Ma (Harmer

17

and Armstrong, 2000), which according to Bryan and Ernst's (2007) redefined definition of LIPs, qualifies the Rooiberg Group to be one of the largest and oldest silicic LIP known.

The 'mysterious' Rooiberg Group and Bushveld Complex poses challenging questions in terms of its petrogenesis. Some of the questions include the following: What is the source and nature of volcanism of the Rooiberg Group? Is the Rustenburg Layered Suite older than the upper three formations of the Rooiberg Group? How many igneous pulses occurred during the life span of the Bushveld magmatic event?
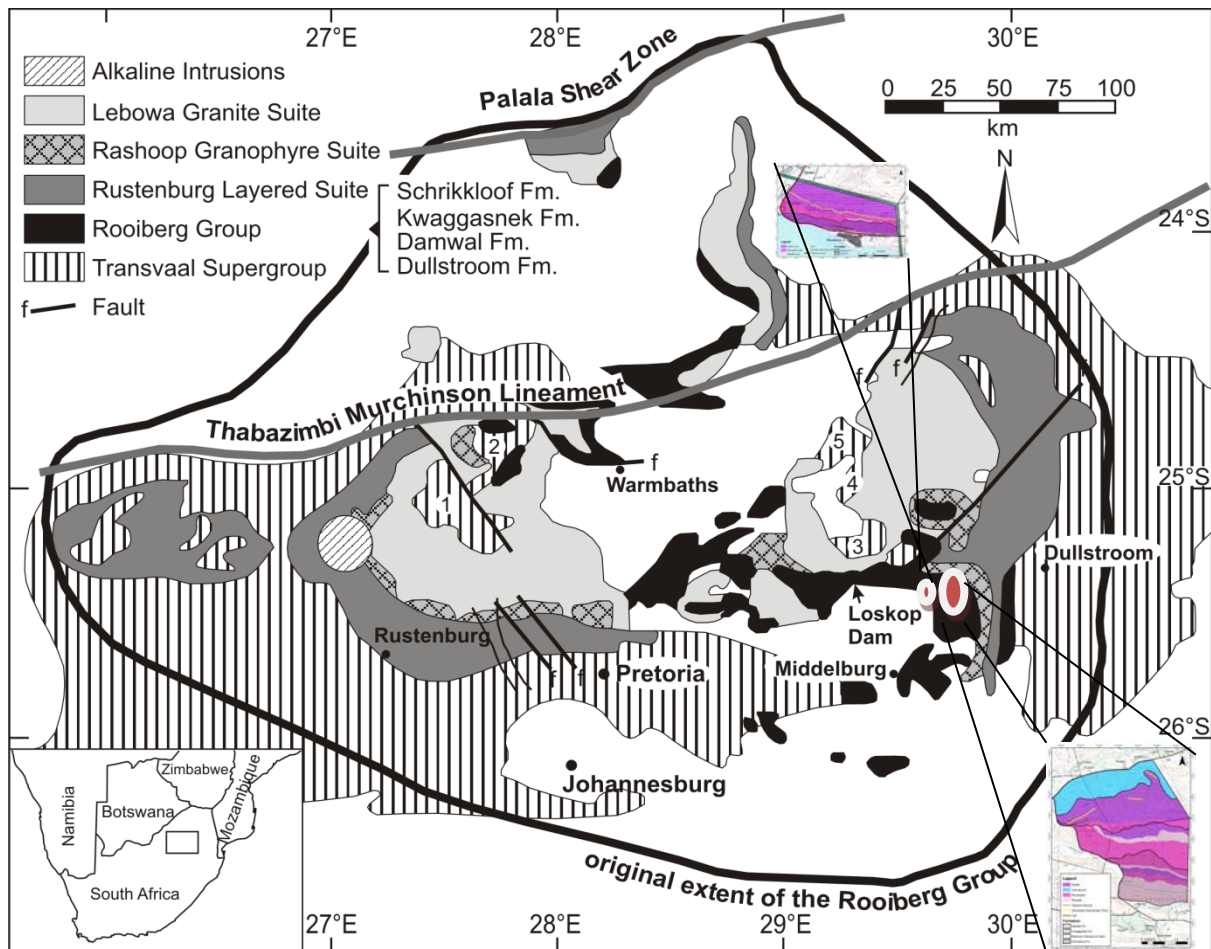
Figure 1. Simplified geological map showing the distribution and the relationship between the rocks of Transvaal Supergroup and the Bushveld Large Igneous Province. The Rooiberg Group, the Rustenburg Layered Suite, the Lebowa Granite and the Rashoop Granophyre suites are almost entirely bound by the basement rocks of the Transvaal Supergroup. The thick black line shows the original extent of the Rooiberg Group. Numbers 1-5 refer to Rooiberg fragments respectively: Rooiberg, Dennilton, Marble Hall, Stavoren/Mekeckaan Fragments. Bottom left inset shows the position of the BMP in South Africa and the study area is inserted on the bottom right the white and red circles (Modified from Lenhardt and Eriksson, 2012).

These questions are still hanging in thin air. However, previous age determinations implied that the complex evolved over a period in excess of 100 million years (Burger and Coertze, 1975), influencing the debate on the petrogenetic relationship of the various components of the BIC. More recently, Letts et al. (2009), suggested a minimum emplacement time of 1.4 Myr, determined by means of seven magnetic reversals found in the Bushveld Complex.

So far, three theories have been postulated in an attempt to resolve the former petrogenetic mystery. Early research (e.g. Elston, 1992), ascribed the formation of Rooiberg Group and the larger Bushveld Magmatic Province to the simultaneous impact of several comets or asteroids. The interpretation is partly based on the observed shape of the complex and partly on petrographic evidence. Akin to the lower Onaping Formation of the Sudbury Complex, Canada, interpreted to have formed due to the former impact theory (Grieve et al., 2008), the lower Rooiberg Group's shape resembles several closely spaced ring features. In the Rooiberg, the ring structures are partially covered by the younger Loskop Formation and the Waterberg Group (2.0-1.7 Ga; Martini, 1998). Elston (1992), interpreted the former ring structures and further, using petrographical studies to suggest that some of the Rooiberg Group melts were superheated and thus could represent impact melts. Among the evidence presented by Elston (1992), was the presence of paramorphs after tridymite in the Rooiberg lava. Buchanan and Reimold (1998), later opposed this hypothesis with strong counter impact evidence, reasoning that the paramorphs after tridymite have been recognised in other terrestrial volcanic provinces such as the North Shore Volcanic Group of north-eastern Minnesota. Further, the micro-deformation structures of quartz do not support the shock metamorphic planar deformation features. The latter authors concluded based on the structural data, including the dips of the Rooiberg Group strata that the lobate shape of the Bushveld Complex and the Rooiberg Group are the result of post-Bushveld deformation. Further on, the second hypothesis, Hatton (1988), proposed a theory using geochemistry, to suggest that the rocks of the Rooiberg Group formed by melting of detrital material subducted under southern Africa at a nearby plate margin along the northern Kaapvaal edge. However, such geochemical evidence with subduction features is contradicted by the lack of geological evidence. Cornell et al. (1996), and Jolayemi et al. (in prep.) point out that this geochemical subduction feature, lacking geological confirmation of subduction, is archetypal of most Archaean and Proterozoic volcanic rocks of the Kaapvaal Craton. Finally, the third theory, which the majority of the scientific community agrees on, suggests that both, the Rooiberg Group and the Bushveld Complex, are formed due to partial melting of subcontinental lithosphere and lower crust by a mantle plume (Harmer and von Gruenewaldt,

1991; Hatton, 1995; Hatton and Schweitzer, 1995). Although the mantle plume model/theory remains contentious, it is highly favoured by the majority of the scientific community, probably due to its ability to explain the enormous volume of magma produced (Kinnard, 1995). Regardless of its significance with regard to the formation of Rustenburg Layered Suite, the world's largest deposit of platinum group elements, chrome and vanadium, and also considering that the Rooiberg Group is one of the oldest and the largest known sLIPs it has not being studied in details.

Recently, more studies were focused on resolving the petrological aspects of the Rooiberg Group and the Bushveld Igneous Complex (i.e. Rustenburg layered suite). In an attempt to unravel the latter aspect, Van Tongeren et al. (2010), proposed that the Rooiberg Group resulted from differentiation of a shallow large body of mafic magma (Rustenburg Layered Suite?). The former hypothesis further explains that the Damwal, Kwaggasnek and Schrikloof Formations are the felsic end product to Bushveld differentiation. Using major and trace elements, Mathez et al. (2013), concluded in support of VanTongeren et al. (2010) that the Rooiberg and the Rashoop ferroan rocks formed due to fractional crystallisation of the Bushveld mafic liquids (Rustenburg Layered Suite liquids?) and that there is no way that the high magnesian liquids of the Dullstroom Formation and the ferroan lavas of the upper Rooiberg Group could co-exist. Jolayemi et al. (in prep.), suggest the Rooiberg Group to have occurred as a result of partial melting of the upper crust with evidence of low degree fractional crystallisation. The main contradicting points of Van Tongeren et al. (2010) and Jolayemi et al. (in prep.), is that the former author suggest that the Damwal, Kwaggasnek, and Schrikloof liquids are the product of differentiation of mafic Bushveld liquids, thus being younger than the Rustenburg layered suite, while the manuscript by Jolayemi et al. (in prep), using major, trace and isotopic data, shows strong crustal origin of the Rooiberg Group. The findings in the manuscript by Jolayemi et al. (in preparation), are thus in support of Rooiberg Group being the first magmatic phase of the Bushveld large igneous province as it was initially proposed.

Németh and Martin (2007), point out that recognizable facies diversity provides an important, useful role in reconstructing both the volcanic processes and the eruptive environment at the area of volcanism. The above idea has and is still used on large igneous provinces and had showed to be an essential measure in understanding the geodynamic settings, nature and the eruptive processes that lead to the emplacement of these unique igneous rocks (e.g. Whitsunday Volcanic Province, Bryan et al., 2000; Gawler Range Volcanics, Roache et al., 2000).

A significant part of facies analysis is the identification and interpretation of primary textures formed during eruption and emplacement of volcanic rocks and, or transportation and deposition of sediments. However, the former maybe practically difficult in ancient terrains, since both the volcanic successions and the intercalating sedimentary beds often constitute modified textures due to diagenesis, hydrothermal activity and metamorphism (Cas and Wright, 1987; McPhie et al., 1993). Further, it is very rare to find facies in volcanic terrains that correspond explicitly to a particular environment or setting, thus facies interpretations have to be based on association of facies rather than on single facies (McPhie et al.,1993; Németh and Martin, 2007). The main aims of this study include:

- the production of a detailed geological map and the stratigraphical section of the study area.
- to provide the properly constrained lithofacies interpretations of the Rooiberg Group of the Bushveld large igneous province near the Loskop Dam (Mpumalanga Province)
- and therefore enabling the construction of a geodynamic model of the Rooiberg Group in the area.

"Lithofacies" refers to a rock body or interval of rock having unique definable character, which may be compositional, textural or structural, that has genetic significance such as the conditions of eruption or deposition that distinguishes it from other facies or intervals of rock or sediment (Cas and Wright, 1987; Song and Lo, 2002).

2. Large Igneous Provinces (LIPs)

Bryan (2007) points out that <u>LIPs</u> are the end product of huge additions of magma to the continental crust, both at the surface and at depth. Nevertheless, for any crustal emplacement to be regarded as a large igneous province (LIP) it must gratify one of the following: The deposits must be massive, constitute principally plutonic and volcanic mafic and/or felsic magma that patents as oceanic plateaux, continental and ocean basin flood, volcanic passive margins, submarine ridges, and seamont groups; a definition originally coined by Coffin and Eldholm, (1994). Recently, Bryan and Ernst (2007), redefined LIPs to be "mainly mafic magmatic provinces (having generally subordinate silicic and ultramafic components, whereas some dominantly silicic) with areal extents $>0.1Mkm^2$, igneous volume >0.1 Mk^3 and maximum lifespan of ~50 Myrs that are emplaced in an intraplate setting and characterised by igneous pulse(s) of short duration (~1-5 Myrs), during which a large proportion (>75%) of the total igneous volume has been emplaced". LIPs are generally sub-divided into two groups (mafic and felsic) depending on the dominant rock (Shellnutt et al., 2012). Mafic LIPs are more common and considerably better studied. Flood basalt provinces are normally characterised by high magma emplacement rates (Storey et al., 2007) occurring at a short duration of ca. 10 Myr (Sheth, 2007; Bryan and Ernst, 2008). On the other hand, the felsic or silicic LIPs experienced less attention and hence little is known about them. Silicic LIPs, as compared to the mafic LIPs are characterised by magma emplacement over ca. 40 Myr (Ernst et al., 2005; Sheth, 2007; Bryan and Ernst, 2008). Chemical characteristics and groupings mostly define LIP magmas. Bryan and Ernst (2008), described the distinct silica gap of LIPs that can be chemically grouped at around 45 – 56 and 65 – 75 wt.%. LIPs with such silica gab are referred to as 'Bimodal' (Pankhurst et al., 2011).

Archetypal to Bryan and Ernst's (2007) LIP examples, is the Bushveld Magmatic Province denoted herein as the Bushveld LIP (i.e. Bryan and Ernst, 2007, Lenhardt and Eriksson, 2012), the Sierra Madre Occidental (e.g. Mcdowell and Keizer, 1977), the Parana-Etendeka Province (e.g. Milner et al. 1992), the Whitsunday Volcanic Province (Bryan et al., 2000) and other LIPs elsewhere. One of the largest silicic large igneous provinces in North America, the Sierra Madre Occidental, is characterised by two main igneous pulses at ca. 34-28 Ma and ca. 24-18 Ma, producing a minimum volume of 400,000 km^3 (Bryan and Ferrari, 2013, and references therein). The Bushveld LIP produced 0.7 $x10^6$ - 1 x 10^6 km^3 of magma within 1-3 Ma, suggesting magma generation rates between 1 x 10^6 km^3 and 0.3 x 10^6 km^3 per Ma (Harmer and Armstrong, 2000). Further, the produced magma of the Bushveld LIP is a

product of three main pulses. The igneous pulses of the Bushveld LIP are described by Rajesh et al. (2013) and are summarised in the chapter 3 (Regional geological setting)

3. Geological setting

3.1. Regional setting

The Kaapvaal Craton of South Africa is one of the best preserved Archaean cratons known. The predominantly granite-greenstone basement of the Kaapvaal Craton host a number of volcano-sedimentary, intracratonic basins of Archaean-Palaeoproterozoic age. Among these basins, the three large and most preserved include the ca. 3.1 - 2.8 Ga Pongola-Witwatersrand Supergroup, the ca. 2714 - 2709 Ma Ventersdorp Supergroup and the ca. 2.66 - 2.05 Ga Transvaal Supergroup (Eriksson and Reczko, 1995; Catuneanu and Biddulph, 2001; Eriksson et al., 2005; Altermann and Lenhardt, 2012; Lenhardt and Eriksson, 2012). By 3.1 Ga the nucleus of the Kaapvaal Craton had formed within intra-oceanic and arc setting through thin-skinned thrusting (De Wit et al. 1992). The Transvaal Supergroup developed subsequently to cratonisation while the former basin-fills were formed during late cratonisation of the Kaapvaal Craton (Eriksson et al., 2005), which served as a stable foundation during the development of the former basins (Lenhardt and Eriksson, 2012).

3.1.1. The Pongola-Witwatersrand Supergroup

The Pongola-Witwatersrand Supergroup is underlain by the ca. 3.1 Ga Dominion Group (Armstrong et al., 1991) and conformably overlain by the Ventersdorp Supergroup (SACS, 1980). Catuneanu (2001), interpreted the Witwatersrand Basin to be the proximal flexural fore-deep and its possible age overlapping Pongola basin represent the distal back-bulge part of the retroact foreland system. The two foreland sub-basins represented by Witwatersrand and Pongola Supergroups are separated by flexural forebulge. Pongola Supergroup hosts the equivalent deposits of the Central Rand Group. The world largest gold-bearing, Witwatersrand Basin, comprises the lower West Rand Group and the economic upper Central Rand Group. The Central Rand Group is dominated by fluvial-deltaic sedimentation processes such as sandy and conglomeritic braidplain deposits while the West Rand Group is dominated by shallow marine systems with miner fluvial and alluvial sedimentation processes (Bumby et al., 2012; Els, 1998).

3.1.2. The Ventersdorp Supergroup

The Kaapvaal Craton experienced a 2.7 Ga global superplume event, which resulted in the formation of the Ventersdorp Supergroup (Armstrong et al., 1991). The volcanic and sedimentary rocks of the Ventersdorp Supergroup rest conformably on the Witwatersrand

strata and are overlain by the Transvaal Supergroup. The Ventersdorp Supergroup forms one of the largest large igneous provinces on Kaapvaal Craton, with aerial extend of ca. 300 000 km^2 from southern Botswana to central South Africa and comprise the stratigraphic thickness of up to ca. 4 - 8 km (Altermann and Lenhardt, 2012 and the references therein). Stratigraphic thickness of ca. 5 km is occupied by sub-aerial lavas and pyroclastic rocks while the ca. 3 km is mostly occupied by lacustrine siliciclastic and carbonate sedimentary rocks (Van der Westhuizen et al., 2006). Based on lithological types and characteristics, the Ventersdorp Supergroup is stratigraphically sub-divided into the flood basalt dominated Klipriviersberg Group, Platberg Group and the siliciclastic and flood basalt dominated the Pniel Sequence/Group (SACS, 1980). The Platberg Group comprises variable sedimentary rocks, such as basal diamictites, wackes, conglomerates, ash and carbonate-rich shales (SACS, 1980).

3.1.3. The Transvaal Supergroup

The up to c. 15 km thick (Button, 1986) basin fill sequences of the Transvaal Supergroup, predominantly comprising of quartz arenites, dolomites, shales and minor volcanic rocks, are preserved in several structural basins, i.e. the Transvaal, Griqualand West (both are found in South Africa) and Kanye (found in Botswana) basins (Eriksson et al. 1996). The Transvaal Supergroup developed subsequently to cratonisation while the former (Witwatersrand Supergroup and Ventersdorp Supergroup) basin-fills were formed during late cratonisation of the Kaapvaal Craton (Eriksson et al., 2005), which served as a stable foundation during the development of the former basin (Lenhardt and Eriksson, 2012). The basin-fills of the Transvaal Supergroup have possibly formed as a response to intercratonic rifting (Eriksson et al. 1991). Prior to the Rooiberg Group volcanic extrusion, the general tectonics of the Kaapvaal Craton were unstable due to the effect of the Eburnean Supercontinent assembly, which possibly resulted in a relative gentle regional shortening and folding of the Transvaal strata (Eriksson et al., 1998). The Pretoria Group, which forms the youngest metasediments and metavolcanics sequence of the Transvaal Supergroup can be stratigraphically divided into: "pre-Magaliesberg Formations" (i.e. Rooihoogte, Timeball, Boshoek, Hekpoort, Dwaalheuwel, Strubenkop, Daspoort and Silverton), the Magaliesberg Formation (predominantly quartzites), and "post-Magaliesberg Formations" (i.e. Vermont, Lakenvalei, Nederhorst, Steenkampsberg, and Houtenbek Formations). The latter mentioned post-Magaliesberg Formations are composed of fluvial and relatively immature, shallow marine

deposits, which were deposited in a set of shrinking basins (Lenhardt and Eriksson, 2012). The former basin-fills are interpreted to form a platform for tectonic instability as a result of shrinking (Schreiber and Eriksson, 1992). The probable, initial factor leading to the instability of post-Magaliesburg basins is the rise of the Rooiberg magma which resulted in rapid uplift and major thermal doming (Eriksson et al., 1993, 1995; Catuneanu and Eriksson, 1999).

The Transvaal Supergroup almost completely bound and forms the floor rocks of the entire Bushveld Magmatic Province (Eriksson et al., 1991). The extrusion of the older part of BMP, i.e. the Rooiberg lavas, terminated the deposition of the clastic Transvaal sediments within the basin. SACS (1980), defined and described the Bushveld Complex as comprising only of the Rustenburg Layered Suite, Lebowa Granites Suite and Rashoop Granophyres Suite, and the Rooiberg Group belonging to the upper Transvaal rocks despite the strong petrogenetic evidence presented by R.A. Daly (1922), (c.f., Elston, 2012) that relates the Bushveld Complex and the Rooiberg Group. Later, Hatton and Schweitzer (1995) and Schweitzer et al. (1995), presented clear petrological evidence that links the Bushveld Complex and the Rooiberg Group. Cheney and Twist (1991), described an unconformity beneath the Transvaal Supergroup and the Rooiberg Group. Lithological contact between Transvaal and Rooiberg is rare and restricted to the eastern outcrop of the lower Dullstroom Formation and the Makeckaan Fragment, which is one of the five fragments (namely: Rooiberg, Crocodile, Dennilton, Makeckaan/Stavoren and Marble Hall) of the Transvaal-Rooiberg lithologies (Eriksson et al.1995). The latter mentioned fragments are sparsely engulfed by the wider Bushveld intrusives. The large roof pendants found in the west of Bushveld LIP include the Rooiberg and Crocodile Fragments (Lenhardt and Eriksson, 2012; Hartzer, 1995). The highly deformed Dennilton, Makeckaan/Stavoren and Marble Hall fragments lie in the east and are characterised by low-medium grade metamorphism (Hartzer, 1995). Hartzer (1995), interpreted them as floor-attached domes since they have dome structure and are in contact with floor of the Transvaal basin.
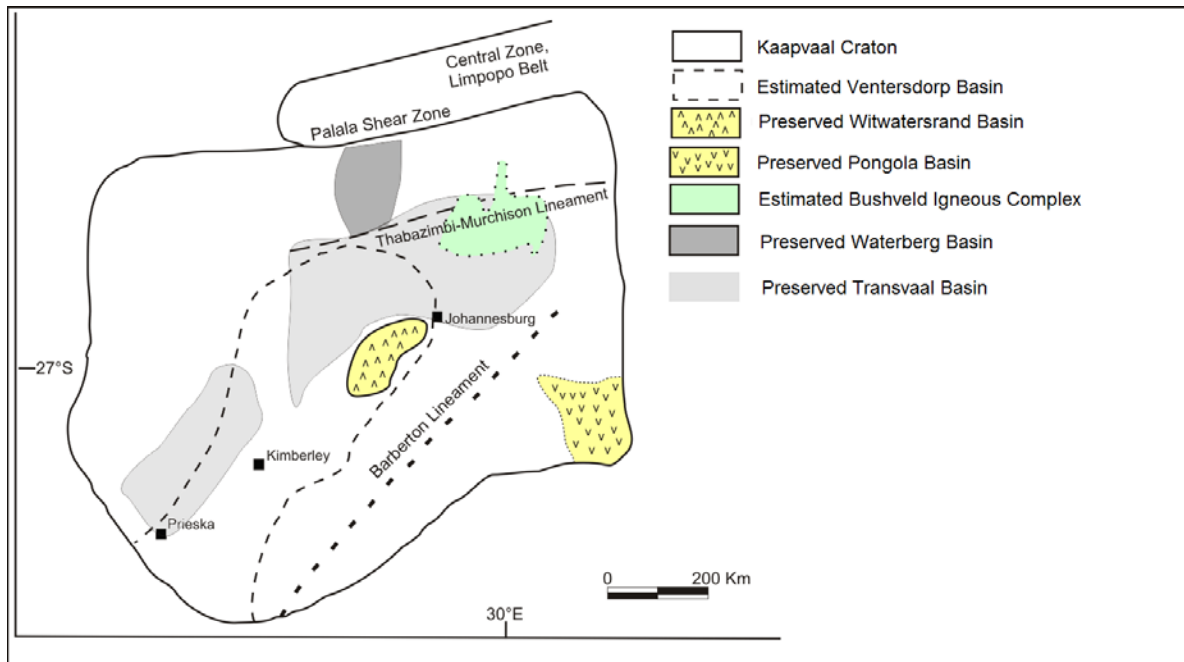
Figure 2. Schematic geological map of the discussed volcano-sedimentary, intracratonic basins of Archaean-Palaeoproterozoic age within the Kaapvaal Craton (after Eriksson et al., 2005; Bumby et al., 2012).

3.1.4. The Rooiberg Group

The up to 6 km thick volcanic sequence of the Rooiberg Group overlying the ca. 2.32 - 2.06 Pretoria Group, has been interpreted as the product of fissure volcanic eruption with minor units of shale and greywacke (Twist and French, 1983; Twist, 1985; Hatton and Schweitzer, 1995; Schweitzer et al. 1995). The Rooiberg Group volcanics are mainly formed of basaltic - andesitic lavas in the lower Dullstroom to dacitic-rhyolitic in the upper Damwal, Kwaggasnek and Schrikkloof Formations with minor intercalated pyroclastic and siliciclastic sedimentary rocks. The erupted volume is estimated at more than 300,000 km^3 (Twist and French, 1983). Its original extend is probably greater than 200,000 km^2 (see figure 1.) (Cawthorn and Walraven, 1997), covering a significant part of the northeast of the Kaapvaal Craton in South Africa and essentially extending towards Botswana, as suggested by the similar age, high silica lavas found in the west of Molopo area (Rajesh et al., 2013). The post erosional outcrop area in South Africa is estimated at 50,000 km^2 to 67,000 km^2 (Twist and French, 1983; Hutton and Schweitzer, 1995; Buchanan and Reimold, 1998).

In most contacts between the Rooiberg Group and the BIC, the Rooiberg Group forms the roof of the BIC, with the exception in the south eastern Bushveld, where parts of the Dullstroom Formation (Hatton and Schweitzer, 1995) and possibly small fragments near Pretoria and south of Middelburg basin form the floor rocks of the BIC (Mathez et al., 2013

27

and references therein). The latter is due to the intrusion of the BIC suites, causing the stratigraphical disruption of the Rooiberg Group (Lenhardt and Eriksson, 2012). The Rustenburg Layered Suite detached or separated the lower Dullstroom Formation from the upper Dullstroom, Damwal, Kwaggasnek, and Schrikloof Formations, consequently forming the roof of the Bushveld Complex (Hatton and Schweitzer, 1995; Schweitzer et al., 1995). The stratigraphical units of the Rooiberg Group comprise several thousand meters of a sequence of predominantly volcanic rocks, representing the initial phase of the Bushveld LIP. In addition to lava flow units, pyroclastic rocks pyroclastic fall, volcanic breccia, frequently occur (Twist, 1983; 1985). Sedimentary inter-beds such as sandstones, pebbly sandstones and conglomerates, showing upward fining, are also present (Twist, 1985). Lenhardt and Eriksson (2012) point out that, in spite of the Rooiberg Group's Palaeoproterozoic age, it is neither deformed nor greatly metamorphosed although contact metamorphism exist. Occasionally, the Rooiberg lavas are metamorphosed and to some extent partial melting (anatexis) occurred (Twist and French, 1983). Twist (1985) distinguished nine units of lava flows within the sequence, based on physical characteristics, such as colour, texture, phenocryst content, internal structure and relationship to the intercalated sedimentary units. Chemical investigation of Rooiberg Group lavas by Schweitzer et al. (1995) led to the description of six compositionally different lava types, and further, of the four Formations the Dullstroom Formation comprises all six different lava types while Damwal constitute two. The overlying Kwaggasnek and Schrikloof Formations each comprise a single similar lava type (Hatton and Schweitzer, 1995; Schweitzer et al., 1995). The lava types described by Twist (1985) in ascending stratigraphical order include the low-Ti basaltic andesite, a basal rhyolite, high-Ti basalt, high-Mg felsites, high Fe-Ti-P andesite and low-Mg felsites are all present in Dullstroom Formation. All the remaining three formations of the Rooiberg Group are mainly composed of low-Mg felsites. In addition to the low-Mg felsites, the lower Damwal Formation also has high Fe-Ti-P which gradually grades into the upper Dullstroom Formation.

Single grain zircon Pb evaporation dating on samples from Rooiberg Group and Rustenburg Layered Suite revealed the age of Rooiberg Group and Rustenburg layered suite to range from 2061 ± 2 to 2052 ± 48 Ma (Walraven, 1997; Buick et al., 2001). Rajesh et al. (2013) recently revealed that the entire Bushveld LIP might have formed between ~2.06 - 2.04, and is related to three major igneous pulses (~2.061 - 2.060 Ga, ~2.059 - 2.054 Ga, and ~2.046 - 2.042 Ga). Minor pulses might stretch up to 2.03 Ga (Rajesh et al., 2013). Dating of the four

Formations of the Rooiberg Group is not yet complete. The Kwaggasnek and the Schrikkloof Formations (formally known as lower and upper Selons River Formations, and Doornkloof and Lilpnek Formations, respectively; SACS, 1980; Twist, 1985; Schwertzer et al., 1995) have not been dated. The Dullstroom and Damwal Formations are the only formations, which have been dated. The Rb-Sr statistical data of the latter Formations yielded a combine age of ca. 2071 +94/-65 Ma (Buchanan et al., 2004). Up to now, the Schrikkloof Formation has not yet been dated, while Harmer and Armstrong (2000) provided an unexplained estimation of the age of the Kwaggasnek Formation to be at 2057.3 ± 3.8 Ma. This Kwaggasnek age estimate was based on all available geochronological data from the Bushveld LIP.

3.1.5. The study area (north east of Loskop Dam)

The study area comprises an area of ca. 50 km^2 and is located ca. 120 km E of Pretoria and ~52 km N of Middleburg in the Mpumalanga Province, where three of the four Formations can be encountered in the field (figure 2). The ca. 50 km^2 area located in the north east of the Loskop Dam is subdivided into two small areas namely the major (42 km^2) and minor outcrop (8 km^2), due to accessibility restrictions. The major outcrop is defined by four corners at 25°23'0"S, 29°29'45"E (top left); 25°23'0"S, 29°33'30"E (top right); 25°26'0"S,29°29'45"E (bottom left) and 25°26'0"S, 29°33'30"E (bottom right), clearly observed in figure 6. Similarly the minor outcrop is also defined by four corners at 25°24'30"S, 29°22'0"E (top left); 25°24'52.5"S, 29°23'54"E (top right); 25°25'07.5"S, 29°21'37.5"E (bottom left); and 25°25'25.5"S, 29°24'0"E (bottom right) (figure 5.). Comparatively to this study, early studies of the Rooiberg Group were located in the west and north of Loskop Dam i.e. by French and Twist (1985), and Twist (1985), respectively. However, their research mostly focused on the area within the Loskop Nature Reserve, located at the north and northwest of Loskop Dam (see figure 1.).

3.1.6. Physiography of the study area

The morphology of the Rooiberg Group in the study area attains elevations greater than ±1600 m above mean sea level (a.m.s.l), with plateaus in higher areas. Most interesting about the landforms of this region is the variety of slope types and deep valleys, which are characterised by flat valley floors.

The study area is covered by dense vegetation and this may limit the outcrop conditions, contributing to ambiguous mapping yet if done gradually and meticulously, a scientific mapping can be achieved as this study demonstrates. The dense vegetation prevails

throughout the seasons, as seen from figure 5. Mucina and Rutherford (2006), described the vegetation of the Loskop Dam Nature Reserve and the surrounding area and concluded that it belongs to the Loskop Mountain Bushveld Vegetation and the Loskop Thornveld Vegetation unit. According to Mucina and Rutherford (2006), the Loskop Mountain Bushveld mainly consist of open, broad leaved woodland while the Loskop Thornveld has deciduous, open woodland.

The Loskop dam is situated in an area of summer rainfall with moderate to mostly very hot summers and mild to cold winters. Frost occurs on the mountain tops and in the low-lying valley bottoms (Theron, 1973; Barett, 2010). The rainfall is associated with strong, south westerly winds and it is in the emergence path of short-lived and high intensity thunderstorms (Barett, 2010). The study of Low and Rebelo (1998), recorded temperature ranges between -7 and 41°C throughout the seasons.
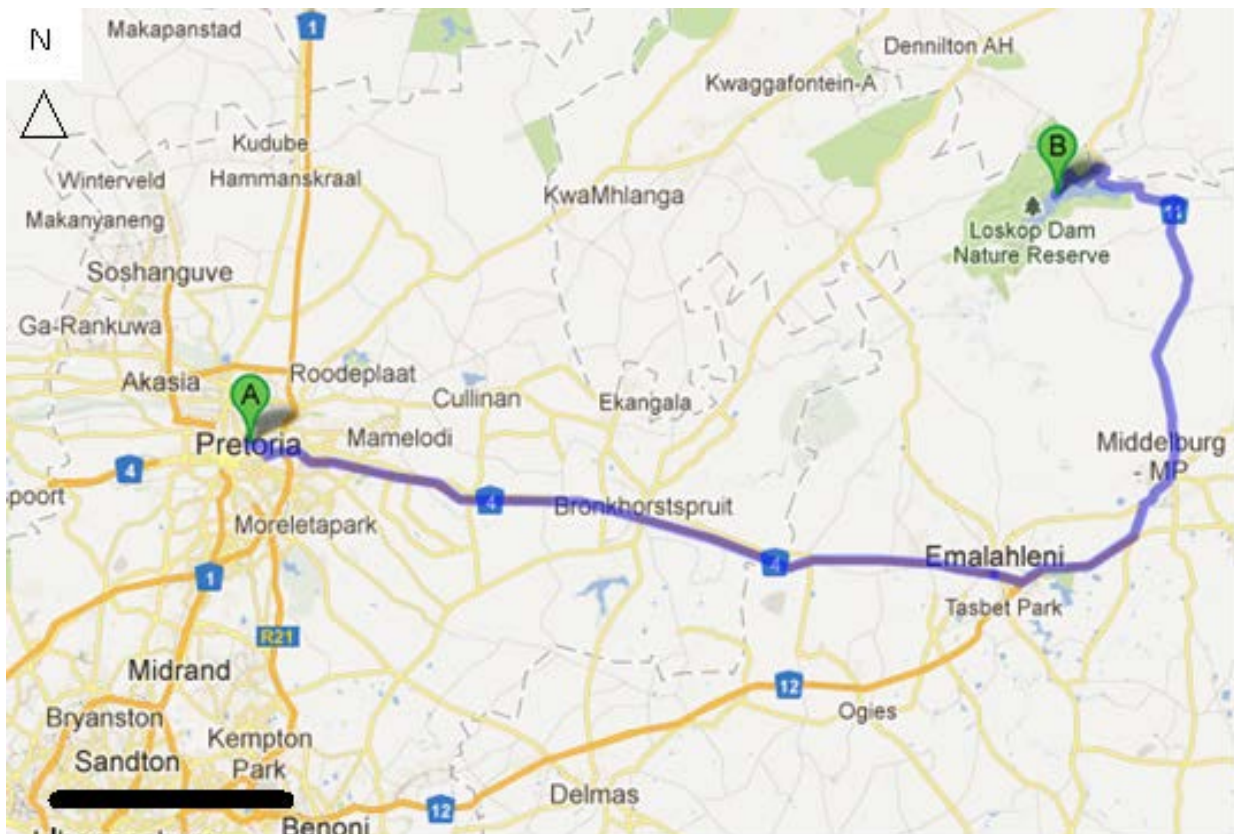
Figure 3. Google road map showing the geographical location of the study area from Pretoria (A) to Loskop dam (B). The study area is 52 km from Middleburg, Mpumalanga. The black thick line (bottom left) represent the scale of 20 km.
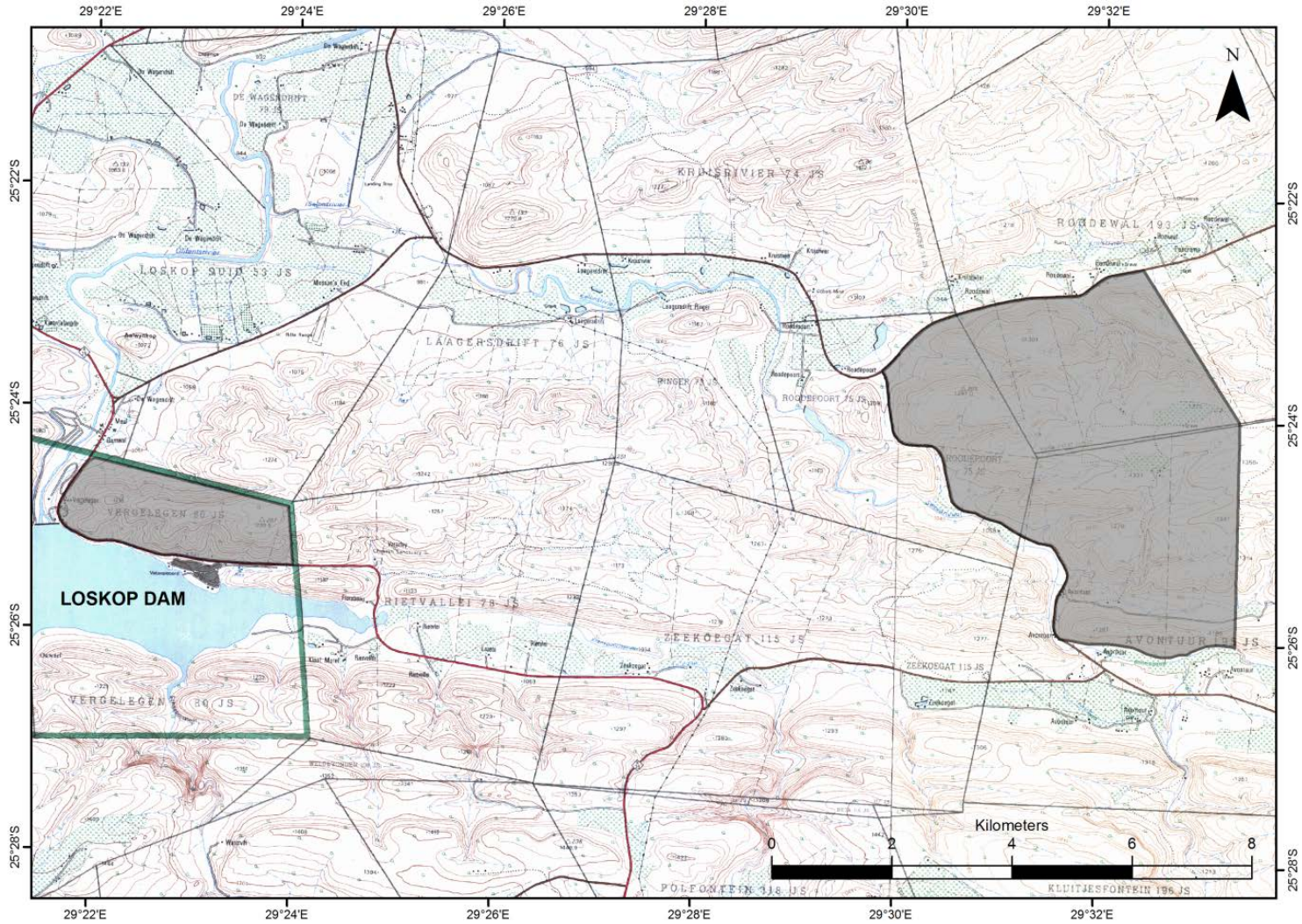
Figure 4. Topographical map showing the location of the two study areas (grey 'blocks'). The areas are ~10 km apart
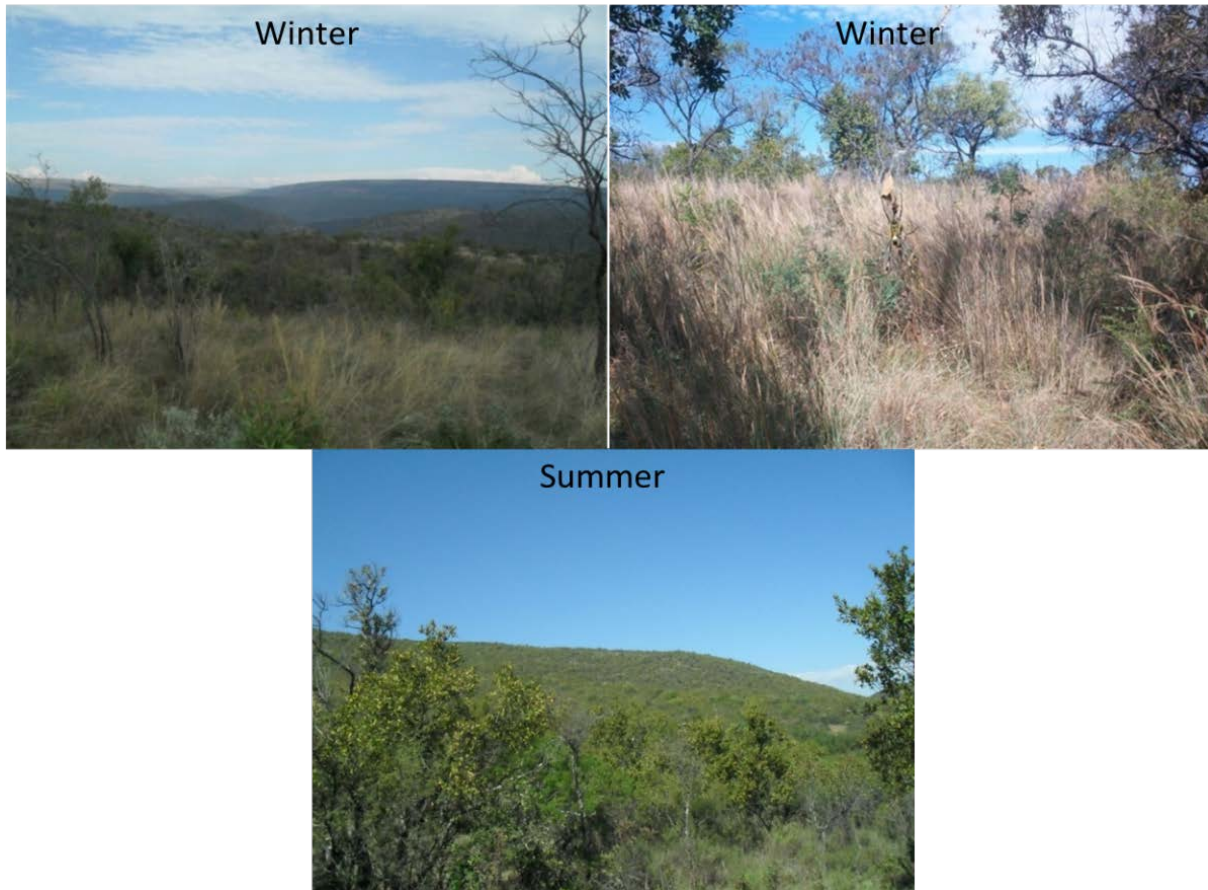
Figure 5. Pictures of the study area depicting dense vegetation as observed throughout the seasons, especially in summer and winter.

4. Materials and methods

4.1. Sample collection and mapping

The mapping began by outcrop description, measurement and fresh samples collection. Fresh samples include the portion of the rock that is most likely to represent the rock as it was originally emplaced, (i.e. not weathered). This was achieved by using a geological and the 1.8 kg domestic hammer. A total number of 105 lavas, one chert and 4 sandstones samples were collected. The next step was to locate the samples on the topographic map of the area and marking the GPS coordinates from a GPS instrument (Geographical Position System). The different rock units were determined using the physical properties such as colour and grain/crystal size change of the rock.

4.2. Sample preparation

Of the 105 collected samples 41 volcanic samples were considered for XRF, XRD, and thin section analysis. 40 lava samples and one pyroclastic rock were considered for XRF and thin section analysis. XRD analysis was done only in cases meant to support the thin section analysis. Chert and sandstone were only analysed petrographically. The selection of the lava samples to be considered for analysis was completely influenced by several aspects; i.e. the sample physical appearance such as secondary features (i.e. veins, filled vesicles, crusting due to weathering and alteration) lead to their exclusion during the analysis. These features may lead to misrepresentation of the rock`s primary chemistry which often result in wrong chemical interpretation of the rock.

The XRF and XRD analysis were performed at the University of Pretoria's Stoneman labs of Geology. Both major and trace elements are analysed using the ARL 9400XP+ XRF wavelength dispersive spectrometer, the samples are prepared as pressed powder briquettes and the analyses were executed using the Uniquant software (Loubser and Verryn, 2008).The software analyse for all elements in the periodic table between Na and U, but only elements found above the detection limits are reported. The loss on ignition is also determined during XRF analysis to determine the crystal water and oxidation state changes. Then, all elements are expressed as oxides in weight percent (wt %). Trace elements are expressed in parts per million (ppm) and are analysed in COLA and TRACE software programs.

The LOI gives an indication of the degree of chemical weathering/alteration of feldspars and other minerals (Soueka et al., 1985). However, the LOI can also be caused by the devolatisation of minerals like carbonates (personal communication, Wladyslaw Altermann,

2014). To determine the percentage LOI, the samples were ground to $< 75m$ in a tungsten carbite milling vessel and roasted at 1000 $^{\circ}$C at the University of Pretoria. The LOI percentages are calculated by determining the weight loss of samples after heating (1000 $^{\circ}$C). Further, the chemical index of alteration is calculated. Nesbitt and Young (1982) demonstrated the importance and usage of the concept of CIA. The CIA is best described by the following formulation (Nesbitt and Young, 1982):

$$CIA = \frac{Al2O3 \; X \; 100}{Al2O3 + CaO + Na2O + K2O}$$

The samples were prepared for XRD analysis using a back loading preparation method (Loubser and Verryn, 2008). They were analysed using a PANanalytical X'Pert Pro powder diffractometer with X'Celerator detector and variable divergence and receiving slits with Fe filtered Co-Kα radiation. The phases were identified using X'Pert High score plus software (Loubser and Verryn, 2008). The phases identified are listed in the attached graphical representations.

Mineral names may not reflect the actual compositions of minerals identified, but rather the mineral group.

The relative phase amounts (weights %) were estimated using the Rietveld method (Autoquan Program; (Loubser and Verryn, 2008)). Errors are on the 3 sigma 3 level. Amorphous phases, if present were not taken into consideration in the quantification, except on the analyses of SM37 (clast and matrix analysis). The quantitative results are listed below.

Thin sections were prepared by the Council for Geoscience in Silverton and the analyses are done at the University of Pretoria.

In order to observe and describe the mineral phases present, thin sections are analysed using the Nikon model Eclipse E200 POL microscope at 0.4A, 50-60 Hz, 220/230/240 V; the observation were done under transmitted light. Pictures of the grains and crystals under the microscope were taken using the Nikon model Eclipse 50i POL AT 0.9/0.5A

A geographical information system (ArcGIS version 10) was used to draw the geological map. Corel draw version 12 was used the rearrange the petrographic micrographs, draw the stratigraphic column of the study area and to modify general diagrams from previous publication.

4.3. Description of bedding thicknesses

Table 1, shows the restriction measurements used during the descriptions of stratification/bedding of strata. The left column (table 1.) represents the thickness ranges of the beds which assign a certain thickness range to a descriptive thickness name in right column.

Table 1: Stratification/bedding thickness (after Ingram, 1954)

<100 cm	Very thickly bedded
30-100 cm	Thickly bedded
10-30 cm	Medium bedded
3-10 cm	Thinly bedded
1-3 cm	Very thinly bedded
3-10 mm	Thickly laminated
>3mm	Thinly laminated

4.4. Descriptive names of clasts based on their origin and size

Table 2: Classification of clasts (after Chough and Sohn, 1990; Sutton, 1993)

Range size of clasts	Non-volcanic	Volcanic
<256mm	Boulder	Coarse block
64-256 mm	Cobble	Fine block
16-64 mm	Pebble	Coarse lapillus
4-16 mm	Granule	Medium lapillus
2-4 mm	Very coarse sand	Fine lapillus
0.5-2 mm	Coarse sand	
0.25-0.5 mm	Medium sand	Coarse ash
>0.25 mm	Fine sand	
	Silt	Medium ash
	Clay	Fine ash

Sedimentary clastic rocks are formed from clast components that may have similar or different processes of deposition. Different sedimentary processes and volcanic activities lead to accumulation of clast components that are characterised by different sizes, shapes and cementation. Chough and Sohn (1990) and Sutton (1993), described the clast that are produced by non-volcanic (e.g. fluvial, wind deposits, etc.) and volcanic (e.g. pyroclast) processes. The description is summarised by table 2.

5. Geological map

The geological maps (figures 5 and 6.) best describe the lithological successions of the Rooiberg Group with clear boundaries of both the rocks and the geological formations. All formations, except the Dullstroom Formation are present in the study area. The boundaries of the formations are determined by their compositional variation as shown by figure 25. These boundaries that define Rooiberg formations are also confirmed by the chemostratigraphy of Jolayemi et al. (in prep.) The absence of Dullstroom Formation is due to the thick sequence of mafic intrusive rocks that extends further north of the study area. The area north of the Damwal Formation representing the base of the stratigraphy is an irregular transition between dacite and granophyres. The Damwal Formation constitutes the majority of dacites with minor rhyodacites, siliciclastic sedimentary rocks forming interbeds, massive tuff and peperite while the Kwaggasnek and Schrikloof consist of rhyodacites and rhyolites respectively, as seen from the geological map in figure 6. Up to 5000 m stratigraphy was logged (figure 8.). Close to the Loskop Dam area the Rooiberg Group attains a thickness of ~3,520 m. This thickness increases towards the east to a maximum of ~5,110 m (Twist, 1985; Clubley-Armstrong 1977). The area north-east of the study area (figure 8.) is characterised by the out-cropping of the Rashoop Granophyre rocks and the Bushveld intrusive rocks of the Rustenburg Layered Suite. The Rashoop Granophyre rocks depict a clear gradational transition with the rocks of the Damwal Formation. This gradational contact is interpreted to be a consequence of partial melting due to the emplacement of the mafic magmas of the Rustenburg layered suite. This observation and interpretation is consistent with previous studies. Walraven (1985), interpreted the granophyres to have been the product of contact metamorphism and partial melting of Rooiberg lavas. Recently, Tegtmeier (2013), also described the red granophyres, containing lath-shaped and acicular-shaped quartz and feldspar phenocrysts, as intrusion-induced (by the Rustenburg Layered Suite) products of re-melting of the basal rhyolite of the Dullstroom Formation, an idea, which was initially proposed by Von Gruenewaldt (1968). Further, Walraven (1982), using geochemistry, also suggested the genetic link between the Rooiberg Group lavas and the granophyres, arguing that the granophyres are the hypabyssal equivalents of the Rooiberg Group lavas.

In the southwards direction, the Damwal Formation crops out with thickness up-to ~750 -110 m. It mainly consists of dacitic and rhyodacitic lava, interbedded with meta-sandstones, peperitic breccia and massive tuff. The Damwal Formation is overlain by the Kwaggasnek and Schrikkloof Formations respectively southwards of the study area. The average strike

direction of the Rooiberg Group rocks is 270° with all sedimentary beds dipping towards the south. Dips are increasing from 15-30° in the north to 55-70° in the south.
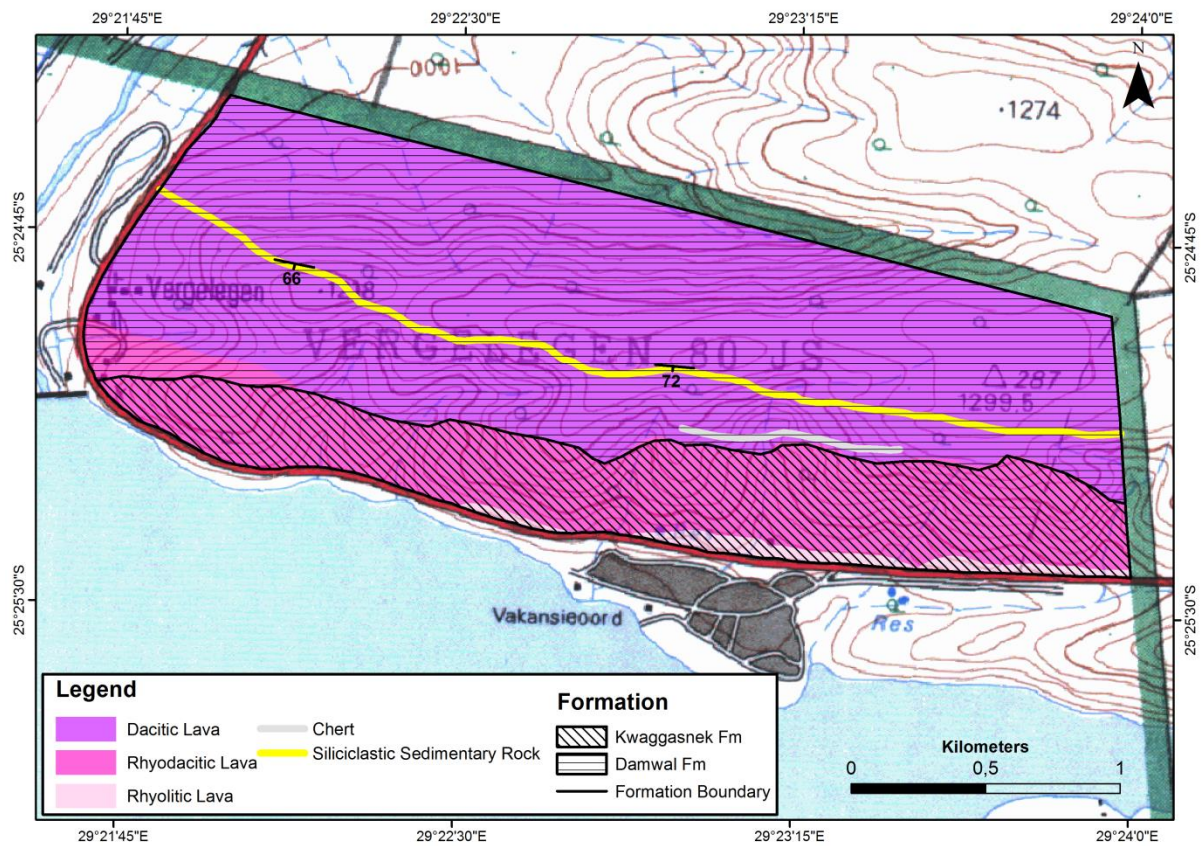
Figure 6. Geochemical map showing clear boundaries of the formations of Rooiberg Group in the study area. Different colours show compositions of lava, sedimentary and pyroclastic rocks in the north east of the Loskop dam (see legend for colour description).
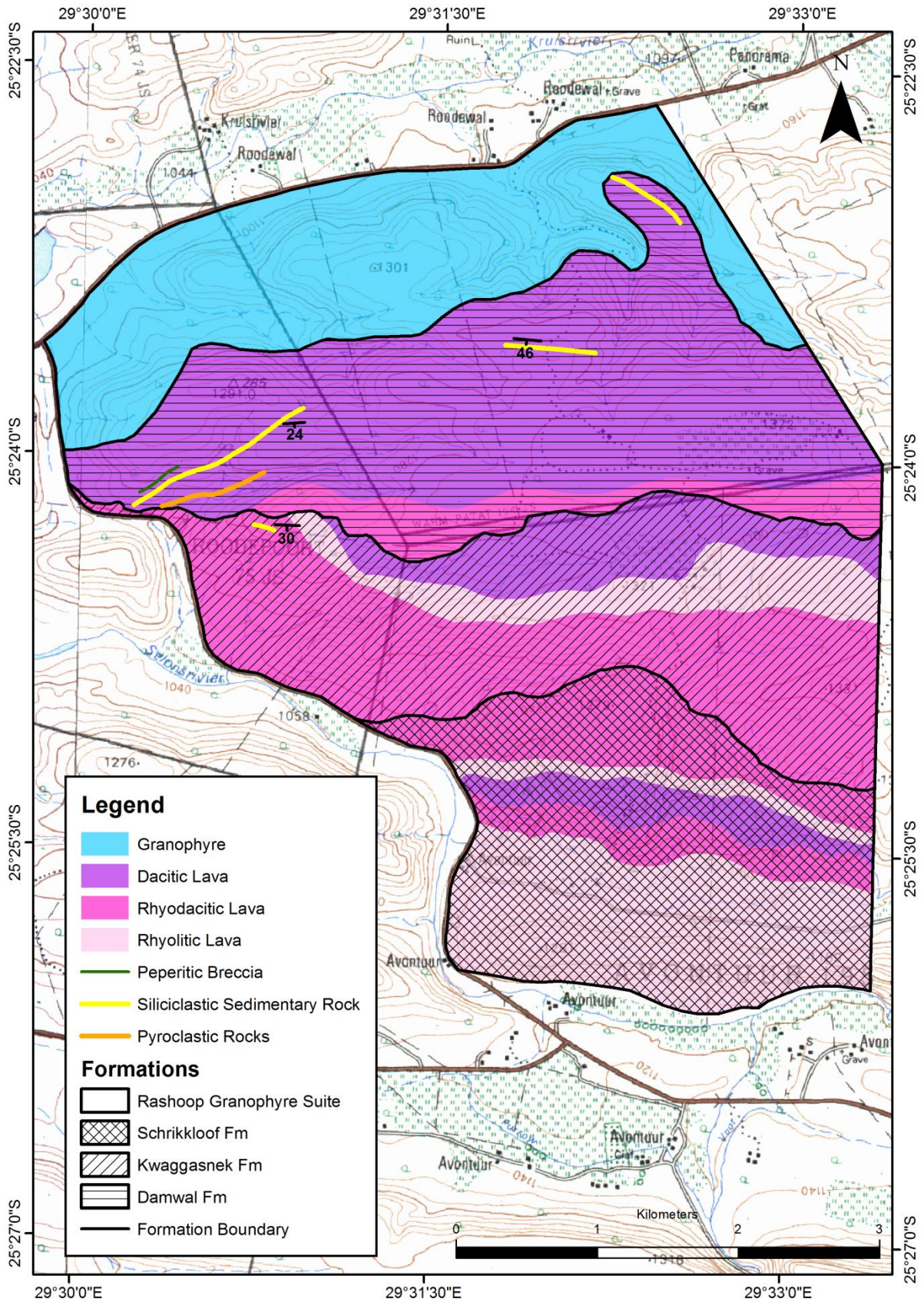
Figure 7. Geochemical map showing clear boundaries of the three formations of Rooiberg Group in the study area. Different colours show compositions of lava, sedimentary and pyroclastic rocks in the north east of the Loskop Dam (see legend for colour description).

Rooiberg Group Stratigraphy near Loskop Dam, Mpumalanga
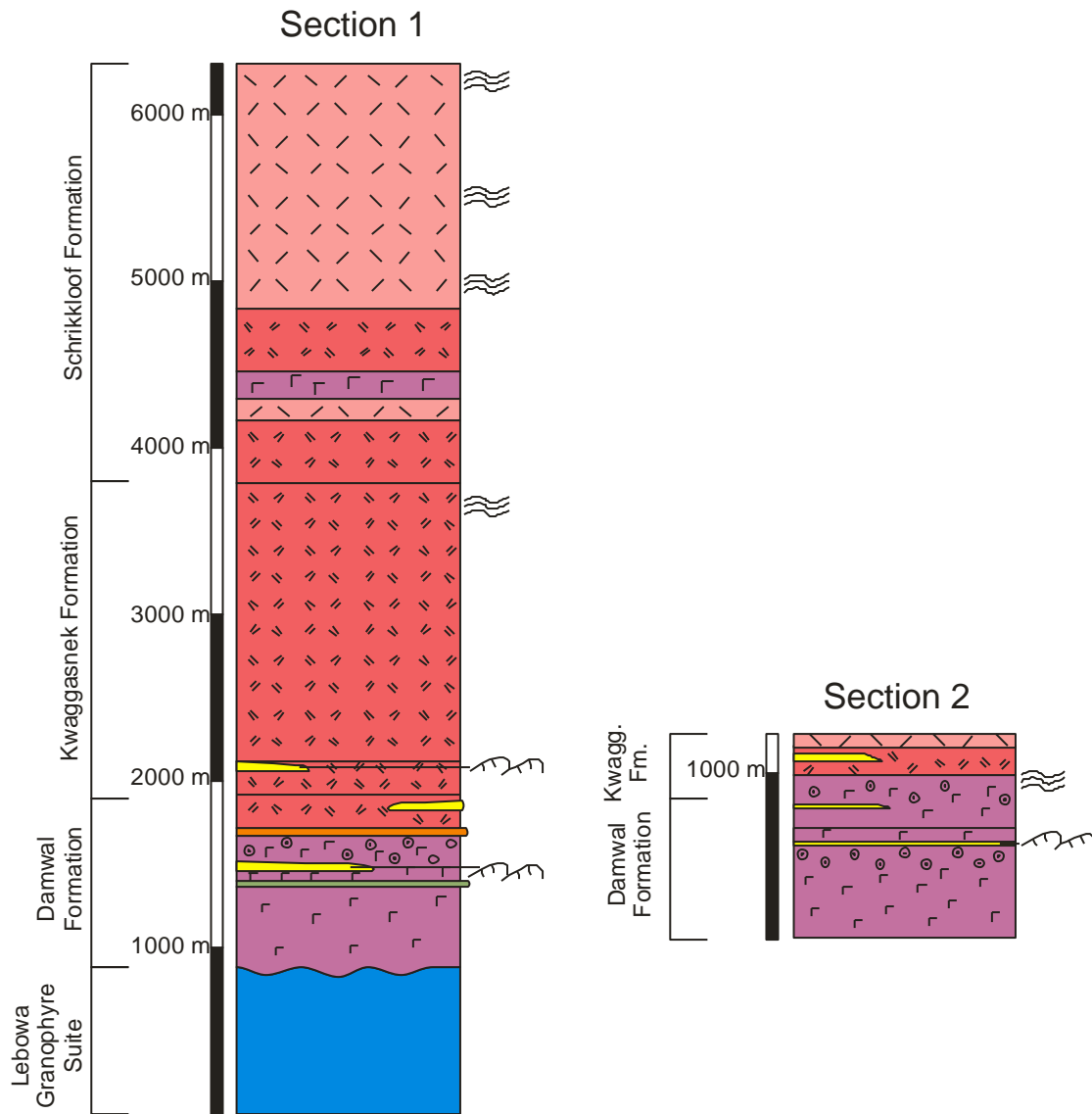
Figure 8. Stratigraphic column of the Rooiberg Group in the northeast of the Loskop Dam area.

6. Lithology and Petrography

The classification diagram of rock composition by Winchester and Floyd (1977), seen in figure (23) and the phenocrysts assemblage (plagioclase, quartz ± K-feldspar) clearly shows the magma clan of the Rooiberg Group rocks in the Loskop Dam area. In this area, rock units include dacites, rhyodacites and rhyolites. Within the ~5 km-thick logged (figure 8.) stratigraphic unit of the Rooiberg Group, each formation contains its major distinct compositional flow unit and rock types as seen from figure (5 - 7.). Table (3) shows that the silica content (65.65 wt.% - 79.84 wt.%.) of the lava units found in the formations of the Rooiberg Group increase stratigraphically from North to South, meaning that Schrikkloof Formation constitute the greatest amounts of silica content. Below are the lithological and petrographical descriptions of the rocks found in the three formations of the Rooiberg Group. The rock names of each sample follow the nomenclature by McPhie et al. (1993). The following is the thin section analysis of selected rock samples in the study area (other samples are briefly described in appendix C):

6.1. Damwal Formation

The Damwal Formation strata lie above the Rashoop Granophyre rocks. The formation was formerly described as units 3 - 6 (by Twist, 1985) predominantly consist of lava flows, with minor tuffs, peperites and metasandstones. The lava flows are massive, dense with local flow banding and occasionally have a blocky carapace intercalated between other depositional units. The base of Damwal Formation mainly consist of dacites with variable textures (aphyric to sparsely porphyritic) and may contain vesicles/amygdales, spherulites and lithophysae. Frequently, the spherulite dominated rocks (towards the top of Damwal Formation) constitute perlitic fractures filled with quartz and opaque mineral phases. The rhyodacites are mainly found at the top of the Damwal Formation and mostly are sparsely porphyritic in texture. Noteworthy, is the observed slight increament of phenocryst content from the base to the top (north to south) of the stratigraphy, yet having almost same sizes of euhedral phenocrysts. The peperites, tuffs and metasandstones are intercalated within the lava flows. Peperite is a genetic term applied to a rock formed essentially in situ by disintegration of magma intruding and mingling with unconsolidated or poorly consolidated, typically wet sediments (Brooks et al., 1982). The following is a detailed microscopic analysis of the selected samples.

6. 1.1. Massive lithophysae/spherulites bearing, dacite (sample SM14)

Rock SM14 is grey in colour and consists of thick brown weathering skin. The aphanitic SM 14 has features such as, polycrystalline growths and amygdales (lithophysea and micro-spherulite) (Davies and McPhie, 1996, Tuffen and Castro, 2009; Kshirsager et.al., 2012).
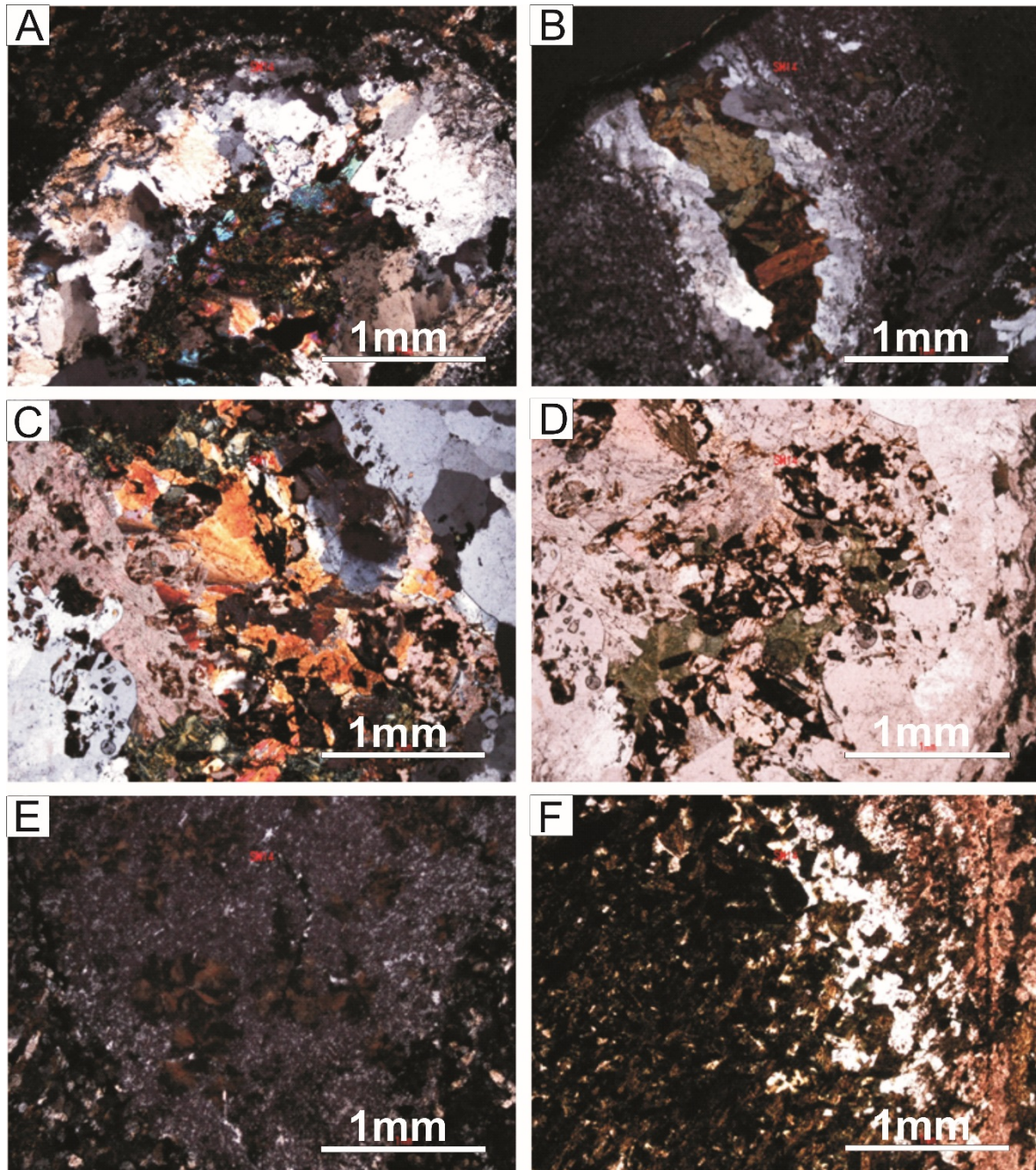
Figure 9. Photomicrographs of dacitic lava (sample SM14), Damwal Formation. A and B, show lithophysea with concentric zones, note the onion skin structure consisting of outer k-feldspar, inner quartz, and most inner phyllosilicate minerals. All pictures are taken in cross polarised light.

The micro-spherulites (figure 9, E.), spherulites and lithophysea (figure 9, A and B) are suspended within a hyaline microcrystalline groundmass mainly made of K-feldspar and possibly altered and thus displaying multiple colored secondary alteration products.

Unlike spherulites, lithophysae (figure 10, A-D and figure 31, B.) lack radial structures (seen when bisected through their centers) yet spherical but more oval and may contain secondary quartz along fractures and inner zone(s) and are however spatially related with the spherulites (c.f., Tuffen and Castro, 2009). The size of the lithophysae (40 vol %) have the range of 1.0 - 1.5 cm. To some extent, the lithophysae appear to constitute concentric distinct occasionally alternating mineralogical zones (inner, middle and outer zones) arranged parallel to the crystalisation front. The zones are mainly composed of quartz and k-feldspar and the 'assortment' of both. The inner zone is made up of large (up to 1.3 mm on the long axis) euhedral calcite crystals (figure 9, A), corroded by recrystallizing quartz. In some cases, the nuclei of the lithophysae are comprised of amphibole, chlorite and quartz. The middle zone is predominantly made up of recrystallized euhedral-anhedral quartz crystals, while the outer zone is comprised of polycrystaline fine quartz and alkali feldspar crystals. Compared to the lithophysae, the spherulites are small in size (0.5 - 1.0 cm) and consist of bundles of radiating fibres from the centre outward. The size of the amygdales (1 %) can be up to 5 mm.

6.1.2. Massive lithophysae bearing dacite (sample SM3)

On hand specimen, unit SM3 or rather massive lithophysae dacite is grey-green in colour with black lithophysae (figure 31, C.). Sample SM3 represents a dense massive slightly greenschist-metamorphosed rock. The lithophysae (1-8 mm diameter and ~15 % vol) are more resistant to weathering and thus give the outcrop its course textured appearance. Occasionally, the lithophysae show a preferred horizontal alignment of up to 1-2 cm thick clustered growth. To some extend the lithophysae displays forms such as twin, triplet and quadruplet of clustered lithophysae. Unit SM3 has an aphyric texture, where the lithophysae are suspended within a glassy greenish groundmass. The former mentioned lithophysea are mostly filled with secondary quartz (figure 9.). The secondary infilling quartz or possibly quartz polymorphs frequently exhibit a star shaped morphology and thus may be referred to as thundereggs (c.f., Kshirsager et al., 2012 and the references therein). The variable sized lithophysae may also be homogenously composed of the rounded to sub-rounded quartz filled voids which are randomly distributed, and entirely engulfed by devitrified glass as groundmass. Some of the lithophysae appear as spheroidal polycrystalline bodies, sparsely distributed and both well rounded and minor amoeboidal quartz filled voids. The voids sizes

range from few microns to 1 mm scale. The appearance of minerals such as chlorite and actinolite as observed and detechted by XRD analysis is typical of low grade metamorphism of greenschiest facies. The presence of spherulites and clay minerals are indicative of devitrification of silicic glass.
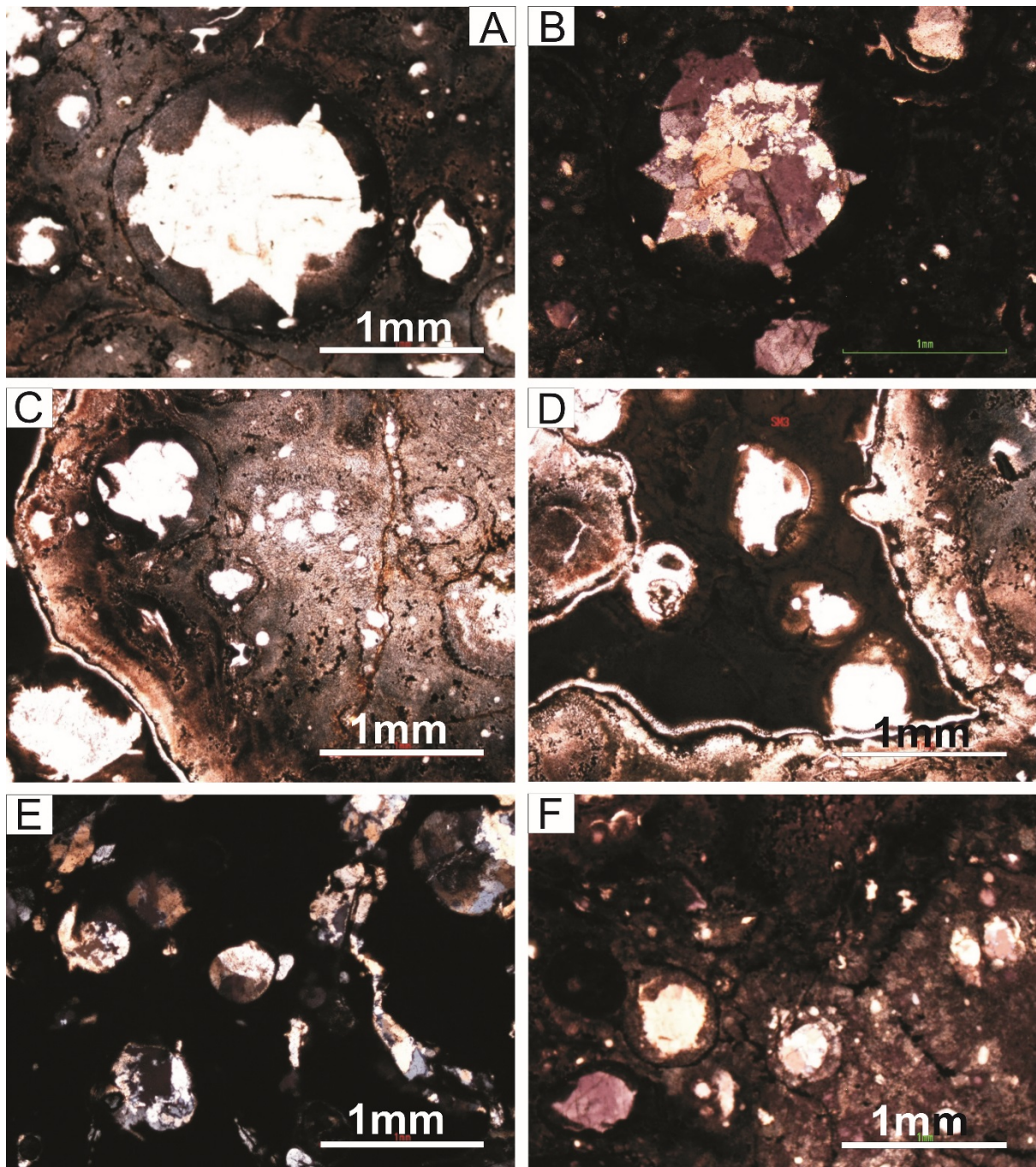
Figure 10. Photomicrographs of dacitic lava (sample SM 3), Damwal Formation. A and B, show star shaped morphology of the lithophysae. C, multiple lithophysae inside the large one. D, shows boundaries of twin shaped lithophysae. E, shows amygdules. B and E are taken in cross polarised light while A, C, D and F are taken in plane polarised light.

© University of Pretoria

6.1.3. Perlitic dacite (sample SM37)

The perlitic dacite is green-brown in colour probably due to the effects of greenschist metamorphism. In the field, SM37 consist of a massive rock with thin petty folding layers ('onion like layers') with thickness up-to 10 cm. Its eye capturing clast-like texture and its association to fine grained, veined silty sandstone could be easily misinterpreted for hyaloclastite. However, the polished slap shows finger like interconnected high silica (cherty) bodies that are sericitised. However, in thin section the rock consist of sericitised, cuspate, shard-like shaped 'bodies' which could be easily misinterpreted for the pyroclastic origin. Photomicrograph C in figure (11, D) shows that these bodies (named CLSM37 in appendix E) consist of very fine radiating structures K-feldspar and quartz. XRD analyses of these bodies reveal the main constituents to be quartz and K-feldapar and minor plagioclase (see appendix). In thin section, the previously glassy groundmass has completely recrystallized to mainly anhedral-subhedral micro-quartz and K-feldpsar. The matrix of this rock is mainly composed of plagioclase quartz and K-felddspar as shown from the XRD analysis. This rock is interpreted to be formerly coherent glassy lava which was affected by post-hydrothermal activity and was later altered producing a false pyroclastic texture. The onion like layers is interpreted as weathering pattern which grades outwards relative to the outcrop.

6.1.4. Massive amygdaloidal dacite (unit SM 17)

The dark grey-brown unit SM17 is aphantic with red flow like fillings (perlitic veins), partchly distributed in a microcrystalline groundmass. The flat lying outcrop of unit SM17 forms the peak with lateral exposure of ~3 m. The fresh surface of this outcrop comprises the huge white (up to 2 cm long axis), oval and spherical quartz filled amygdales which are to some extent zoned. Also present is the red-brown lithophysae which are quartz filled. Perlitic cracks are filled mainly with haematite and secondary quartz

Microcrystaline groundmass of unit SM17 includes variable proportions of quartz, alkali feldspar, plagioclase and minor opaque respectively. Subhedral plagioclase (2 %) phenocrysts are corroded by recrystalised quartz (figure 12, A). Minor quartz amygdales (<1-10 mm radius) and lithophysae (up to 3 mm) are present. The lithophysae may be filled with actinolie crystals. This unit also consist of quartz veins/fractures which cut through lithophysae (figure 12, B). Minor chlorite, actinolite and magnetite are also reported by XRD analysis.

45
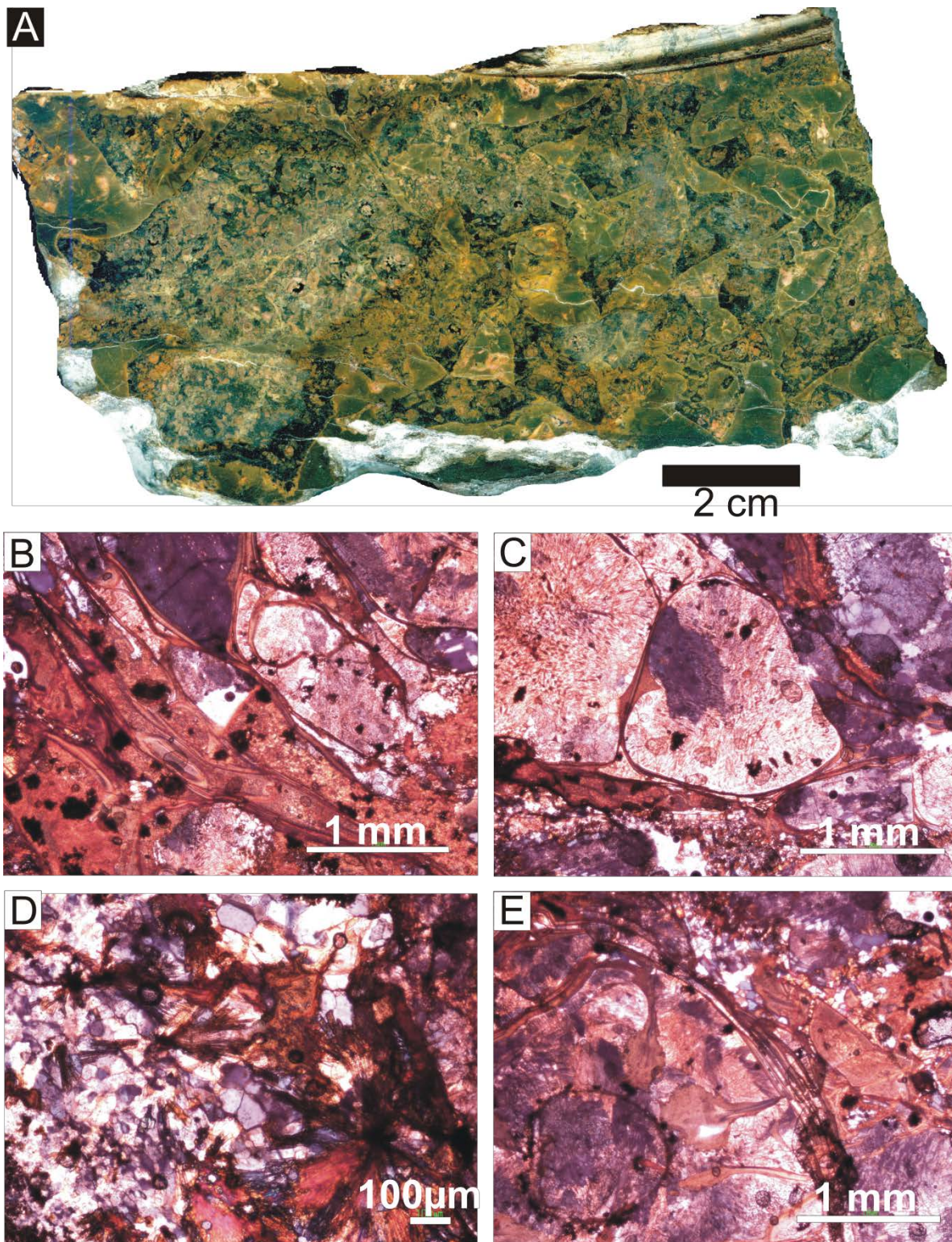
Figure 11. False pyroclastic texture in altered hydrothermally affected dacitic glass (perlitic dacite).   A, shows a polished slab (SM 37). B, C and E show sericite filled perlitic fractures. D, shows recrystallized glass. B-E, in cross polarised light.
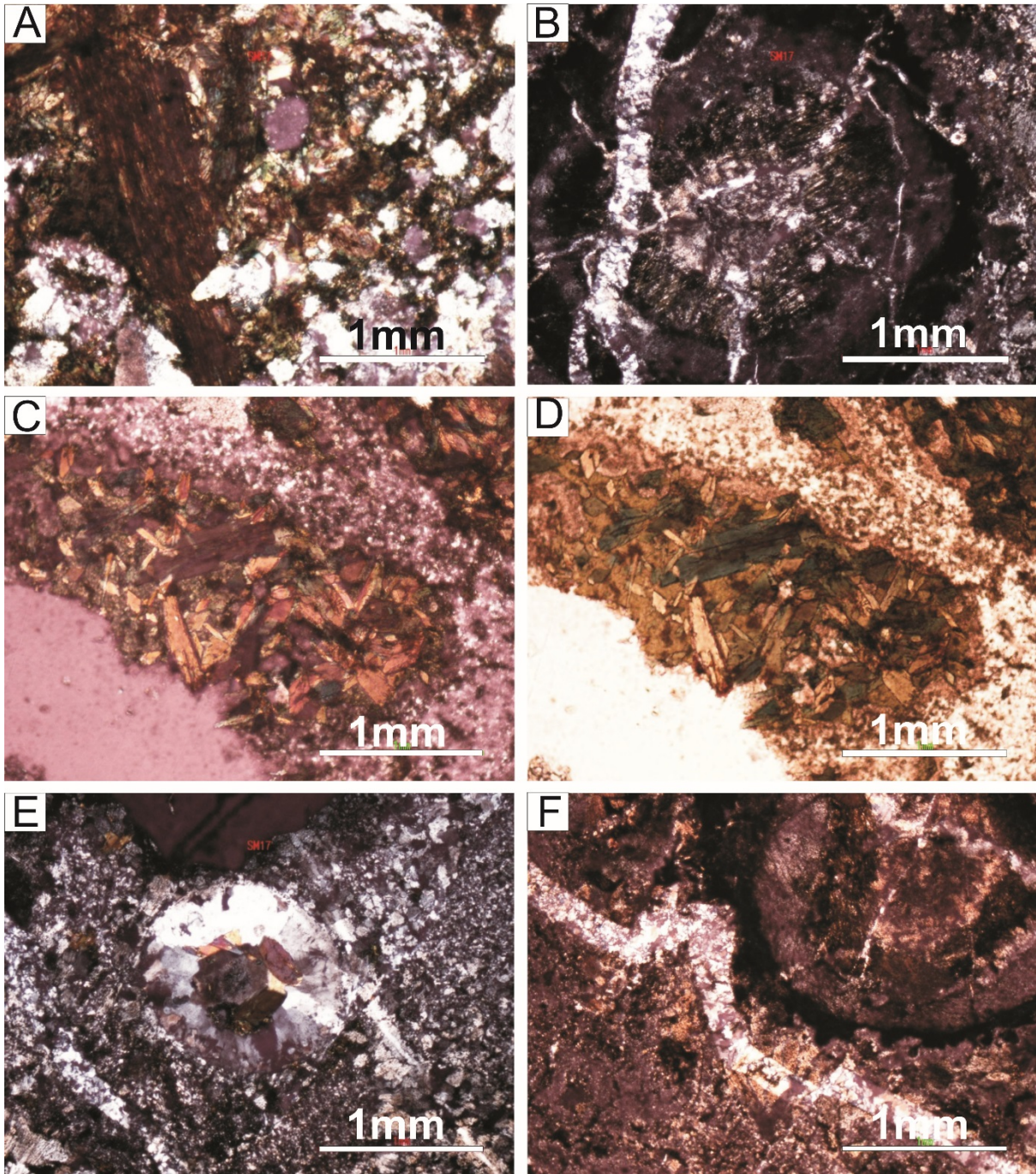
Figure 12. Photomicrographs of amygdaloidal dacitic lava (sample SM 17). A, shows pseudomorph after plagioclase in a recrystalised glass. B, E and F show quartz veins and amygdales. Well rounded (E) and oval amygdales with concentric zones depicting crystallisation pulses, are filled with quartz (outer core) and phyllosillicates. Vein cut through the amydale (B), while on F it surrounds the amygdale. A, B, C, E, in cross polar while D and F are in plane polarised light.

6.1.5. Massive pseudospherulitic dacite (RL1)

The brown black unit RL1 letarally extends for ~5m outcrops very limitedly in a dense grassy area found on the flat lying morphology near the middle west of the study area. The hand specimen shows red rounded and dark grey rounded spots or rather polycrystalline bulbous aggregates of quartz and feldspar. Occationally, the polycrystalline aggregates (pseudospherulites) show concentric zoning composed of k-feldspar and quartz. Thin section shows that this massive dacite (RL1) consist cryptocrystalline groundmass. Patches of chlorite are also observed. In this case, chlorite is accounted for as an alteration product of hornblende minerals.

XRD analysis report that quartz (probably secondary) and plagioclase are the abundant minerals with minor k-feldspar and chlorite.

6.1.6. Sparcely porphyritic dacite (Unit SM 6)

Unit SM 6 is brown grey lava, found on the north east of the study area. The feldspar-phyric unit SM 6 is exposed as thin outcrop of ~1m, but unlimitedly continuous on the east-west direction of the study area. Dominant minerals are euhedral-subhedral plagioclase and k-feldspar set in a quartofeldspartic microcrystalline groundmass. The overall texture of the rock is sparcely porphyritic. Euhedral plagioclase (0.5-1 mm) crystals forms <7 % and are often associated (edge contact) with unhedral K-feldspar, forming glomeroporphyritic texture. K-feldspar is seldom euhedral and may attain maximum size of up to 1.5 mm. Further investigation reveals groundmass to be microcrystalline and predominantly composed of plagioclase, minor K-feldspar, quartz and patches of chlorite.

6.1.7. Massive dacite (sample SM 44)

Unit SM44 consist mainly of plagioclase and quartz with rare k-feldspar. The dominant texture is the bulbous clasters of devitrtified glass consisting of recrystallized quartz and K-feldspar and large tabular bulging plagioclase phenocrysts are corroded by minor recrystallised patchy quartz. Plagioclase appears to be severely altered to white-brown clay mineral, probably kaolinite. Minor amygdales are filled with quartz and calcite. Opaque minerals minerals are present, but are rare,

XRD report the existence of actinolite. This phase occur as an alteration product of probable feldspars.

48
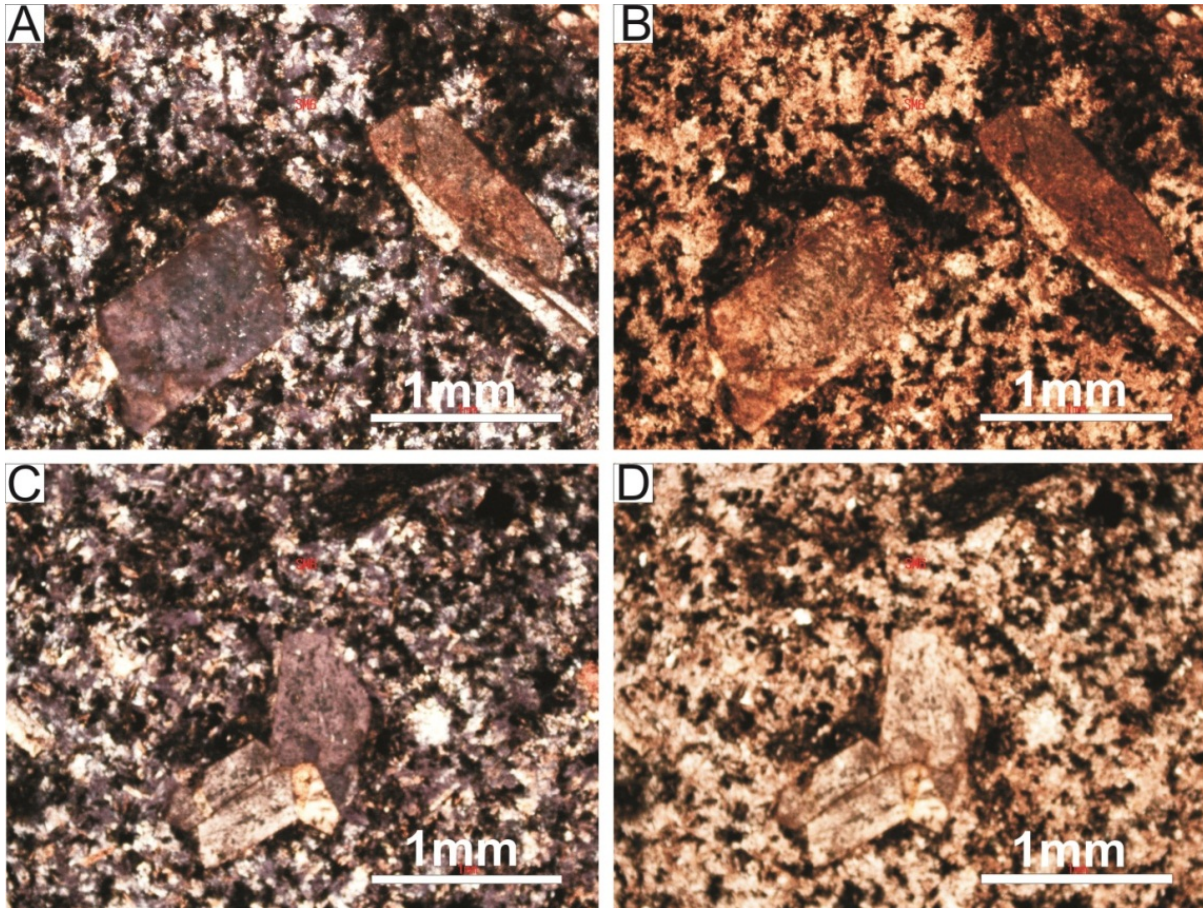
Figure 13. Photomicrographs of dacitic lava (unit SM 6). A and C, show poorly porphyritic texture and contains only minor euhedral-subhedral plagioclase and K-feldspar phenocrysts set in a quartzofeldspathic microcrystalline groundmass, pictures in cross polarised light. B and D in plane polar while A and C are in cross polarised light.
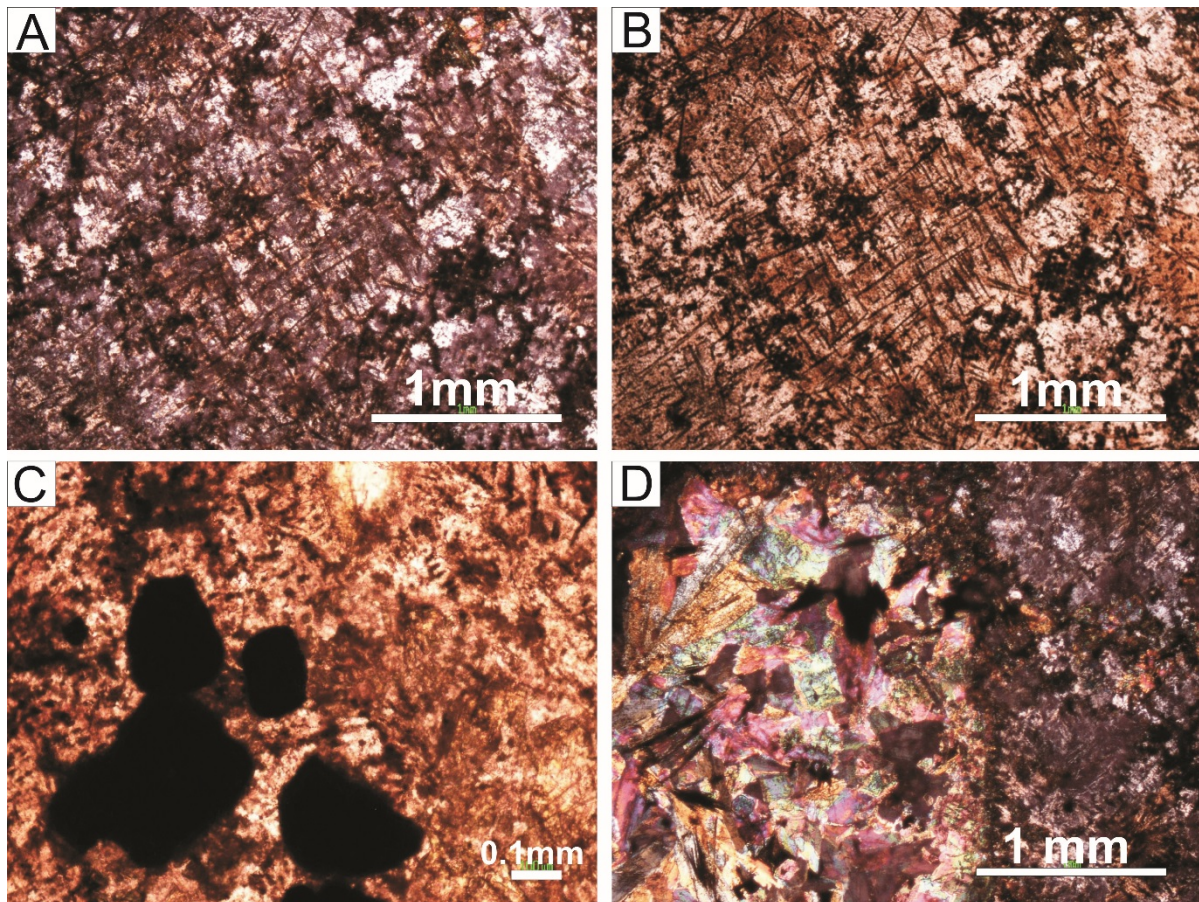
Figure 14. Photomicrographs of dacitic lava (sample SM 44, Damwal Formation). A, shows bulbous clasters of devitrtified glass consisting of recrystallized quartz and k-feldspar. C, shows opaque minerals. D, shows quartz and calcite filled amygdales. A and D are taken in cross polarised light while B and C are in non-polarised light.

6.2. Kwaggasnek Formation

Within the study area the Kwaggasnek Formation (sample 7-8 of Twist, 1985) consist mainly of lava flows and minor sandstone rocks. The lava flows are massive dense and lack brecciated units (carapace), with local flow banding and occasionally are dominated by zoned amygdales/vesicles. At the flow margins the amygdales are both rounded and rarely amoeboidal with sizes up to 7 cm. Unlike Damwal and Schrikkloof Formations, the Kwaggasnek Formation is dominated mostly by porphyritc rhyodacites and minor dacites and rhyolites. The highest number of phenocrysts (5-40 %) are found in this formation, however they seem to increase from the base to the top of the stratigraphic section. The interbedded sandstones forms minor individual outcrops at the base of the formation. Horizontally bedded chert can be followed for tens of meters along strike. Three samples were considered for microscopic analyses.

Qaurtz appears as microcrystaline of euhedral and anhedral crystals while plagioclase is mostly found as unhedral crystals. K-feldspar is occationally found as inclusion of plagioclase. The groundmass is predominantly composed of quartz, plagioclase and minor k-feldspar. Patches of chlorite are also observed. In this case, chlorite is accounted for as an alteration product of hornblende minerals.

6.2.1. Rhyodacite (sample SM 48)

Unit SM 48 is the near base unit in the Kwaggasnek Formation. It has masive fine grained texture. It is dark brown in colour. Microscopically, unit SM 48 shows dispersed mostly 1 mm crystals of plagioclase (up to 3%) set in a matrix of plagioclase, K-feldspar (microcline) quartz, and very rare pyroxene. Chlorite appears as an alteration product of pyroxene (figure 15).

6.2.2. Pseudospherulitic dacite (sample SM 10)

Unit Sm10 is found close to the base of the Kwaggasnek Formation.The handspecimen display massively textured, brown-grey colour influenced by semi-rounded brown aggregates. Thin section reveal the presence of altered polycrystaline bodies (0.5-1 mm) held together by fine matrix, of possible predominantly plagioclase, K-fedspar and quarts. The altered polycrystaline bodies or rather bolbous aggregate (pseudospherulites, figure 16) are generally composed of K-feldspar and quartz (Figure 16).
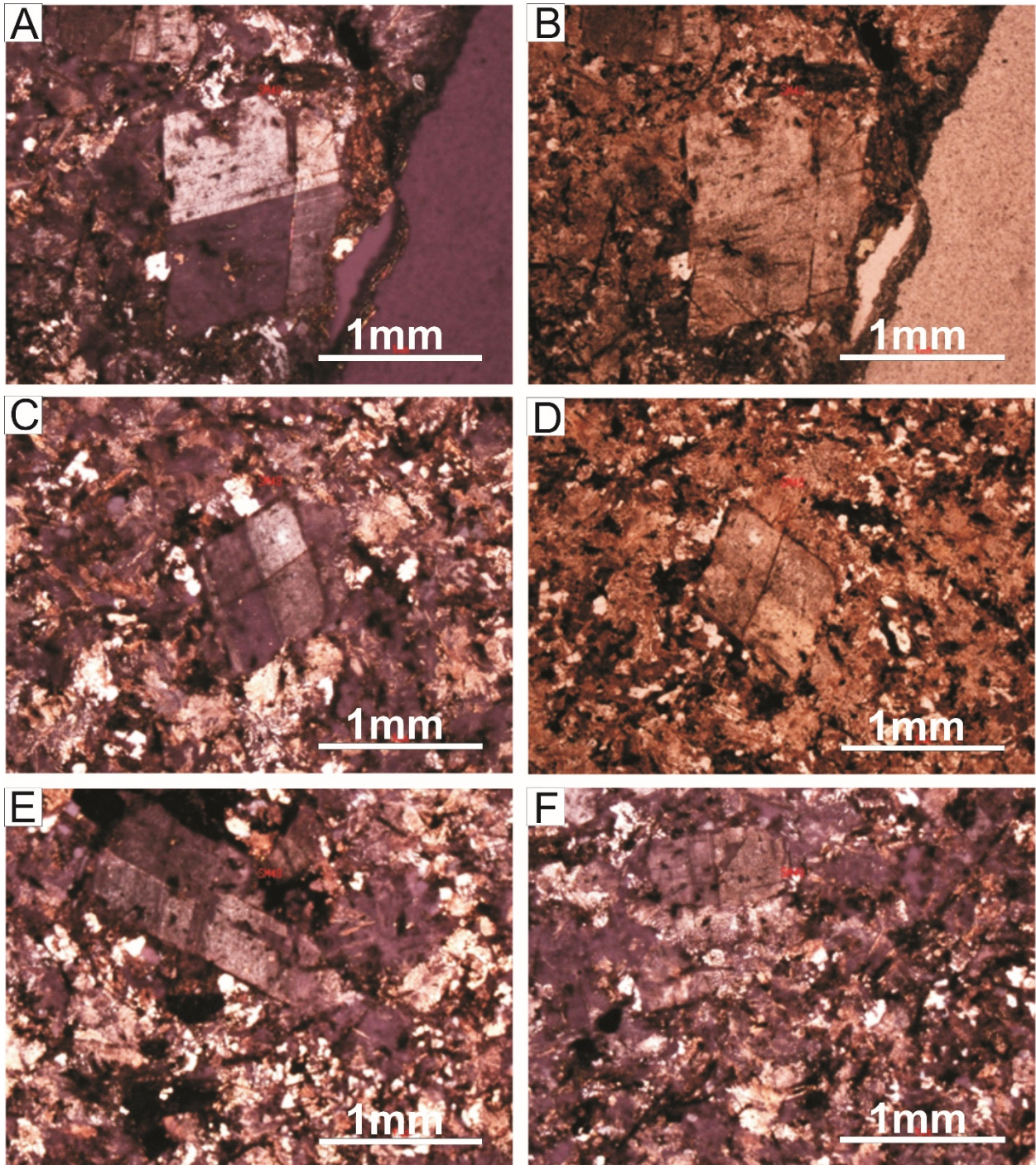
Figure 15. Photomicrographs of rhyodacitic lava (sample SM 48, Kwaggasnek Formation). A, B and C show size range of plagioclase phenocrysts (1-3 mm). The matrix consists of microcrystalline plagioclase, quartz and k-feldspar. A, C, E and F are taken in cross polarised light while B and D are in plane polarised light.
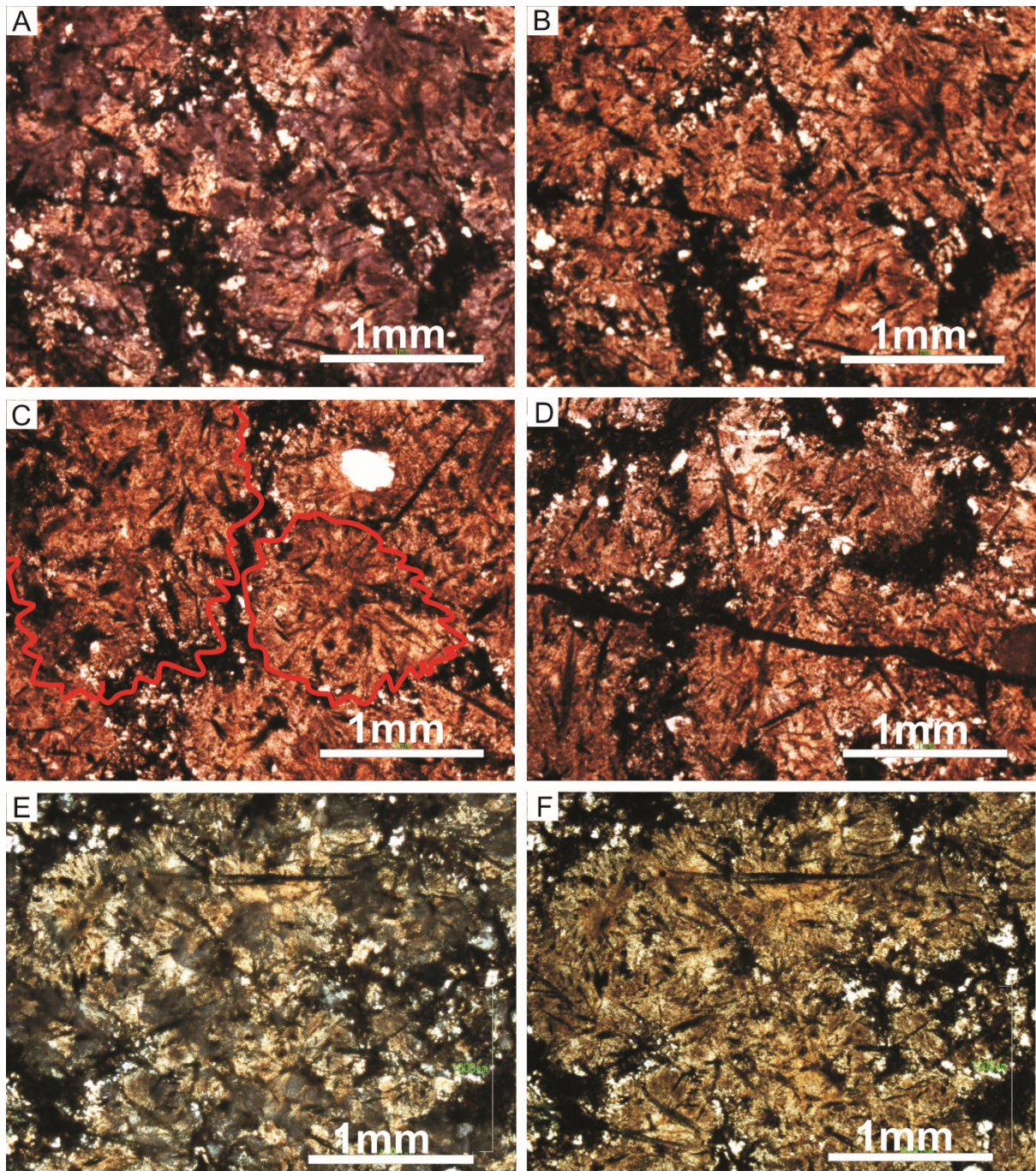
Figure 16. Photomicrographs of rhyodacitic lava (sample SM10). This unit mainly consist of bulbous, polycrystalline 'bodies' (pseudospherulites) as indicated by red sub-cicles. A-D are taken in non- polarised light. E and F are taken in cross polarised light.
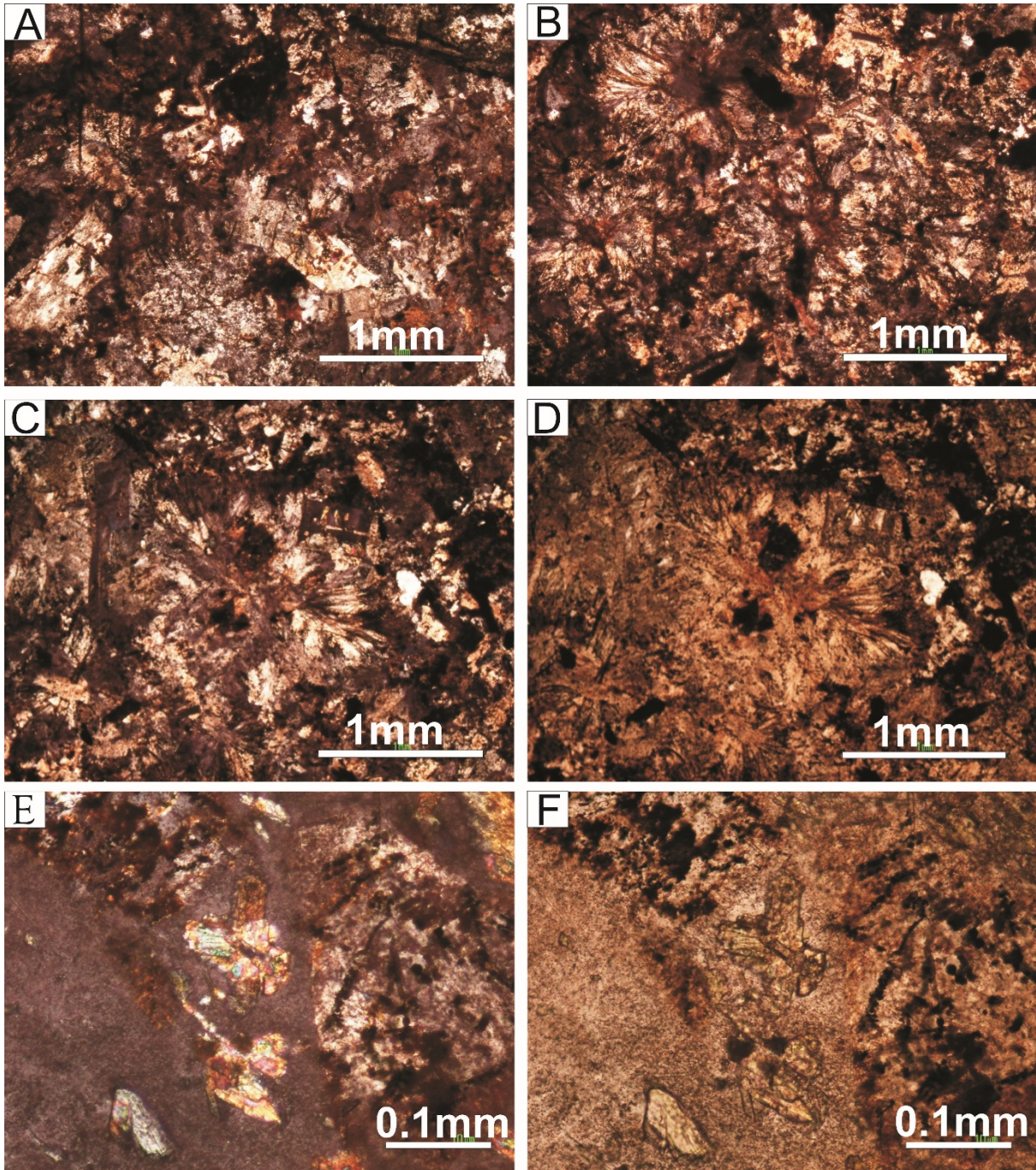
Figure 17. Photomicrographs of rhyodacitic lava (sample SM 51). This unit mainly consist of bulbous, polycrystalline 'bodies' (pseudospherulites) on the top left of B and centre of C and D. A, B, C and E are taken in cross polarised light. D and F are taken in cross polarised light.

6.3. Schrikkloof Formation

Within the study area the Schrikloof Formation (unit 9 of Twist, 1985) consist mainly of lava flows. The lava flows have massive dense core, further, parallel concentric fractures are frequently observed within the rhyodacites. The lava flows consist mainly of rhyolites and minor rhyodacites. The rhyolites have aphyric to porphyritic textures, while the rhyodacites exhibit porphyritic textures. The highly porphyritic rhyodacites (5 - 25% phenocryst, predominantly plagioclase) forms the base of this Formation, while a sudden decrease of phenocrysts occurs when approaching the top of the formation. Spherulitic textures although rare, are also observed. The spherulites consist of outer coarse zone and finer centres. The flow margins are normally vesiculated (up to 10%) with prominent flow banding. The following is a detailed microscopic analysis of the selected samples.

6.3.1. Porphyritic rhyolite (SM 5.2)

Porphyritic rhyolites (SM5.2) contain 5% of feldspar crystals which are suspended in a dark brown to grey microcrystalline groundmass. The overall texture is sparsely porphyritic, with thin section revealing the microcrystalline plagioclase, quartz, k-feldspar and parchy distributed chlorite. Rarely, this unit shows cumulophyric sieve texture of k-feldspar enclosed in plagioclase. Plagioclase the dominant phase, has euhedral phenocrysts (up to 1.5 mm) with rare anhedral-subhedral k-feldpar phenocrysts (<1.0 mm) (figure 18.). Quartz grains may appear rounded.

6.3.2. Porphyritic rhyodacite (SM 28)

The pink-red, Porphyritic rhyodacites (SM 28) of the Schrikkloof Formation comprise large crystals and crystal fragments (<5 mm) of quartz (5% vol), plagioclase (15%) and k-feldspar (5 %). Dominant textures include symplectite, corona, granophyric and sutured crystals. Plagioclase is the dominant feldspar and appears both as subidiomorphic to allotriomorphic crystals. Anhedral plagioclase crystals are edge corroded by secondary amphibole. In rare cases, plagioclases occur as in a subpoikilitic and poikilitic on the sanidine crystals. Large crystals (up to 6 mm across) of alkali feldspar mainly occur as idiomorphic crystals and commonly contain granophyric rims. Frequently, the amphiboles replace the feldspar. Quartz (3 mm in size) appears to be partially resorbed and embayed. Idiomorphic quartz is engulfed in blebs of quartz and feldspar (figure 19.).

6.3.3. Sparcely porphyritic rhyodacite (sample SM22)

Unit SM22 is rhyodacite rock consisting of micro-spherulites and perlitic fractures. The texture of the rock is hyaline with minor plagioclase crystals (0.7 mm in size) constituting 1 % of the rock. The spherulites are well rounded and show polycrystalline assortment of k-feldspar and quartz (and quartz polymorphs) radiating from the centre (figure 21, C.). The quartz filled perlitic fractures within the hyaline texture cut through plagioclase phenocrysts (figure. 21, D.).
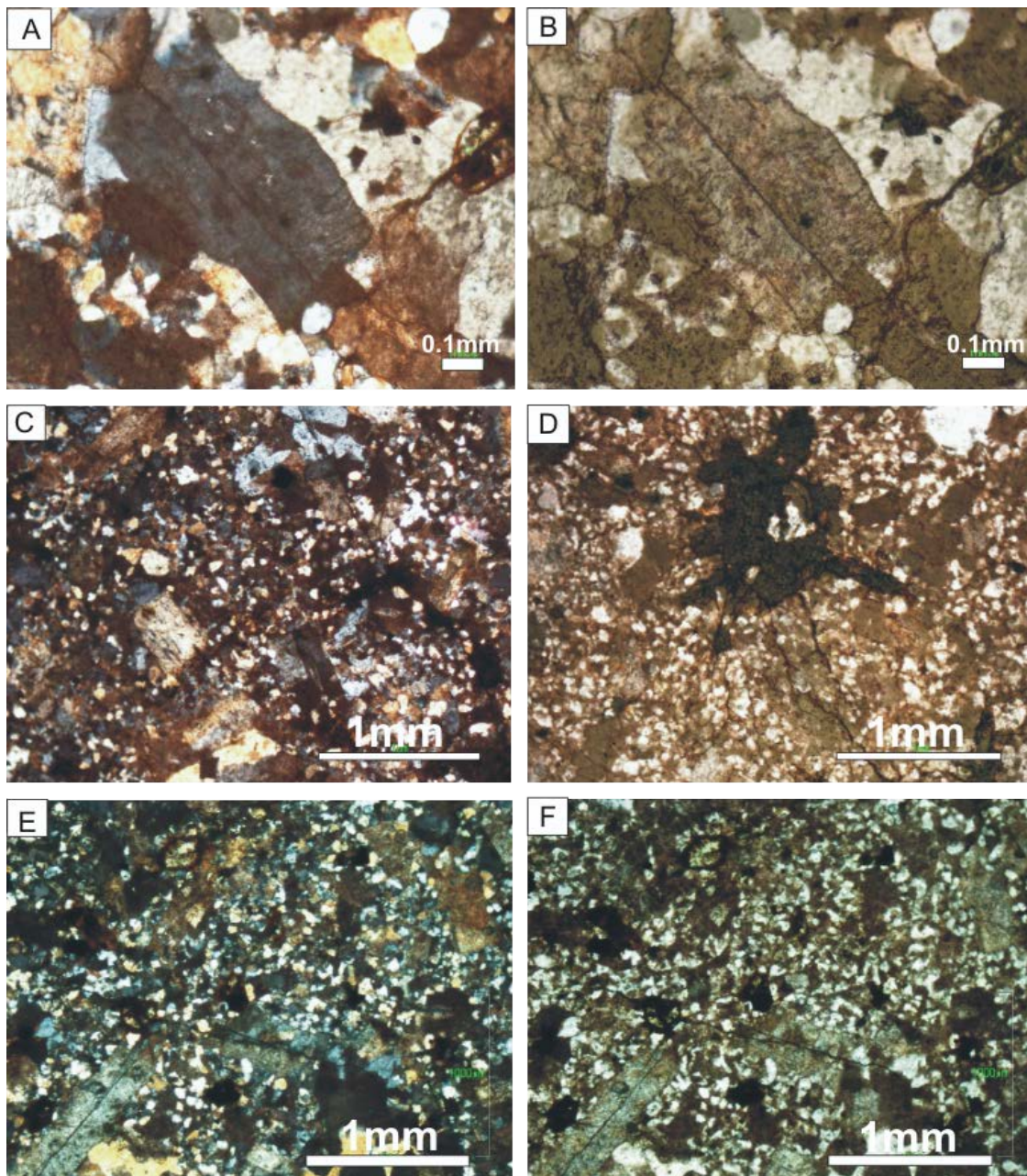
Figure 18. Photomicrographs of dacitic lava (sample SM5.2). SM 5.2 consists of plagioclase and K-feldspar phenocryst suspended within the cryptocrystalline groundmass of plagioclase,

k-feldspar, and quartz. A, C and E are taken in cross polarised light while B, D and F are taken in plane polarised light.
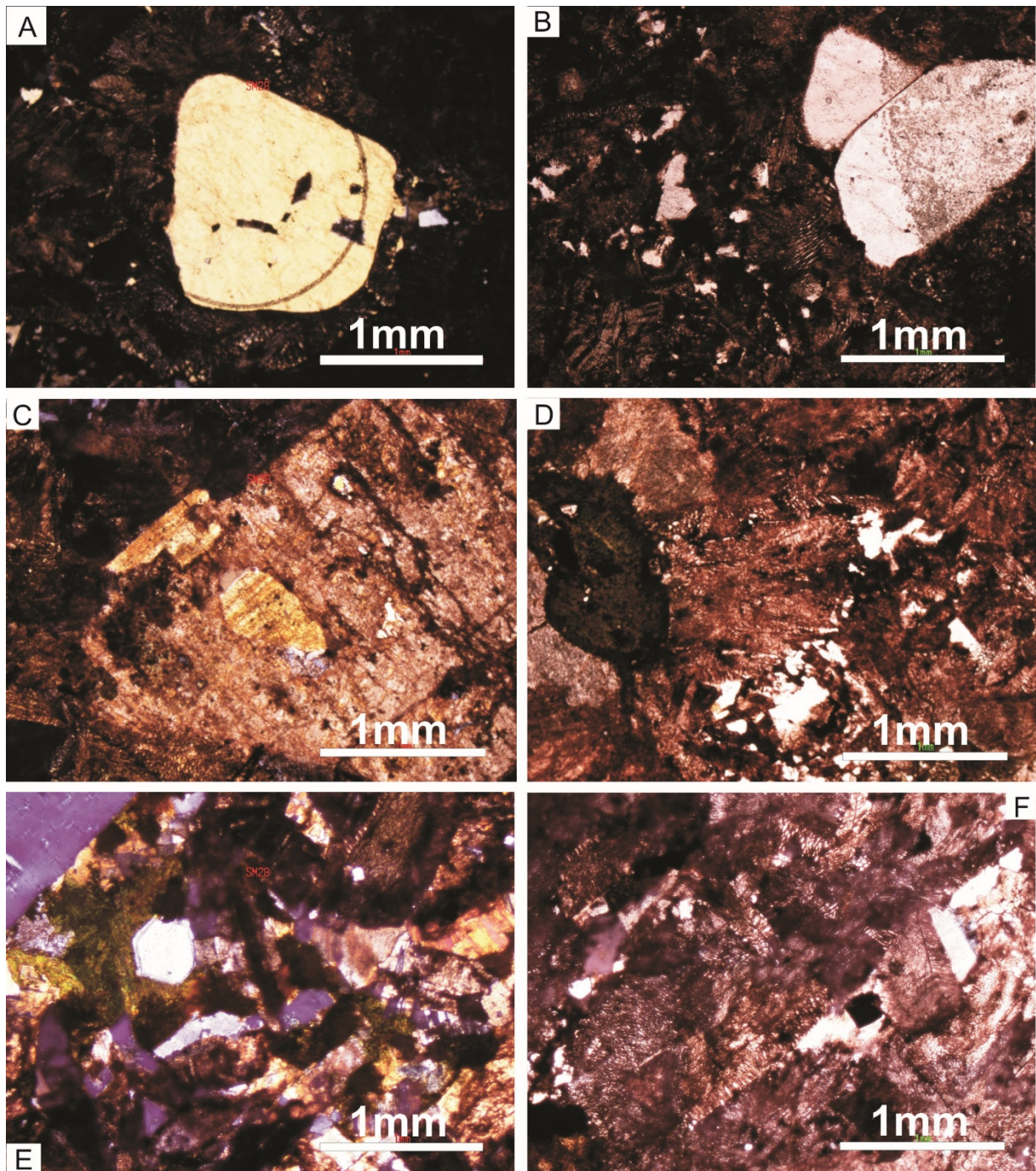
Figure 19. Photomicrographs of rhyodacitic lava (SM28, A. See B in the appendix). All pictures are taken in cross polarised light. A and B show subhedral quartz crystals submerged in a granophyric textured groundmass. The granophyric material surrounds all other crystals, indicating that it is the product of late crystallisation. C, shows K-feldspar enclosing plagioclase crystal. D, show secondary amphibole (green porphyroblast). E shows

plagioclase, perthite, euhedral quartz and amphibole within biotite. F shows the K-feldspar with granophyric rim.
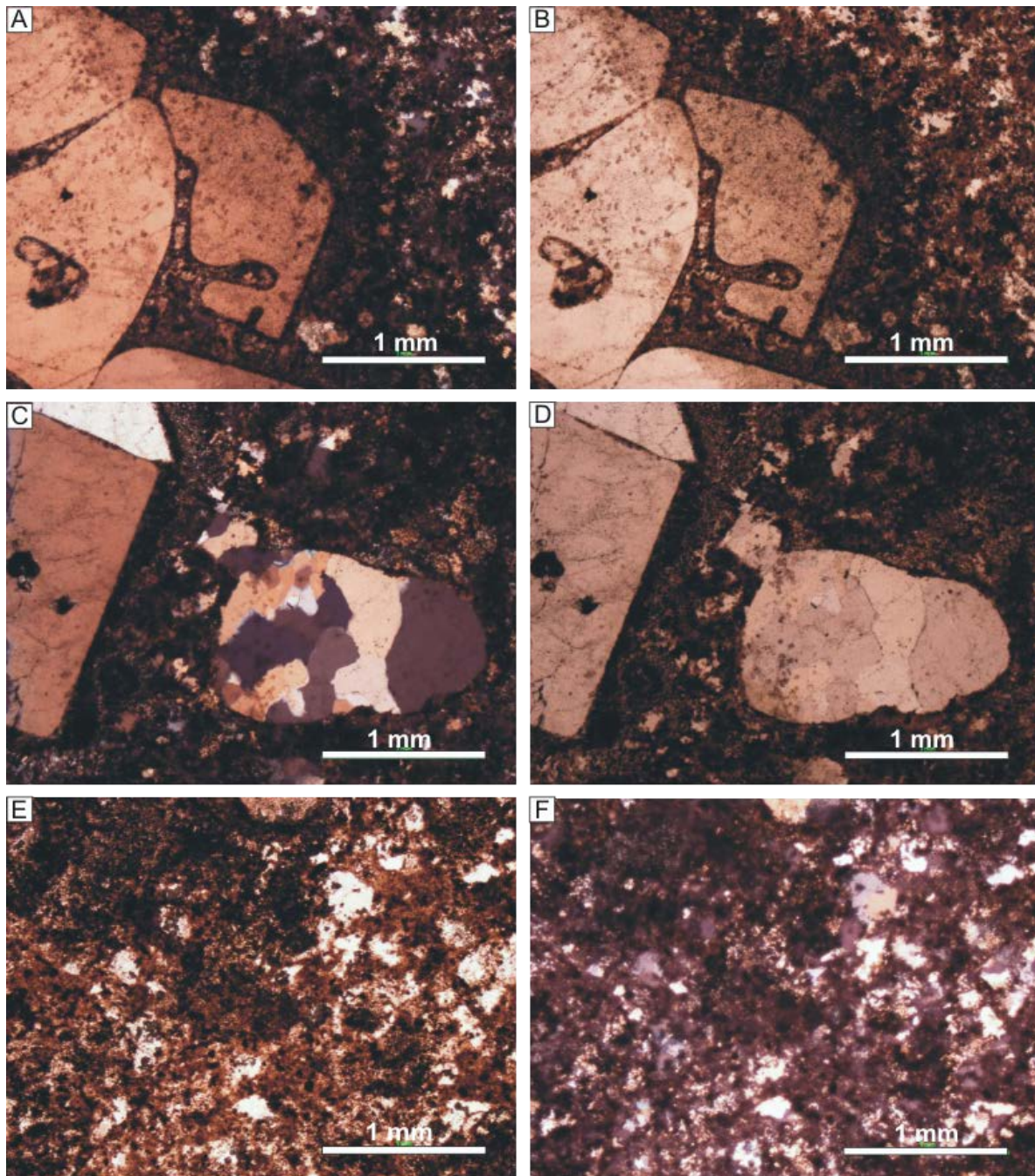
Figure 20. Photomicrographs of rhyolitic lava unit (sample SM25) found in Schrikkloof Formation. Photos A and B show embayed and resorbed textures of quartz. C and D show euhedral plagioclase crystals (primary) and bulbous recrystallised quartz (secondary). Photos E and F show devitrified glass. Scale bar is 1 mm, A, C and F are taken in cross polarised B, D and E in plane polarised light.

58

6.3.4. Porphyritic rhyolite (sample SM25)

On hand specimen, the porphyritic rhyolite sample SM25 resemble sample SM28 rhyodacite in texture, but the difference is only noticed when analysed geochemically and microscopically. Further, field features (outcrop scale) such as flow banding are observed on SM25 only. Stratigraphically, these units are in contact with unit SM28 found at the base while unit SM25 is on the top. The groundmass of unit SM25 is microcrystalline and brown in colour. Like SM28, SM25 consist of large crystals and crystal fragments of quartz, plagioclase and k-feldspar in almost the same proportion and sizes of phenocrysts. Textures such as symplectite, corona, granophyric and sutured crystals are absent. In SM25 quartz crystals are larger (up to 2 mm) and like SM28 appear to be partially resorbed and embayed. However, SM25 has minor flow banding.
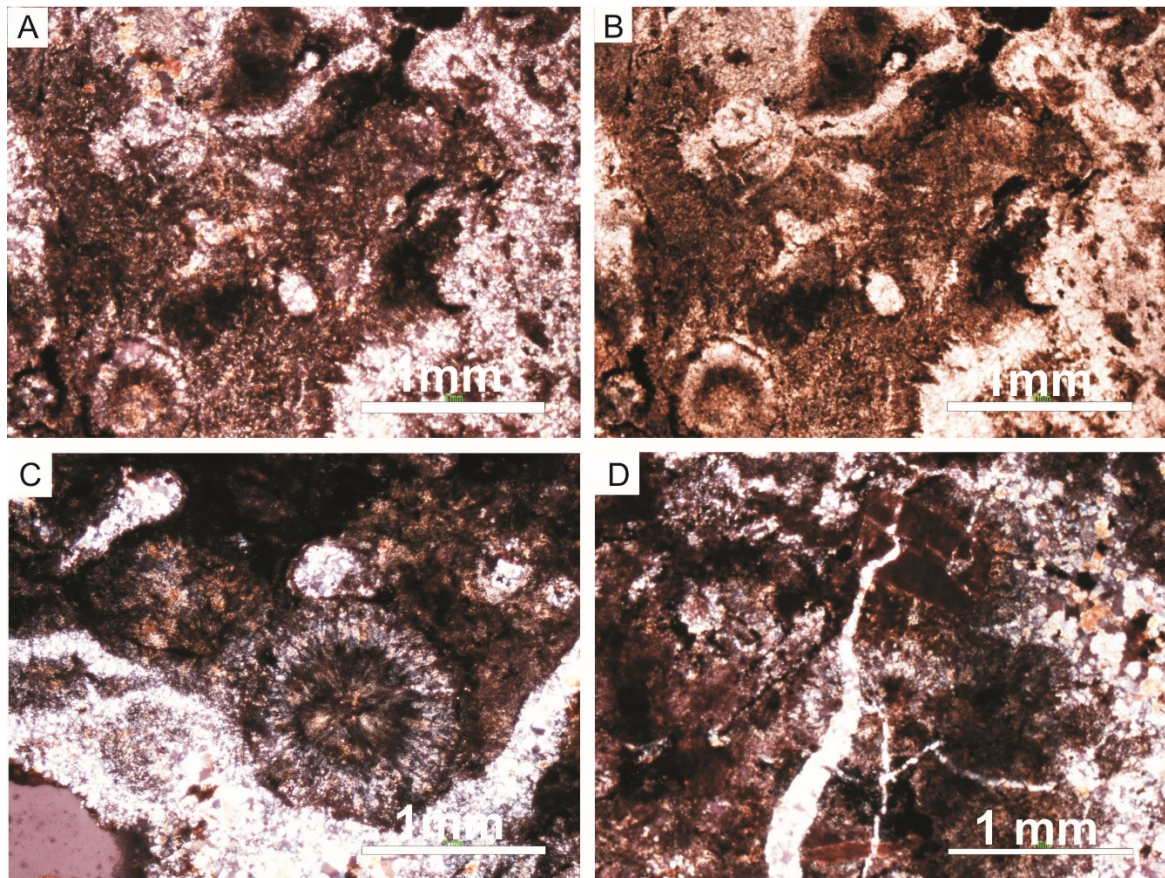
Figure 21. Photomicrographs of rhyodacitic lava (sample SM 22). A and B show spherulitic textures (micro-spherulites size range from 0.5 - 2 mm. D, postdepositional veins cutting the altered plagioclase. C is taken incross polarised light, while A, B and C in plane polar.
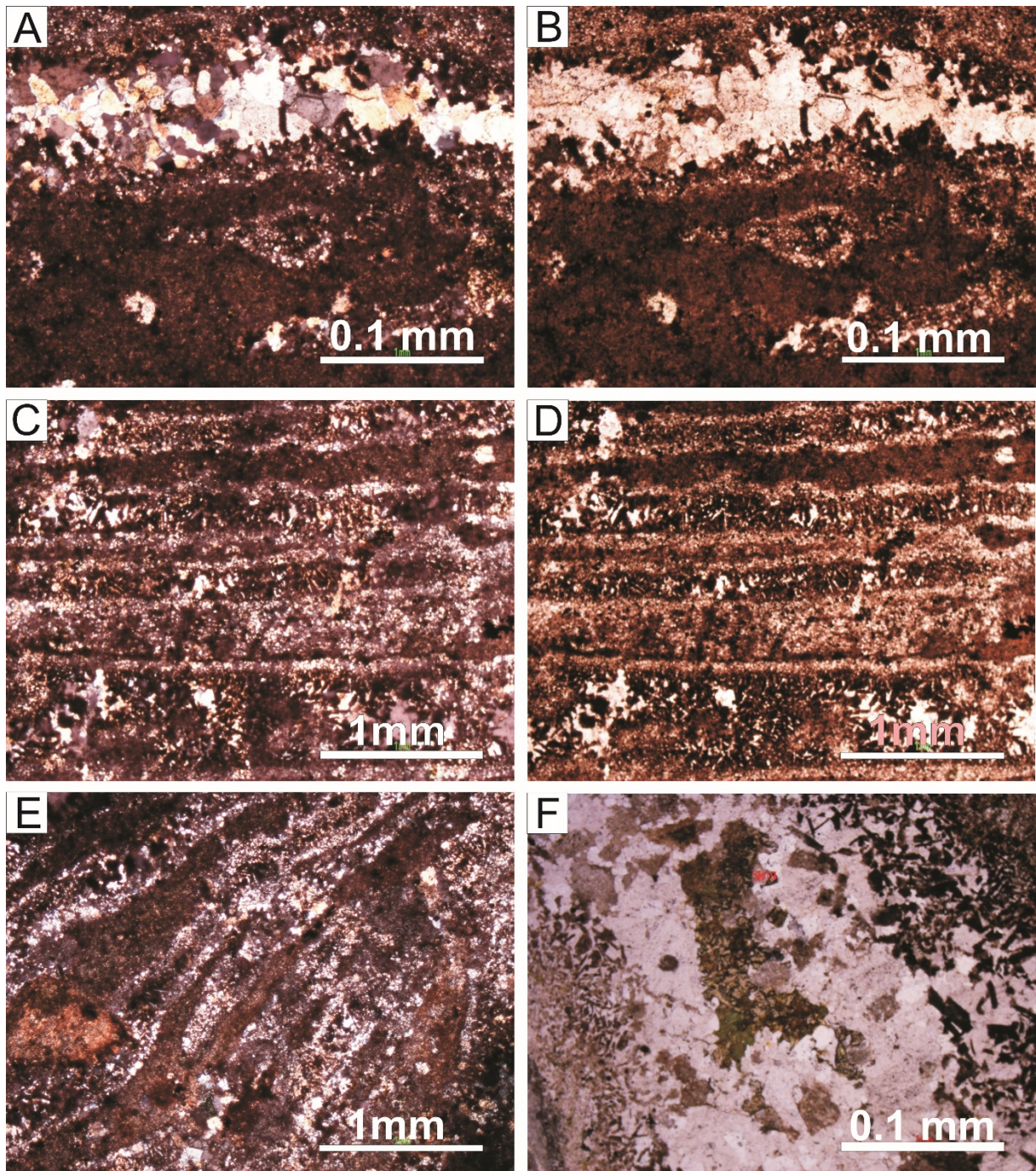
Figure 22. Photomicrographs of rhyolite lava (sample SM19) found in Schrikkloof Formation. This rock show prominant flow banding which is filled secondary quartz and amphibole. A and B shows an 'eye like' structure filled with recrystallized quartz. A, C, E and F are taken in non-polar light while B and D are in polarised light.

6.3.5. Flow banded rhyolite (sample SM19)

Sample SM 19 (predominantly flow banded rhyolite) (figure 37) represent the most abundant rocks in the Scrhikloof Formation. These rocks form the uppermost Schrikkloof Formation. The main lava characteristics include; lobate flows, directional flow banding and contorted

flow banding. The flow bands are filled with recrystallised quartz and minor chlorite. Of note is the 'eye like' structure (figure 22, A and B.). This structure is interpreted to be the stretched bubble produced during lava flow. The groundmass is pink-red and has a cryptocrystalline texture. Minor vesicles are also observed.

7. Geochemistry

Most lava samples experienced relatively low but varying degrees of alteration as can be seen in thin sections and low LOI values. The values of LOI of the samples range from 0.84 wt. % to 2.39 wt. % (average 1.54 wt. %) (table1). During chemical weathering/alteration, the chemistry of a rock may be slightly changed, especially common in Precambrian rocks.

The rocks of the Rooiberg Group in the study area have CIA values of 58.09-58.56 % in the Kwaggasnek Formation, 58.84-59.19 % -55.15-57.08 % Schrikloof Formation. In actual fact, the CIA is used to measure the extent of feldspar group minerals` alteration to form aluminous clay minerals (Nesbitt and Young, 1982) under low temperatures. Peat (1997), suggested that during low temperature alteration progressions, incompatible high field strength elements such as Ti, Zr Y, Nb and Hf are immobile. According to Altermann and Lenhardt (2012), and the refernces therein, CIA values above 90 are the result of removal of alkali and alkaline earth metals and this assume an intensive weathering and alteration of minerals. Fedo et al. (1995), speculate that the CIA values for the unaltered granites are 45-55, while illite and montmorilonite possess values between 75 and 85, indicating less intense weathering and alteration. On the other hand, CIA values close to 100 and mostly indicated by kaolinite and chlorite exhibit severe intense weathering and alteration. The CIA values for the Rooiberg Group lava samples therefore indicate that the lavas are not intensely weathered. Thus, post-eruptive silicification and elemental re-mobilisation processes such as hydrothermal and metamorphic activities minimally altered and changed the chemistry of the Rooiberg Group rocks. During this processes, more susceptible mobile elements are likely to be added or removed (Pearce and Cann, 1973). Despite this fact all previous work compositionally classified the Rooiberg Group rocks based on the plots of the total alkali versus silica (TAS classification scheme).

Low "field strength" elements (Gast, 1972) and elements such as Ca, K, and Na are habitually mobile and susceptible to change during alteration. In order to avoid the effect of alkali mobility, common especially in Precambrian rocks, SiO_2, Ti, Zr Y, and Nb elements are plotted (after Winchester and Floyd, 1977). However, the TAS diagram is also plotted to emphasise the classification errors. As a consequence of post-eruptive silicification which affected the chemistry of the Rooiberg Group rocks, this study strongly, recommends the review of compositional nomenclature of previous studies to be based on the discrimination plots of Winchester and Floyd, (1977).

The volcanic rocks of the Rooiberg Group in the study range in composition from dacites-rhyodacite-rhyolites (figure 23). Figure (23) depict that the Damwal Formation (red cycle) is

62

predominantly dacitic, the Kwaggasnek Formation (green cycles) is rhyodacitic while the Schrikloof Formation (yellow cycles) is predominantly rhyolitic in composition. The change from dacitic to rhyolitic composition is thought to be a result of fractional crystallisation. The criteria used to assign the Rooiberg Group volcanics into distinct formations is described by Hatton and Schweitzer (1995) (see figure 25). The graphs of TiO_2 (wt %) versus SiO_2, MgO, P_2O_5, and Fe_2O_3 total (wt %) show the chemical boundaries that discriminates the Formations of Rooiberg Group (Fig 7). Table 4 and 5, show major and trace elements composition ranges and averages of the Rooiberg Group in the study area (actual compositions are found in the Table 12). The upper Schrikkloof Formation has a higher SiO_2 (>75 wt. % average) content with lower TiO_2 (~0.25 wt. %). In contrast, the lower Damwal Formation shows higher TiO_2 (~0.61 wt. %) and lower SiO_2 (~69 wt. % average), while the Kwaggasnek Formation (between Damwal and Schrikloof) comprises intermediate composition of the former Formations averages of SiO_2 and TiO_2 content of ~74 and ~0.42 wt %.
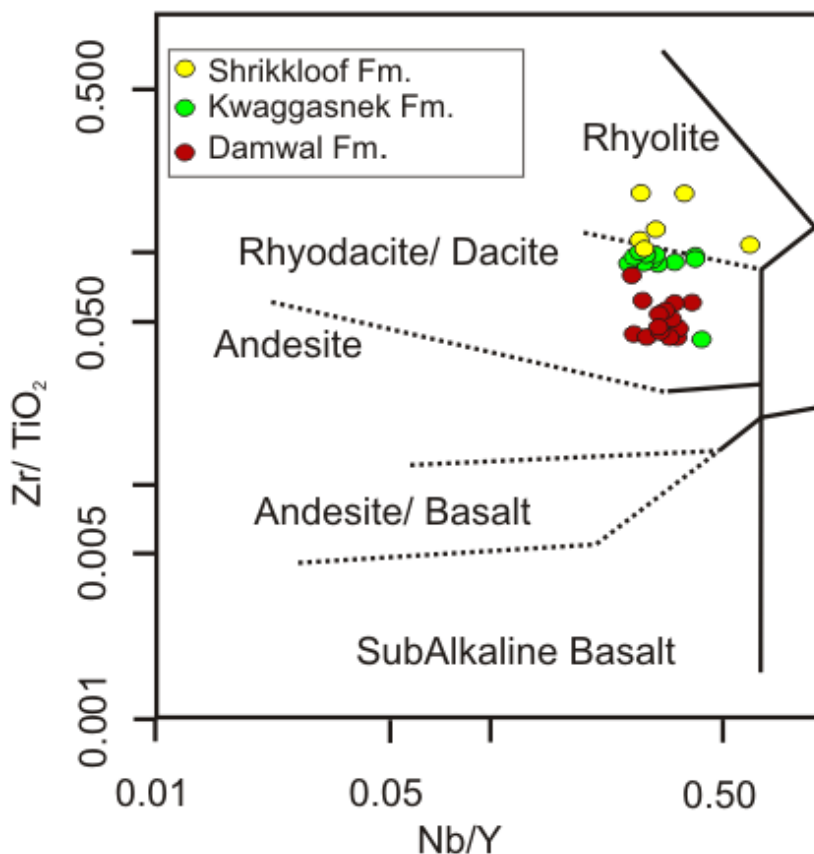
Figure 23. Compositional classification of the three upper Formations of the Rooiberg Group volcanic rocks in the north east of Loskop Dam (boundaries after Winchester and Floyd,

1977). The insert colour legend representing the three formation of Rooiberg Group, apply in all the figures in chapter 7.
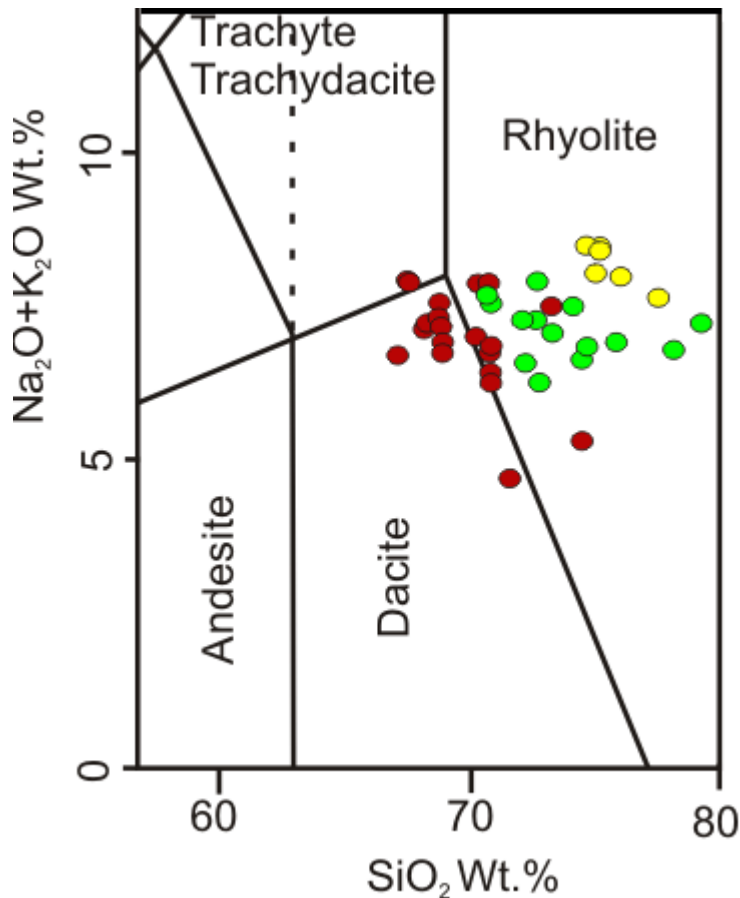
Figure 24. Compositional classification (TAS diagram) of the three upper Formations of the Rooiberg Group volcanics in the north east of Loskop Dam (boundaries after Le Bas et al., 1986).

As observed in the rocks from the Loskop Dam area, there is a negative trend of TiO_2, CaO, P_2O_5, and $FeO_{(t)}$ with increasing SiO_2 (c.f., Jolayemi et al., in preparation). MgO, although not a major constituent in these rocks, shows to some extent a negative trend. However, K_2O, Na_2O_3 and Al_2O_3 (all major constituents of both sodium-rich plagioclase and K-feldspars that have been observed in thin sections) do not show any preferential trend. The initial crystallization of early forming plagioclase and Fe-Ti-rich minerals (±apatite) is responsible for the decrease in TiO_2, CaO, P_2O_5, and $FeO_{(t)}$ with increasing SiO_2. This resulted in the subsequent enrichment of the melt in K_2O, Na_2O_3 and Al_2O_3, resulting in a late formation of sodium-rich plagioclase, K-feldspar and quartz as phenocysts. The REE and trace elements show trends that support partial melting, fractional crystallization, and crustal contamination. Negative anomalies of Ba, Ti and Sr (figure 26a) demonstrate the partitioning ability of these elements during crystallization of feldspars (White et al., 2003). Depletion of the light rare

earth elements (LREEs) and slight enrichment of heavy rare earth elements (HREEs) is depicted by figure 26b. Fractional crystallization is also supported by the negative Eu anomaly as observed by the REE (figure 26b). The negative Eu anomaly is furthermore usually associated with a deep mantle residual melt (White, 1999). A mantle plume origin as suggested for the Rooiberg lavas by various authors (Hatton and Schweitzer, 1995; Hatton, 1995; Buchanan et al., 1999; Buchanan et al., 2002) is supported by the tectonic discrimination diagram according to Pearce et al. (1984) (figure 26). Here, the majority of samples plot in the within-plate granitoid (WPG) field. Only few samples (samples LD013, 014 and 020) plot along the boundaries of WPG and the volcanic arc granitoid (VAG) and syn-collisional granitoid (syn-COLG) fields while few others (samples LD 01 and SM 04.1) plot within the VAG and syn-COLG field. This can be interpreted as a result of crustal contamination (c.f., Pearce et al., 1984). However, trace and rare element signatures such as the negative Eu anomaly are also exhibited by the upper crust (White, 1999) due to fractionation and crystallization of plagioclase as a major mineral phase in the lower crust. Therefore, crustal origin for the Rooiberg Group is again vocalized. Jolayemi et al. (in preparation) proposed partial melting of the crust that underwent fractional crystallization as the origin of the Rooiberg Group. The interpretation of the origin of the Rooiberg Group from partial melt of the crust is based on the variety of both trace and rare earth elements similarities of these volcanic rocks to the upper (continental) crust.
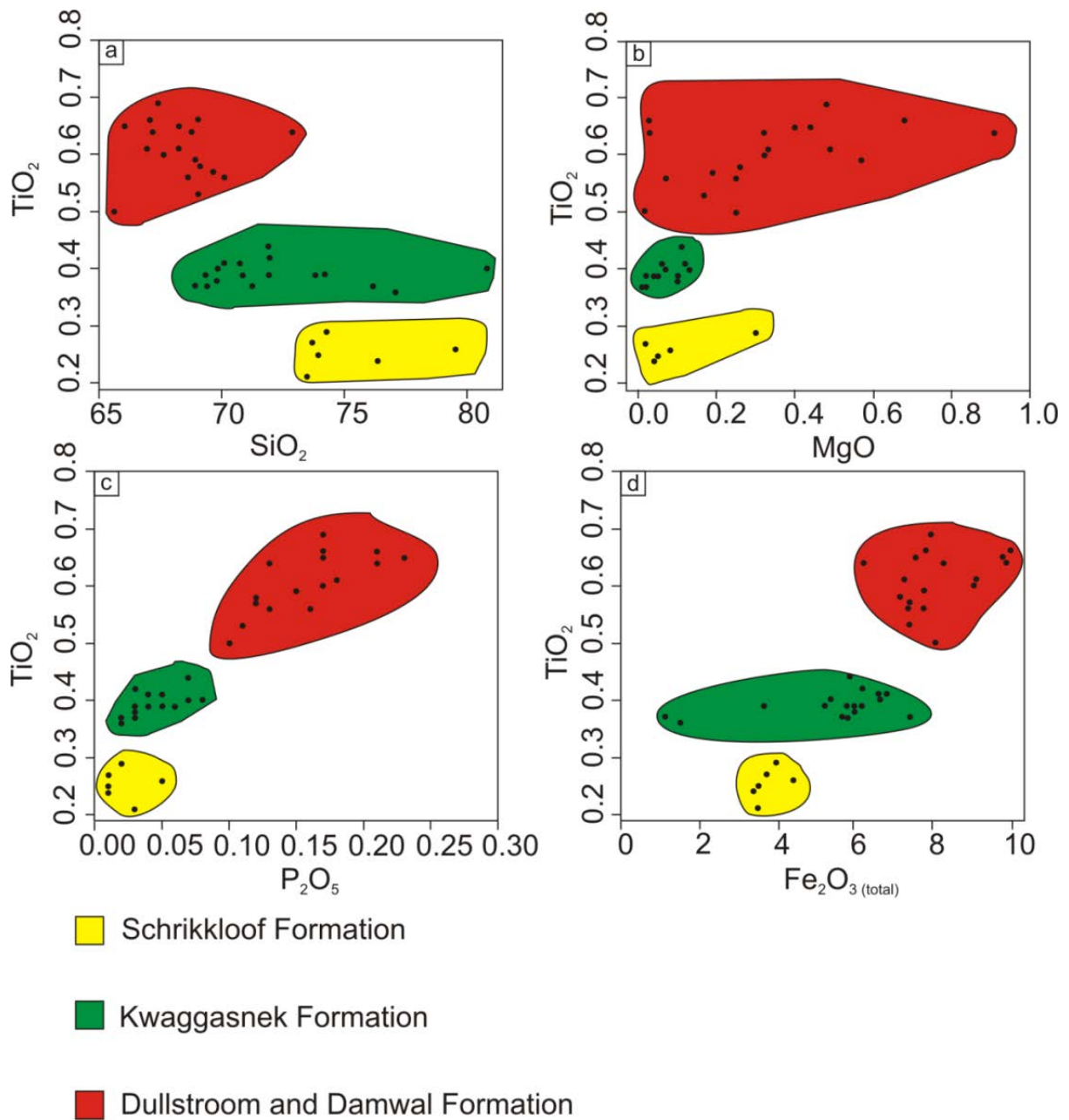
Figure 25. Major element distribution (wt. %) of the Rooiberg Group in the Loskop Dam area. The graphs show clear discrimination of the Damwal, Kwaggasnek and Schrikkloof Formations. Field boundaries (red, green and yellow) are from Hatton and Schweitzer (1995).
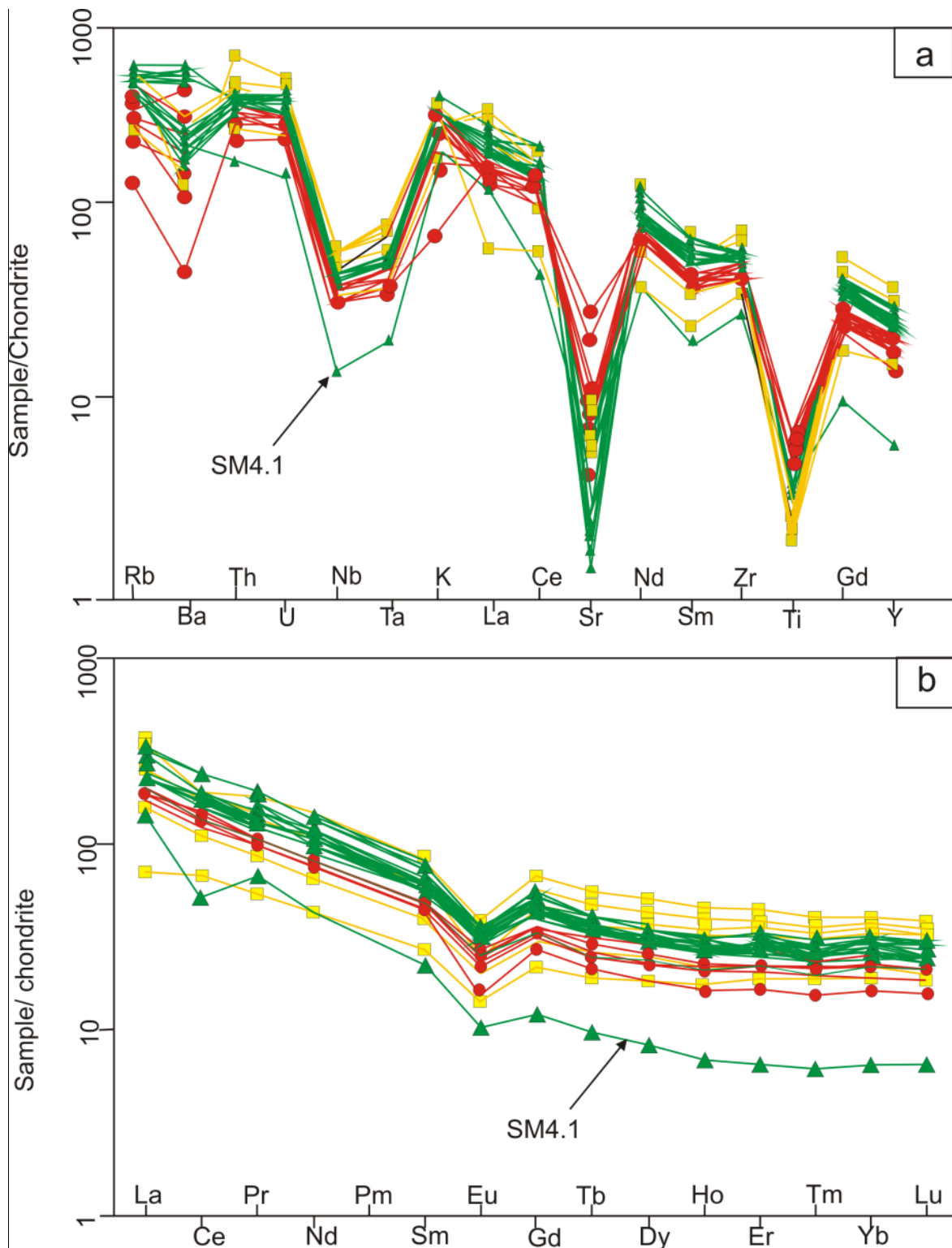
Figure 26. Spider diagrams showing the trace and rare earth (REE) element distribution of the Rooiberg Group rocks in the Loskop Dam area. (a) Trace element distribution normalized according to Sun *et al*. (1980); (b) REE distribution normalized according to Boynton *et al*. (1984). Colours indicate the Damwal Formation (red), Kwaggasnek Formation (green) and Schrikkloof Formation (yellow).
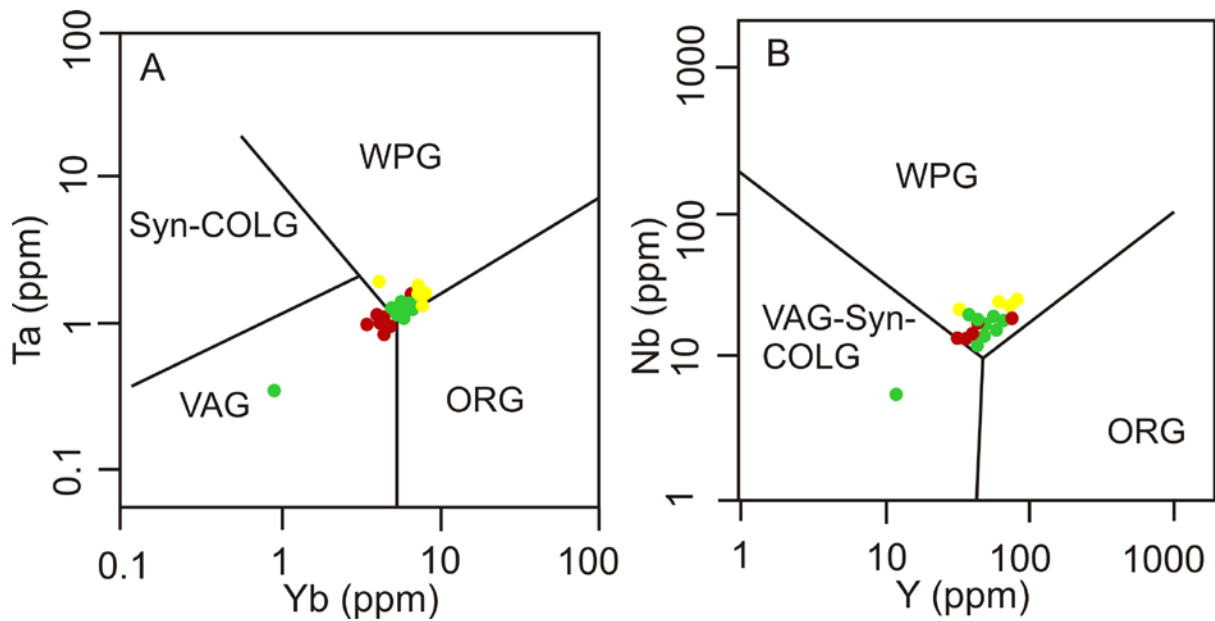
Figure 27. Trace element discrimination diagram according to Pearce *et al.* (1984), showing the tectonic setting of the Rooiberg Group according to (a) Yb vs. Ta and (b) Y vs. Nb discrimination diagrams for granitoids. VAG, volcanic-arc granitoids; ORG, ocean-ridge granitoids; WPG, within-plate granitoids; Syn-COLG, syn-collisional granitoids. A; the VAG character of the Damwal Formation (red plots) is interpreted to be the effects of assimilation of the Kaapvaal Craton`s basement rocks. B; within plate setting is high suggested.

Table 3: Distribution ranges of whole rock composition (trace elements in ppm) in the formations of the Rooiberg Group with calculated mean values for these formations.

Ppm	Schrikkloof Formation (SC)	Kwagganek Formation (KG)	Damwal Formation (DW)	Mean values		
				*SC	*KG	*DV
Li	6.51-17.60	5.3-59.2	52.4-74.66	10.80	26.89	18.71
Sc	0.78-1.63	3.96-4.48	4.90-13.82	0.40	4.24	9.13
V	0.19-8.91	0.30-29.1	1.70-46.15	2.16	9.92	10.33
Cr	0.61-3.40	0.70-57.9	0.39-60.70	1.91	19.78	5.96
Co	107.10-321.70	99-532	54.08-181.60	188	290.32	110.88
Ni	0.60-5.48	0.64-23.5	0.11-15.96	2.33	8.65	5.84
Cu	9.53-41.97	10.9-25.3	7.22-61.20	21.4	17.21	29.16
Zn	62.65132.50	28-164	73.91-216.10	101	88.53	144.71
Rb	103.40-207.40	140-186	54.19-179.80	166	159.77	126.49
Sr	52.95-101.30	57.7-90.5	60.30-353.10	70.33	76.30	144.10
Y	34.93-87.24	12.6-69	32.09-53.16	62.62	46.43	45.57
Zr	226.00-480.00	170-368	269.20-384.80	340.08	297.47	316.46
Nb	13.53-24.20	5.38-18.2	12.94-17.47	20.90	13.85	15.64
Ba	571.30-1269.00	900-997	197.70-1216	918.00	955.80	847.75
La	22.06-117.40	43.6-82.5	57.02-66.08	75.70	66.07	61.64
Ce	54.81-180.50	40.6-150	106.90-138.10	129.67	109.52	121.18
Pr	6.63-22.89	7.74-17.7	12.22-14.41	16.20	13.62	13.34
Nd	25.87-88.69	25.4-66.3	45.31-54.83	61.92	50.76	50.66
Sm	5.27-16.33	4.28-12.6	8.08-10.35	11.50	9.30	9.34
Eu	1.04-2.88	0.73-2.22	1.19-2.25	1.96	1.63	1.79
Tb	0.92-2.63	0.44-1.84	1.02-1.58	1.80	1.29	1.34
Gd	5.64-17.55	3.04-12.0	7.12-10.55	11.54	8.41	8.82
Dy	5.94-16.30	2.53-11.6	5.91-9.83	11.33	8.11	8.29
Ho	1.25-3.27	0.47-2.38	1.18-1.97	2.31	1.65	1.67
Er	3.93-9.25	1.31-6.96	3.52-5.70	6.80	4.79	4.84
Tm	0.61-1.31	0.19-0.99	0.51-0.81	0.99	0.70	0.70
Yb	4.17-8.36	1.31-6.46	3.43-5.35	6.47	4.57	4.62
Lu	0.61-1.22	0.20-0.98	0.52-0.79	0.95	0.69	0.69
Hf	6.69-12.11	4.56-9.53	6.97-10.07	9.1	7.78	8.23
Ta	0.88-1.86	0.45-1.59	0.94-1.32	1.52	1.10	1.12
Pb	10.99-53.06	12.8-33.9	19.03-137.10	29.10	22.52	45.33
Th	15.01-35.10	9.68-21.7	15.81-22.67	24.99	17.21	19.14
U	3.47-7.00	2.17-5.59	3.78-5.31	5.00	4.31	4.73

*(SC = Schrikloof Formation, KG = Kwagganek Formation, DW = Damwaal Formation)

Table 4: Distribution ranges of whole rock composition (major elements in wt%) in the formations of the Rooiberg Group with calculated mean values for these formations.

wt %	Schrikkloof Formation (SC)	Kwagganek Formation (KG)	Damwaal Formation (DW)	Mean values wt %		
				SC*	KG*	DW*
SiO_2	73.72 - 79.54	73.93 - 74.28	66.07 - 72.86	75.22	74.28	68.45
TiO_2	0.21 - 0.29	0.40 - 0.44	0.53 - 0.69	0.25	0.42	0.61
Al_2O_3	7.70 - 12.90	7.13 - 11.59	11.22 - 12.94	11.24	10.04	11.98
Fe_2O_3	3.37 - 4.38	5.35 - 6.78	6.21 - 9.77	3.73	5.99	7.92
MnO	0.02 - 0.08	0.05 - 0.14	0.07 - 0.16	0.05	0.08	0.12
MgO	0.02 - 0.30	0.11 - 0.13	0.07 - 0.91	0.09	0.12	0.38
CaO	0.00 - 0.74	0.00 - 1.04	0.09 - 3.63	0.15	0.65	1.90
Na_2O	1.98 - 3.39	0.01 - 2.47	2.23 - 3.59	2.74	1.60	2.92
K2O	2.97 - 5.73	3.61 - 4.99	1.23 - 5.31	4.72	4.39	3.79
$P2O_5$	0.01 – 0.05	0.05 – 0.07	0.11 – 0.23	0.02	0.06	0.15

*(SC = Schrikkllof Formation, KG = Kwagganek Formation, DV = Damwal Formation)

8. Lithofacies analysis

The Rooiberg Group lithofacies types near Loskop Dam can generally be categorized into syn-eruptive and inter-eruptive deposits (terms derived from Smith, 1991) which define primary and secondary (reworked/epiclastic) deposits respectively. The primary products include all deposits that formed due to either non-explosive or explosive fragmentation and did not undergo any re-deposition such as lava flows and volcaniclastic rocks of all sorts. The secondary or epiclastic deposits include all deposits that are related to reworking of older deposits (including the primary deposits) via debris flow and grain flow processes. The nomenclature for fluvial deposits is derived from Miall, (1985, 1996). The Rooiberg Group stratigraphic section (figure 8) and geological maps (figure 6 and 7) illustrate the general lithofacies distribution. Table 3, 4 and 5 summarises the descriptions, processes and interpretations of varies lithofacies found at the area northeast of Loskop Dam.

Table 5: Descriptions, processes and interpretations of coherent volcanic lithofacies

Lithofacies Code	Lithofacies	Description	Process	Interpretation
DF	Dacitic Coherent	Massive dense aphyric to porphyritic flows; blocky carapace has monogenic angular fragments (2-30 cm in size) arranged in a jig-saw fit pattern; Flow margins are highly concentrated with less collapsed and more rounded vesicles/amygdales; Sparsely distributed microlites groundmass; Flow tops may contain spherulites and lithophysae; Columnar jointing, radial and concentric fractures perpendicular to columnar jointing.	Effusive lava flow	Subaerial flow
RdF	Rhyodacitic Coherent	Massive aphyric to porphyritic flows; Minor vesicles/amygdales; Significant increment of phenocrysts (both size and number) from to the base-top of the sequence. Partially resorbed and embayed quartz crystals.	Effusive lava flow	Subaerial flow
RF	Rhyolitic coherent	Massive aphyric to porphyritic flows; Flow margins are highly concentrated with vesicles/amygdales; Significant increment (both size and number of phenocrysts from to the base-top of the sequence.	Effusive lava flow	Subaerial flow

71

Table 6: Descriptions, processes and interpretations of volcanicaniclastic lithofacies

Lithofacies (thickness) and code	Characteristics	Process	Interpretation
Peperitic Breccia (1-3 m) Bp	Non-stratified breccia, clast-matrix supported, clasts are monomictic, blocky, ragged and made of lava clast that often show jigsaw-textures, Brown colored clasts with non-chilled margins are mostly angular,while others show shard-like structures with curviplanar margins. Clasts are suspended or separated by a matrix of pale-grey massive siltstone.	Mingling of magma with unconsolidated wet sediments, at the margins of intrusions Schmincke, 1967; Spera and Whte, 1987; Kano, 1989; Goto and McPhie, 1996, 1998; Hunns and McPhie 1999; Doyle, 2000; Squire and McPhie, 2002; Galerne et al., 2006)	Subaerial to shallow water deposits, possibly near lakes, ponds and/or rivers
Massive tuff (0.5-1 m) sAT	Coarse ash, dominant crystal grains and minor pumice fragments (all altered). Plagioclase forms the abundant mineral phase, with minor k-feldspar and quartz. Plagioclase crystals are mostly broken, and have the size range of 0.3-0.5 mm (and 2 % vol). Resorption embayments texture on quartz. Original matrix is replaced by cryptocrystalline silica.	Fall from eruption column (Cas and Wright, 1987)	Fall deposit

72

Table 7: Summary of classification of epiclastic lithofacies

Lithofacies Code and thickness	Lithofacies	Description	Process	Interpretation
Sp 0.5- 2 m	Planar-trough cross-bedded sandstone	Planar- trough cross-bedding, coarse to fine grained sandstone; grains are poorly sorted and well rounded. Traces of interstitial mineral phases include feldspar, quartz, rock fragments and opaque minerals	2 D dunes, channel deposit (Miall, 1996)	Braided stream
Sl 0.3-0.5 m	Cross bedded sandstone (low angle)	Low angled (<10°) cross bedding, medium to coarse grained. Poorly sorted and rounded grains	Longitudinal bar deposit (Miall, 1985).	
Sh 0.3-1 m	Horizontally bedded sandstone	Low angle (<10°) cross-bedded sandstone is coarse – fine grained with parallel bedding. Coarse to fine grained. It lacks the parting lineations.	Scour fills (Miall, 1996)	Scour fills
Gm <1 m	Sub-horizontally bedded sandy conglomerate	Matrix-clast supported, poorly defined sub-horizontal bedding, minor clast imbrication		

Table 8: Architectural elements in the Rooiberg Group (northeast of Loskop Dam) (After Miall, 1996)

Symbol	Element	Lithology	Interpretation
CHS	Major ss sheet	Gm, Sh, Sl, Sp	Braided channel
CS	Minor ss sheet	Sh, Sl	Sheet splay

Table 9: Description and field characteristics of chemical sediments (thinly laminated chert)

Lithofacies code	Lithofacies	Thickness (m)	Field characteristics
bc	Bedded Chert	~3 - 10 m	Intercalated lense sandwiched between lava flow and massive fine grained sandstone. Chert is very thinly bedded and with thin laminations. White in colour.

73

8.1. Syn-eruptive deposits

8.1.1. Primary volcanic deposits

The Primary deposits within the Rooiberg Group can be subdivided into three broad classes: coherent volcanic rocks (three lithofacies type), pyroclastic fall deposits (one lithofacies type), and deposits originating from magma-wet sediment interactions (one lithofacies type).

8.1.2. Coherent volcanic lithofacies

Generally, the coherent lavas can be described based on four properties that characterise the rock (McPhie, 1983), i.e. the mineral composition, lithofacies, texture and the degree of alteration based on alteration minerals as summarised in (Tables 13 – 16). These lithofacies with felsic composition defines three sub-classes of coherent volcanic lithofacies (terminology after McPhie et al., 1993) namely the dacitic coherent lithofacies, the rhyodacitic coherent lithofacies and the rhyolitic coherent lithofacies.

The coherent lithofacies has a dense, mostly massive emergence and shows red-pink-brown to grey-black colours. These massive lava flows have the thickness range of ~20-450 m. Clubley-Armstrong (1977; 1980) pointed out that multiple lava flow units are commonly hundreds of meters to more than a kilometre in thickness, without any variation in a rock type. The primary textures range from aphyric to porphyritic and lava features such as amygdales, vesicles, spherulites, and lithophysae are frequently observed. Occasionally, the top of the flow units show planar to contorted flow banding and is locally highly amygdaloidal. This lithofacies is interpreted as massive lava flow [i.e. lava flow lithofacies, (LF)].

Figure 28. Massive, dense lava outcrop of the coherent volcanic lithofacies. Scale: the person is 1.4 m tall.

Figure 29. Coherent volcanic lithofacies outcrop. Scale: the person is 1.7 m tall.

75

8.1.2.1. Dacitic coherent lithofacies (DF)

Description: The dacitic coherent lithofacies is characterized by SiO_2 contents, ranging from 65.65 – 69.67 wt.% (average of 68.37 wt.%), and it has varying colours, ranging from pinkish to greenish grey. Cooling units attain a maximum thickness of 350 m. Single flow units are very hard to identify in the field and could only be observed locally. In the majority, this lithofacies is characterized by massive, dense lava. Also good estimation of lava flows is assumed from the presence of spherulites and concentric pseudospherulites. Only locally, a rubbly carapace could be noticed at the base and around the dense core. The sparsely vesiculated carapace is made of angular fragments (2 – 30 cm) arranged in a jig-saw fit pattern. The dense core exhibits occasional columnar jointing, and radial and concentric fractures perpendicular to columnar jointing. Were visible, this lithofacies exhibits irregular contacts to the underlying lithology. Locally, DF can vary from porphyritic, non-vesicular (figure 30 and SM 17) (generally at the base of a unit) to porphyritic, vesicular, and non-porphyritic (aphyric), vesicular dacite, depending on the varying amounts of phenocryst and vesicle / amygdale content. Phenocryst contents generally range from 5 - 40%. They exhibit euhedral to subhedral shapes and mainly consist of plagioclase (0.25 - 2 mm), k-feldspar (perthite) (0.2 – 1.0 mm), and minor quartz (0.5 - 2 mm). The matrix of DF is characterized by a microcrystalline texture comprising plagioclase and quartz as the dominant minerals, with minor k-feldspar, enstatite, diopside and chlorite, which could also be reported from x-ray diffraction analysis and may be an indication for greenschist metamorphism. Locally, spherulites made of radiating fibers of k-feldspar, quartz and probable quartz polymorphs, ranging in size from 0.5 - 2 cm, and lithophysae can be observed. Spherulitic texture is generally present at the base and the flow of thicker units. Very often, the spherulites are associated with perlitic fractures. Towards the top of a unit, an increase in vesicle size can be noticed. The vesicularity of this lithofacies usually ranges from 3 – 20 % and is characterized by well-rounded and elongate amygdales. The amygdales are mostly filled by quartz and phyllosilicate minerals.

Interpretation: The dacitic coherent volcanic lithofacies is interpreted as the deposits of subaerial lava flows. The massive to brecciated units display the attributes of a coherent flow in which autobrecciation processes were prevalent and produced breccia during flow advance (Bonnichsen and Kauffmann, 1987; Lenhardt et al., 2011). The locally preserved carapace suggests an origin from lava flows that may be described as rubbly pahoehoe (Keszthelyi and Thordarson, 2000; Santos Barreto et al., 2014) to a'a flows. The concentric zones of

lithophysae may reflect crystallisation pulses (Breitkreuz, 2013). Perlitic fractures reflect post-depositional hydration (McPhie et al., 1993). Higher temperatures and alkali rich solutions result in high rates of hydration. Inferring from the geometry of the concentric banding in relation to columnar joints, the radial and concentric fractures are not related to flow patterns but rather to thermal contraction during rapid cooling (Palinkaš et al., 2008; Pilote et al., 2012).
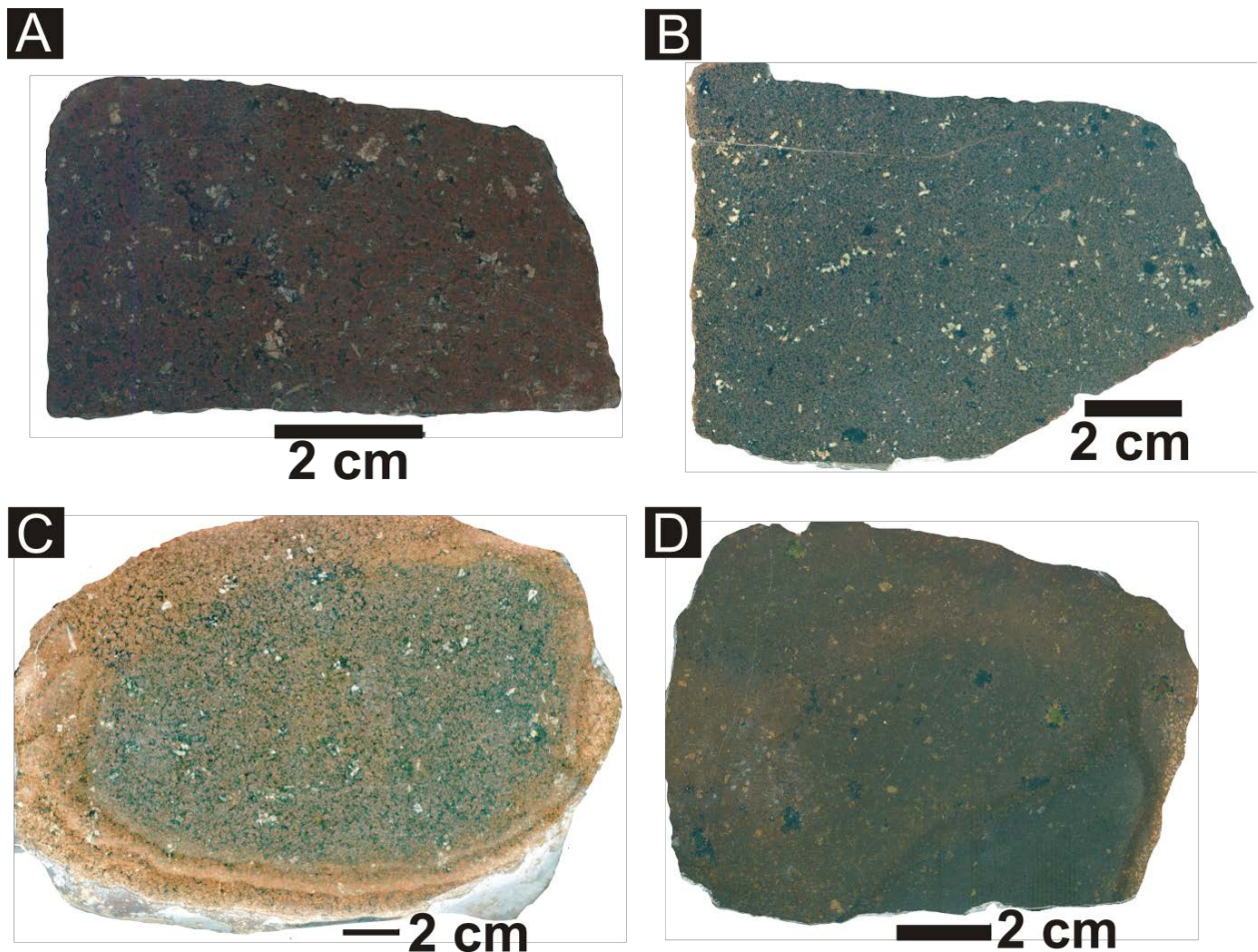
Figure 30. Macrographs of polished slabs of rocks, showing sparsely porphyritic dacites. A, B and C show clustered arrangement of feldspar phenocrysts. D shows sparcely distributed feldspar phenocrysts. A has spherulites, in thin section it also shows pseudospherulites.
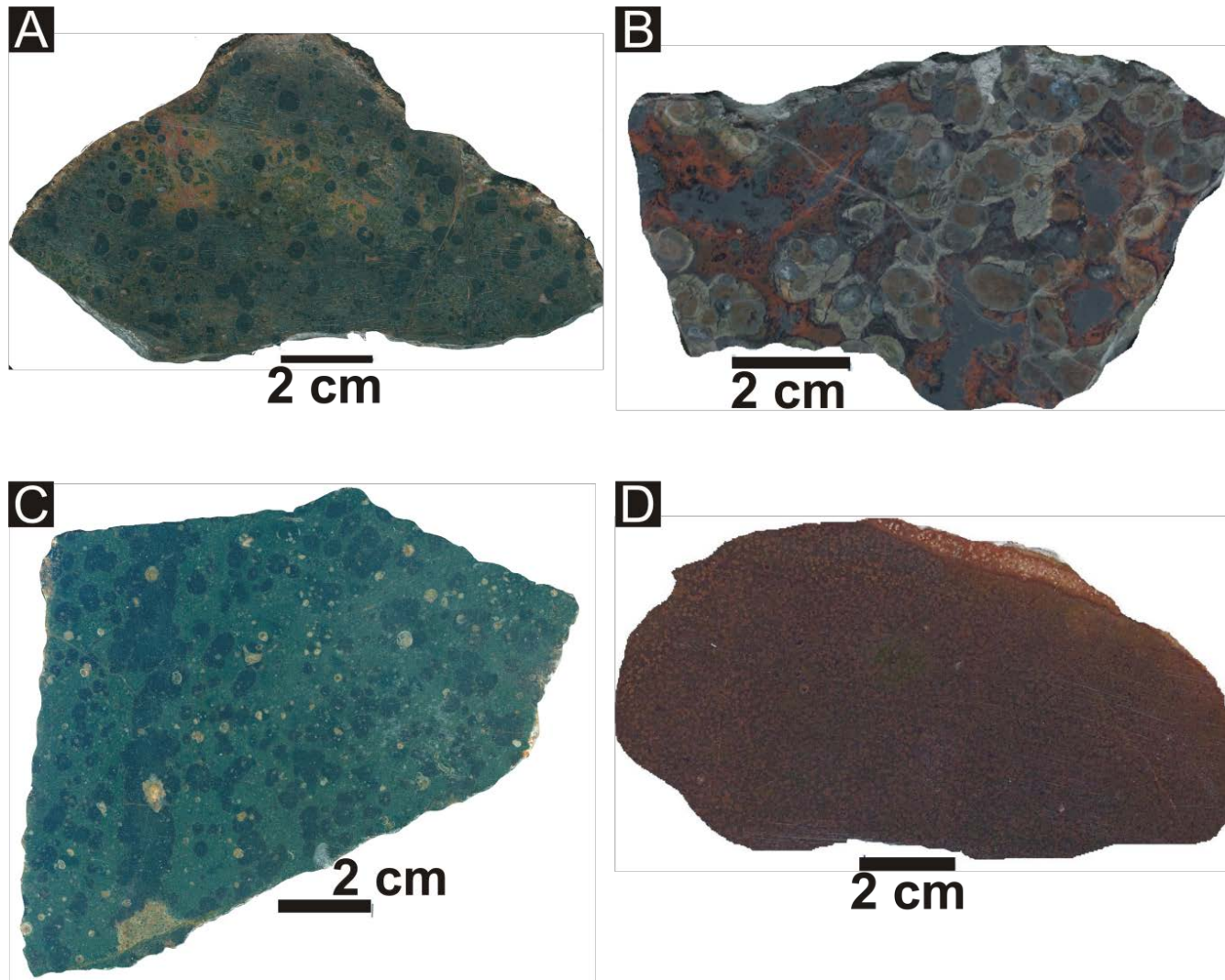
Figure 31. Polished slabs of spherulitic dacites. D, pseudospherulites. C, spherulites and quenched crystal fragment. Note the elongate band of spherulites produced by adjacent spherulites impinging on each other.
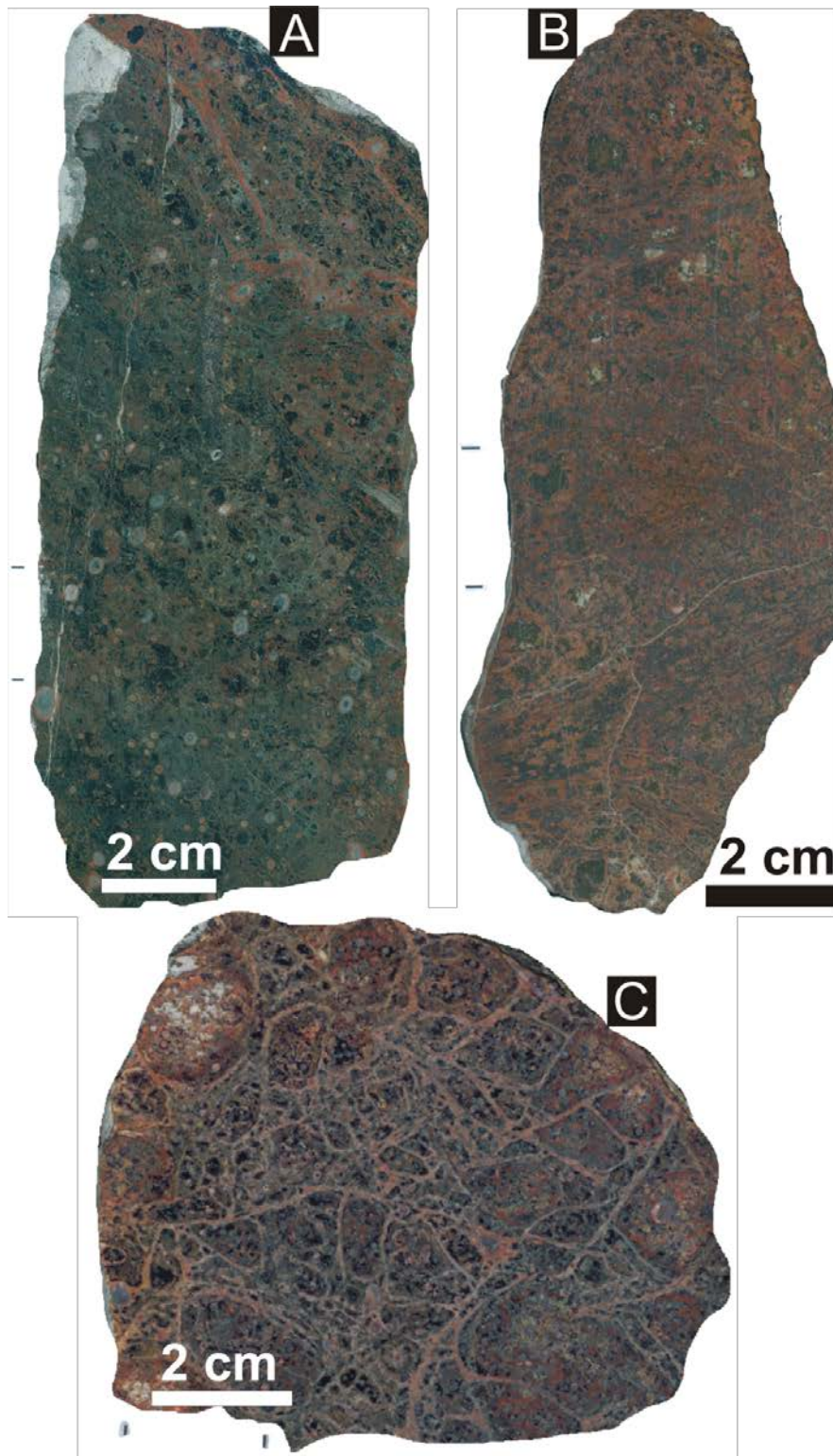
Figure 32. A, B and C depicts polished slabs of perlitic dacites. Picture A shows zoned amygdales and haematitic fractures. A and B show banded perlites while C, shows classical perlite.

8.1.2.2. Rhyodacitic coherent lithofacies (RdF)

Description: The pinkish-red to grey rhyodacitic coherent volcanic lithofacies exhibits SiO_2 compositions between 68.94 - 77.08 wt.% (average 72.95 wt.%) SiO_2, and attains thicknesses, ranging from ~10-50 m. It appears massive and dense, and unlike DF lacks a brecciated carapace. Textures of this lithofacies can vary between vesicular, sparcely porphyric, and non-vesicular, porphyritic. Rare pseudospherulitic textures are also observed. The vesicular, sparcely porphyritic units usually have a phenocryst content of up to 5%, dominated by plagioclase and k-feldspar. Possible upper flow margins are characterized by high accumulations of amygdales (figure 35). The non-vesicular, porphyritic rhyodacites units are characterized by phenocryst contents, varying between 5-35%. The phenocrysts dominantly comprise of plagioclase, k-feldspar and quartz with crystal sized ranging from 1 mm to 3 cm. All phenocrysts of this lithofacies appear to be subhedral to euhedral. The quartz crystals may show signs of resorption at its rims and internally. Minor flow banding can be observed at the flow tops (figure 36). The vesicle content ranges between 5 and 20%. The amygdales are usually round but can also exhibit amoeboid shapes. They are general filled wih quartz. Like DF, this lithofacies shows irregular and conformable contacts to the underlying rocks.

Interpretation: The rhyodacitic coherent volcanic lithofacies can be interpreted as the deposits of subaerial lava flows. As no carapace or other surface feature are visisble or preserved it is hard to say if the lava was in a form of a pahoehoe, aa or blocky lava flow. Nevertheless, due to the possible division into non-vesicular, dense and vesicular parts of the flows, one can differentiate between the dense core and the possible upper or lower margins of the flow (c.f. Aubele et al., 1988; Óskarsson and Riishuus, 2013). The embayment and resorption textures of quartz have occured in response to rapid decompression during the magma ascent (Simões et al., 2014).

Figure 33. Images of rhyodacitic coherent lithofacies (A and C). (A, SM10) sub-vertical cooling joints; (B) Noteworthy is the thermal overprint of the bedding of sandstone (quartzite) (C, SM22) show massive dense core of the lava flow.
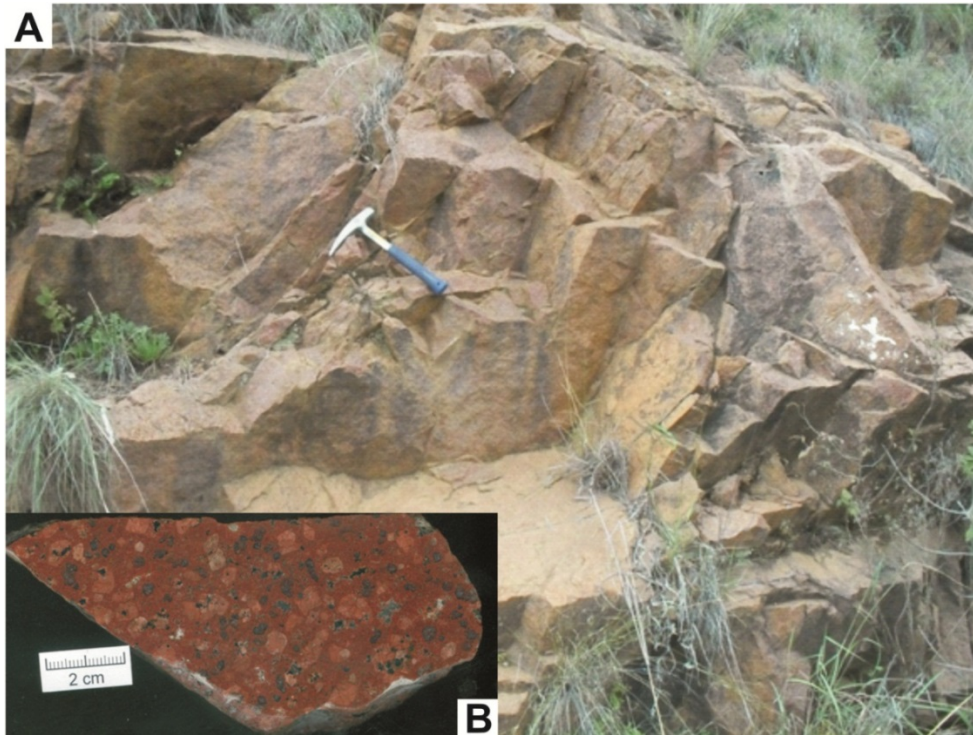
Figure 34. Picture A shows a macrograph of massive rhyodacitic lava. The insert picture B is a polished slab of sample SM28, showing porphyritic texture.

Figure 35. Handspecimen of amygdaloidal rhyodacitic lava. The amygdales are mainly rounded. The spherical characteristic of vesicles is normally associated with pahoehoe lava flows and indicates that gasses were still exsolved when the lava solidified. The coin is 2.3 cm in diameter.

Figure 36. Macrograph of rhyodacite. This picture shows minor flow banding in the rhyodacitic rocks.

8.1.2.3. Rhyolitic coherent lithofacies (RF)

Descriptions: The rhyolitic coherent lithofacies attain 20 to 500 m in thickness and mainly found but not restricted to the southern region of the study area. The brown-pink and brown-grey, rhyolitic coherent lithofacies is characterised by SiO_2 content ranging between 76.37 – 73.47 wt. % (average of 74.37 wt. %). The basal, quartz-feldspar phyric rhyolite (up to 35 % phenocrysts content) is massive and lack vesicles/amygdales. The phenocrysts have a size range from 0.5 – 2 mm. The top flows are non-porphyritic, rhyolites (SM 18.1 and SM 19) displaying red-pink colour, exhaustively wavy flow banding, and quarts filled amygdales. The amygdales display both rounded and minor amoeboidal shapes. The main lava characteristics include; lobate flows, directional flow banding and contorted flow banding (figure 37, B and C) are filled with secondary quartz crystals. Associated with flow banding are the 'eye like' structures filled with quartz. Most textures are of this facies are dominated by micro-spherulites and pseudospherulies.

Detailed textures of each unit are described in chapter 5 (rock units: SM 25, SM 19, SM 18.1, and SM 5.2).
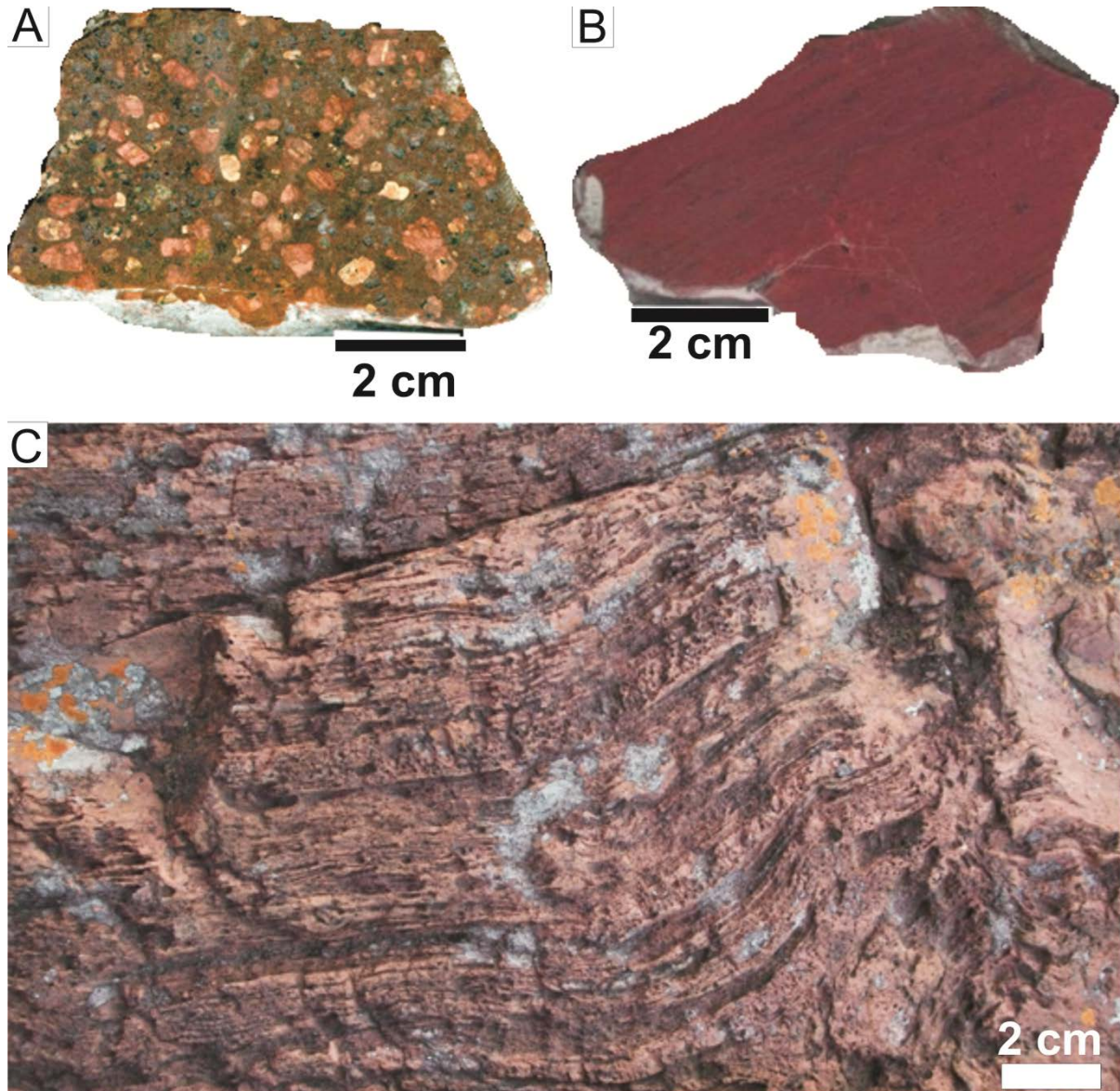
Figure 37. Rhyolites of the Schrikkloof Formation. A and B are polished slabs. A shows porphyritc texture while B shows flow banding aphyric texture. C depicts outcrop macrograph of B.

Interpretation: Like for the two coherent volcanic lithofacies before, an origin from subaerial lava flows is suggested for this lithofacies. The mostly aphyric nature of this lava suggests fast cooling. The prominent flow folding is generated during stretching, shearing and attenuation during flow (Cas and Wright, 1987). The 'eye like' structures are interpreted to be

the stretched bubble produced during lava flow with the sharp end of the bubble orientated perpendicular to the flow.

8.1.3. Volcaniclastic lithofacies

8.1.3.1. Massive stratified tuff lithofacies (sAT)

Description: The pinkish-brown massive, stratified tuff lithofacies is characterized by relatively thin, horizontal beds, attaining thicknesses of ca. 10 cm. It consists of fine- to medium-grained ash particles with rare volcanic lithic fragments (up to 0.5 mm). However, in thin-section, moderately- to well-sorted coarse ash particles, predominantly consisting of crystals (50 %) and subdominant pumice fragments (5 %), of same size. Although all particles appear altered, it can be seen that plagioclase forms the most abundant mineral phase with minor k-feldspar and quartz. The plagioclase crystals (30 %) are mostly broken and have the sizes ranging from 0.3-0.5 mm. K-feldspar (0.1-0.3 mm) is rarely found but whenever it is encountered it also appears mostly broken. Resorption embayment texture is observed on the quartz crystals (0.3-0.5 mm) within thin-sections. The original matrix is almost completely replaced by cryptocrystalline silica.

Interpretation: The fine parallel bedding of this lithofacies, together with the good sorting and lack of larger fragments lead to the interpretation of this tuff as pyroclastic fall deposit (Cas and Wright, 1987). Due to the high crystal content, this lithofacies can be described as crystal tuff (c.f., Cas and Wright, 1987). Crystal tuffs have been described as the near-vent ash-fall deposit produced from crystal-rich magmas during explosive eruptions (Cas and Wright, 1987). The localized preservation of the pyroclastic fall deposits within the study area may have depended on the rapid accumulation of a protective cover, either as reworked or additional primary volcanic material (c.f. Lenhardt et al., 2011).
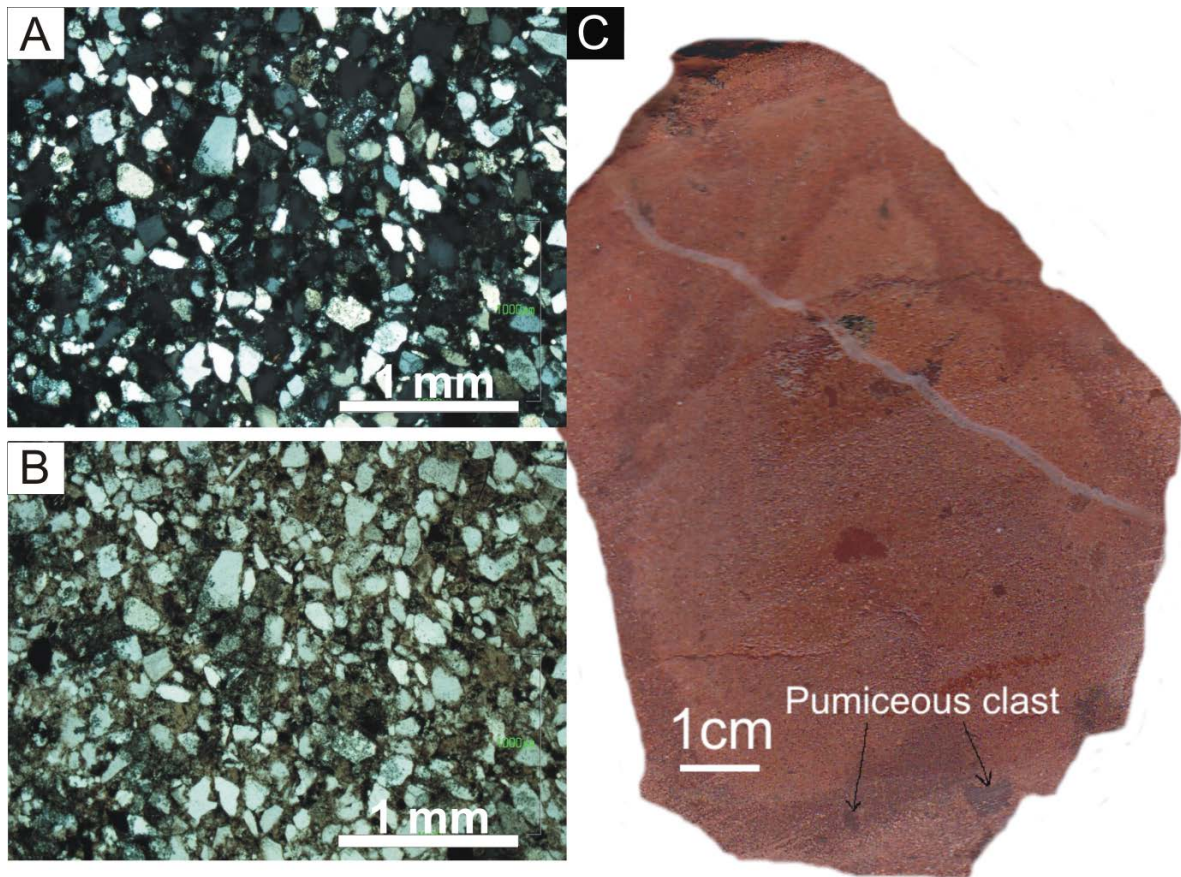
Figure 38. Photomicrographs of massive tuff in Damwal Formation. A and B in polar and non-polarised light (SM4.1). The crystals of quartz and feldspar crystallised prior to eruption.

8.1.3.1. Peperitic breccia lithofacies (Bp)

Descripion: The peperitic breccia lithofacies is non-stratified and attains thicknesses of up to 3 m in the field. It appears clast- to matrix-supported and contains monomictic, blocky, ragged clasts of lava (1-8 cm in size), set in a matrix of pale grey to beige, massive siltstone. The clasts do not have chilled margins and include angular and shard-like clasts with curviplanar margins that often show jigsaw-textures.

The peperitic breccia forms a complex contact with fine-grained, veined sandstone-siltstone and has no definable contact with lava. A clear grading, which is defined by an increment of the matrix from the base up is observed.

Interpretation: This lithofacies is interpreted as peperite. Peperites form due to mingling of magma or lava with poorly consolidated wet sediment, i.e. at the margins of intrusions (Kano, 1989; Goto and McPhie, 1996; 1998; Hanson and Hargrove, 1999) or the base of lava flows (Schmincke, 1967; Hunns and McPhie 1999; Luchetti et al., 2014; Zhu et al., 2014), possibly near lakes, ponds and rivers. The magma, in contact with wet sediment was interrupted by

86

quench fragmentation processes where the quenched debris and the wet sediment may be dynamically mixed. During this complex process, turbulent mixing of wet sediment and quenched debris may occur mainly due to superheating of pore water resulting in boiling and fluidized aggregates (Kokelaar, 1982). The jig-saw textures of the blocky peperite suggest an *in situ* fragmentation of the Rooiberg magma (c.f., McPhie et al., 1993). The former is achieved during quench fragmentation of the magma and/or mild phreatomagmatic reactions as the *domino effects* of break-down of the insulating vapour films at the magma/wet sediment (Cas and Wright, 1987). The blocky peperite forms when the magma was cooler and had high viscosity (Goto and McPhie, 1996).
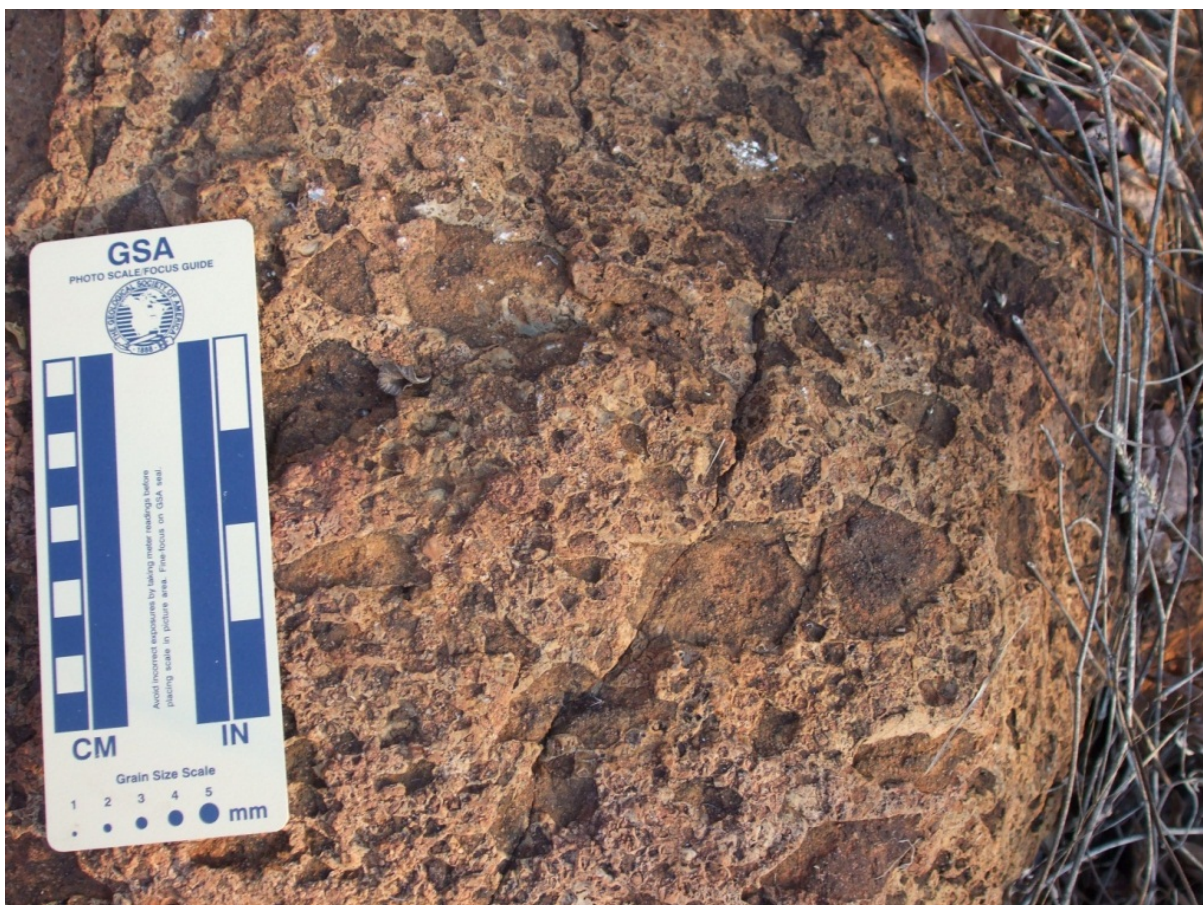
Figure 39. Photomacrograph showing peperitc breccia. The breccia is made of monomictic, blocky, ragged lava clast. Clasts are suspended or separated by a matrix of pale-grey siltstone.

8.2. Inter-eruptive deposits

8.2.1 Epiclastic lithofacies

Epiclastic deposits occur as succession of continuous and discontinuous sandstones, pebbly sandstones and basal conglomerates comprising a thickness of up to 1-5 m. Elsewhere within Rooiberg Group, sandstone interbeds vary in thickness from a few meters and to a maximum of 100 m (Wolhuter, 1954; Clubley-Armstrong, 1977; Eriksson et al., 1994). In the Loskop Dam area these sedimentary interbeds can be followed along strike up to about 10 km. Individual sandstone outcrops are, however, fairly small, with exposed thickness seldom 1-5 m, making it difficult to establish vertical successions. Many of the sandstones are recrystallized to quartzite.

8.2.1.1. Lithofacies Sp: Planar trough cross-bedded sandstone

Description: The planar cross-bedded sandstone lithofacies (05 - 2 m) is the most abundant facies (figure 40). Physically, this facies has a white to light-brown colour and consist of quartz, feldspar, minor rock fragments, matrix material and opaque mineral phases in extensive variations throughout the succession. The lithofacies form planar cross-stratification beds of 0.7 - 1 cm with local planar laminae with parting lamination occurring on bedding planes. The bounding surfaces have discontinuous ridges and troughs. The sandstone shows well rounded and overall poor sorting textures. Authigenic crystal overgrowth and intergrowth of quartz, due to contact metamorphism, are present in thin sections. Grain size is dominantly in the medium to fine sand ranges. Generally, feldspar is more abundant in the finer-grained sandstones and ranges in content from 3-6 %. Rock fragments are form 2-5% of the rock, are sub-rounded to sub-angular and elongate to spherical in shape. Pebbly sandstones and conglomerates layers are present locally at the bases of repetitive upward fining cycles of several meters thickness

Interpretations: Generally, cross bedded sandstone lithofacies association is interpreted to have formed from the migration of bedforms and the infilling of erosional scours in shallow braided streams (Picard and High, 1973; Cant and Walker, 1975; Miall, 1977; 1978; Rust, 1978; Miall, 1996). Planar cross-bed forms are the products of upper flow regime (Allen, 1963; Miall, 1996). Planar or flat laminae are due to the migration of low relief bed forms (2-D dunes). Parting lineation or rather stream lineation/primary-current lineations are created by small longitudinal vortices at the base of the inner turbulent layer (Miall, 1996). Trough

cross-bed is interpreted be produced by sinuously crested and linguoid (3-D) dunes within fluvial channel.

Figure 40. Planar-trough cross bedded sandstone. See the edge of the geological hammer (10 cm) for scale.

8.2.1.2. Lithofacies Sh: Horizontally bedded sandstone

Description: The horizontally bedded sandstone facies has a thickness of 0.3 - 1 m. The individual horizontal beds vary from 1 – 9 cm. This facies is characterised by thin beds of sandstone that are coarse - fine grained (figure 41). The bedding planes carry flat, parallel lamination with primary-current lineation.

Interpretations: Lithofacies Sh, is interpreted to represents movement of larger bedforms (Cant and Walker, 1975; Collins, 1996). According to Collins (1996), when this facies is medium to fine grained and does not contain mica, it represent the upper flow regime (sheet floods). Flat, parallel laminations with primary-current lineation hosted by bedding plane are produced by small longitudinal vortices at the base of inner turbulent layer (Miall, 1996).
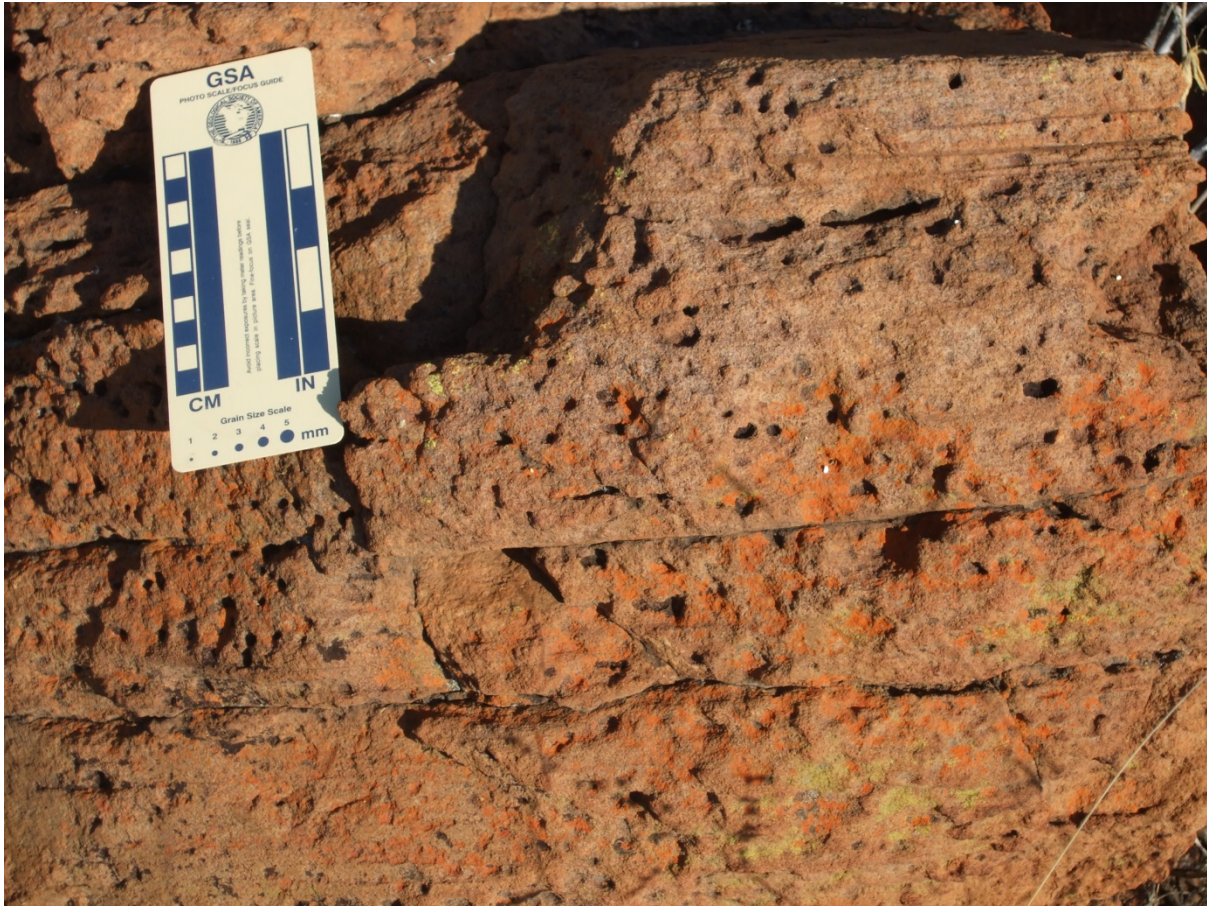
Figure 41. Horizontally bedded sandstone. Fine to coarse grained textured.

8.2.1.3. Lithofcies Sl: Low angle (<10º) cross-bedded sandstone

Description: The lithofacies Sl: Low angle cross-bedded sandstone is coarse – fine grained with parallel bedding. The beds have thickness of 1 – 4 cm. The coarse to fine grained and parallel bedding nature are similar to those of lithofacies Sh, except that it lacks the parting lineations observed from lithofacies Sh. However the lithofacies Sl has a very low angle estimated at lower than 10º.

Interpretation: This facies is interpreted to be the product of migration of low-relief bedform (Miall, 1996).

90

Figure 42. Low angle crossbedded sandstone. See a coin (diameter 2.6 cm) for scale.

Figure 43. Sub-horizontally-bedded conglomerate. The clasts are semi-rounded and composed of sandstone, quartz and chert.

8.2.1.4. Lithofacies Gm: Sub-horizontally-bedded conglomerate

Description: The 0.2-06 m thick conglomerate facies association form normal upward-fining units. The latter upward fining amalgamated units comprise of the basal conglomerate form normal grading that extentends to pebbly sandstone.

The lowermost clast to matrix supported conglomerates deposit (40 cm - 1 m), comprise sub-horizontal stratified conglomerate displaying light-brown colour and consisting of sandstone lithics and minor chert pebbles. Individual bed forms stacks of ~10 cm each. The pebbles and lithics (2 to 8 cm) are angular to sub-rounded and cemented by sand size matrix. Few sub-rounded sandstone cobbles (70 mm sized) are also observed in a sandy matrix. The overall arrangement of clasts display minor imbrication.

The uppermost horizontally stratified pebbly sandstone displaying a gradational contact with the lower conglomerate is characterised by mostly angular chert and minor sandstone pebbles (<3 cm).

Interpretations: This facies is interpreted as longitudinal bar deposit (Miall, 1985). Transport and deposition take place by traction and very limited or no suspension in a turbulent current, producing crude stratification and clast imbrication hence the system is a mesoform occurring in a proximal braided system (Nemec and Postma, 1993; Reading, 1993).

8.3. Lithofacies CT: Chemical sediments (Bedded chert)

8.3.1. Bedded chert facies

Description: The bedded chert facies is restricted to the upper Damwal Formation, interbedded within the dacitic rocks and also in contact with minor fine sandstone lens without notable sedimentary structure. The bedded chert facies can be traced along strike for at least ½ km in the east-west direction. Its thickness ranges from 1-2 m. This facies consist of thinly bedded chert, white in colour with black-reddish (opaque) thin lamination. The laminations consist of scoured opague minerals, heamatite and probable goethite. This bedded chert is largely composed of microcrystalline or cryptocrystalline quartz. Polycrystalline quartz appears as either thin veins or rare clusters randomly in a microcrystalline chalcedony matrix and other silica polymorphs. Chalcedony is recognised by its fine radiating structures.

Interpretations: This facies is interpreted as inorganic precipitation of a silica gel in closed lake basin mainly due to its association with volcanic rocks and fine sandstone (Blatt et al.,

1980; Eriksson, et al 1994). Hickman (1983) described and interpreted the red, white and bluesh layering (laminations) in bedded chert of to be caused by slight changes in Eh, pH and geological setting during inorganic precipitation of a silica gel from waters enriched in silica by magmatic solutions. Pure white colour of chert is attributed to a relatively high content of extracrystalline water (Blatt et al., 1980).

Figure 44. Shows a polished slab of thinly laminated chert. Note the white and reddish parallel lamination.

9. Discussion

9.1. The palaeoenvironment of the northeast Loskop Dam

The facies analysis provides a clear record of volcanism and concomitant sedimentation. The lithofacies analyses, together with information gained during mapping are used to reconstruct the depositional environment as summarised by figure 45. The environment was dominated by volcanic activity over large areas, accompanied by concomitant short-lived fluvial sedimentation with localised lake environment. Syndepositional tectonics and the volcanic activity were the main controlling factors during fluvial sedimentation. The stratigraphic section records various facies sequences indicating sequential changes in volcanic eruption and sedimentation. These sequential changes in volcanic eruption and sedimentation show syn- and inter- eruptive sedimentation as marked by volcaniclastic and epiclastic, depositional processes.

Effusive volcanism, affecting tectonic development, produced abundant extrusive felsic material. This volcanic activity has alternated rapidly with some periods of volcanic quiescence, as indicated by the thin intercalated siliciclastic sediments deposited by braided rivers and blanketed by flash floods. Lake conditions and composition allowed and encouraged the formation of laminated chert. Lava was extruded in an active water system, producing peperitic deposits. Volcanic units present no easily recordable proximal to distal variations, but single lava flow display relatively uniform textures, compositions and thicknesses.

Lava flows were effusively deposited over a large area with minor explosive eruptive character in a subaerial setting. Minor crystal-rich tuff layers also suggest that the pyroclastic material occurred in a subaerial environment (Asvesta and Dimitriadis, 2010). During the times of volcanic eruptions, the Rooiberg Group was a topographic basin as indicated by thin intercalated sediments characterising relative time of quiescence. The fluvial sediments, such as basal conglomerate and sandy channel fills were deposited predominantly across the Damwal Formation. The lack of volcanic clasts and sediments (palaeosols) in the siliciclastic sedimentary rocks of the Rooiberg Group suggests an already active system with frequent eruptive activity and immediate subsequent reworking and sedimentation. Sedimentary rocks from nearby terrains are the likely source for the siliciclastic sedimentary rocks of the Rooiberg Group. Readily available sediments from the eroding nearby terrains were transported through braided river system. The former mentioned absence of Rooiberg

94

volcanic detritus in the siliciclastic interbeds suggest that the quiescent periods were of short duration. In this regard there was less time to erode and transport the Rooiberg felsic detritus. This finding parallels the study of Eriksson et al. (1994), in the area north (-west) of Loskop Dam. Eriksson et al. (1994), found that only Pretoria Group detritus are the likely source of sediments in the upper Rooiberg Group siliciclastic interbeds. Additional components of sediment in the form of chert were deposited in probable nearby lake.

The existence of peperitic breccia facies also supports the topographic basin scenario. The peperitic breccia facies, record the periods were the volcanic activity was concomitant with sedimentary processes (c.f., Skilling et al., 2002; Galerne et al., 2006; Lenhardt and Eriksson, 2012). In principle, the subaerial flowing lava glided into active water system (probable river, lake, pond, etc.) were it mingled with wet unconsolidated sediments, forming the peperitic texture.

The bedded chert facies in close association with volcanic rocks and sandstone depicts a probable lake setting. The chemistry and the inorganic formation of chert in lakes have been described by several authors (O'Neill and Hey, 1973; Jones et al., 1977). Blatt, et al. (1980) described how volcanic rocks can have a significant influence in formation of chert in non-marine basins. The increase in pH of a sodium carbonate brines of lakes cause corrosion of the volcanic rocks and fragments and allow the water to retain the released silica in solution. Later the periodical runoff from surrounding streams dilutes the system and lowers the pH of the lake waters causing the super-saturation with respect to amorphous silica. Then the process of chert formation probably taking time in the order of 10^2-10^3 years will occur during the diagenesis of hydrated sodium silicate precursor.

The dacites of upper Damwal Formation show evidence of post-depositional hydrothermal activity that resulted in hydration forming perlites and consequently the formation of spherulites. Marshall (1961) suggests that perlitic fractures depict strain due to rapid cooling, consequently providing pathways for hydration. Hydration of volcanic glass generates perlitic fractures. Two independent formational conditions favoured the crystallization of spherulites. (1) The spherulites in the lower Damwal Formation were formed in temperatures at or above glass transition at high temperatures. This is depicted by the field observation were spherulites were seen cutting across flow layers (c.f., Kshirsagar et al., 2012). (2) The spherulites in the upper Damwal, Kwaggasnek and Schrikkloof Formations were formed due to the effect of low grade metamorphism and hydrothermal effect at low temperatures. Spherulites may form during devitrification of a natural glass at high temperature (700 – 450

ºC), forming radiating fibers (McPhie et al., 1993). Each fiber is a single crystal that consists of slightly different crystallographic orientation from adjacent crystals (McPhie et al., 1993). Generally devitrification processes occurs in hot glass, and is produced by rapid cooling; however, further slow cooling may allow nucleation and growth of crystals, thus producing spherulites and related features such as lithophysae and micropoikilitic textures (Kshirsagar et al., 2012, and the references therein). Further, Kshirsagar et al. (2012), postulated that low temperature conditions of spherulites formation requires a highly viscous and supercooled (>150 - 200°C) melt and essentially will form by heterogeneous nucleation on submicroscopic seed crystals, bubbles/vesicles, or fractures. However, spherulites may also form as a result of metamorphism, hydrothermal activity or hydration by meteoric water (Friedman and Long, 1984; Kshirsager et al., 2012). Polycrystalline bulbous aggregates or rather pseudospherulites have been described by McPhie et al. (1993), to be the result of alteration and recrystallisation of spherulitically devitrified glass.
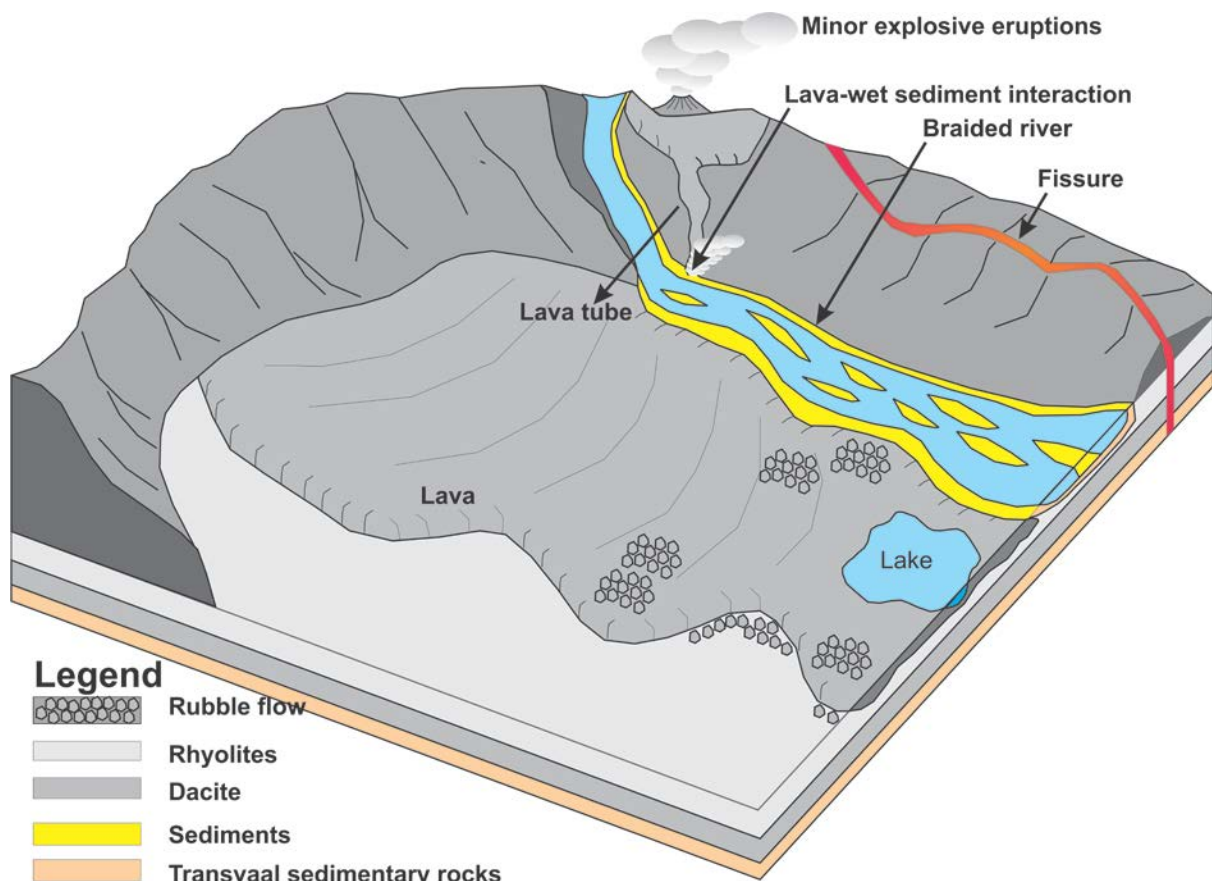
Figure 46. Reconstruction of the palaeoenvironment proposed for Rooiberg Group in the northeast of Loskop Dam area.

9.2. Eruptive mechanism and style of silicic Rooiberg Group

Scrutiny of intermediate felsic composition of volcanic lithofacies has been neglected in most previous studies. However, this study suggests the consideration of the intermediate composition (i.e. rhyodacitic) if present, as a separate entity (facies) since it may shed information that link the eruptive history of the whole range (dacitc – rhyolitic composition). Generally, the literature (e.g. Bryan et al., 2000; Roache et al., 2000; Asvesta and Dimitriadis, 2010; Kshirsagar et al., 2012; Pilote et al., 2012), except few, describe the composition of felsic extrusions to be either dacitic/rhyolitic or the range of both. In this case, facies analysis of both compositions is used together with field data to generalise and infer their depositional processes (cf., Bryan et al., 2000). Field data, produced during mapping together with rock composition of the rocks in the northeast of Loskop Dam reveal the eruptive style of the silicic Rooiberg Group. The volcanism produced three almost distinct compositionally varied Formations, namely the dacitic Damawal with monor rhyodacites, the rhyodacitic Kwaggasnek with minor dacites and rhyolites and the rhyolitic Schrikkloof with minor rhyodacites and dacites. Volcanism of effusive nature emplaced voluminous lava flows over a large area with minor explosive eruptions. Generally and relatively, the lack of major pyroclastic material suggests and supports the effusive nature of volcanism of the Rooiberg Group in the study area. However, minor explosive materials were ejected during volcanism as revealed by minor stratified crystal rich tuff. Considering the inferred original extend of the Rooiberg Group (see figure 1.), probable significant pyroclastic deposits might have been eroded. Further, this lower Rooiberg Group volcanism records volcanic-break as indicated by intercalated siliciclastic rocks such as conglomerate and sandstone interbeds. Field data reveal lava characteristics such as columnar jointing, minor vesicles, and absence of flow banding, spherulites formed during both above and below glass transition temperatures and syn-depositional perlites in the Damwal Formation.

The volcanic activity that produced the rhyodacitic lavas of Kwaggasnek Formation became effusive with no records of pyroclastic material. The former lava flows were moderately viscous and volatile rich as indicated by more vesiculated and abundant plagioclase and quartz phenocrysts with minor flow banding than any of the Rooiberg Group formations. In contrast the rhyolitic Schrikkloof Formation lava flows were very viscous and highly siliceous with prominent flow banding. The latter characteristic is normally the reflection of tabular flow (Cas and Wright, 1987). The magma that formed the transitional boundary rocks between the top of Kwaggasnek Formation and the base of Schrikkloof Formation

97

presumably extruded below its liquidus temperatures. Far less (in Kwaggasnek Formation) or absence (in Schrikkloof Formation) of active sedimentary processes occurred during the stages of volcanism that accounts for the emplacement of both Kwaggasnek and Schrikkloof Formations which produced mainly rhyodacitc to rhyolite lava flows. This lack of sedimentary interbeds in the upper Rooiberg Group is interpreted to be the results of rapid successive volcanism. The study area records the absence of associated dyke swarms. Further, there are no eruptive centres or volcanic vents observed in the study area. The only record of volcanic vents in Rooiberg Group is by Schweitzer (1987), however, this discovery was not supported by any substantial evidence such as illustrations or descriptions of the lithofacies, and no information on the locations (i.e. geographic coordinates) probably due to the former author's nature of study (mainly geochemistry). Thus this study confirms the absence or rather lack of definable volcanic vents in Rooiberg Group. However, the thick accumulated lava flows observed in the Loskop Dam area suggest that these lava flows were dispensed through volcanic centres, most likely fissure vents.

9.3. Geodynamic setting

The volcanic sequence of the Rooiberg Group in the northeast of Loskop Dam has felsic (dacites, rhyodacites and rhyolites) composition with geochemical character consistent with within – plate setting. This setting corresponds well and suggests an origin from the mantle (c.f., Pearce et al., 1984). The observation presented by the tectonic discrimination diagram according to Pearce et al. (1984) and the trace and REE showing negative Eu anomaly (figures 26, 27 and 28 respectively) are also consistent with the mantle plume origin as suggested by the literature (Hatton and Schweitzer, 1995; Hatton, 1995; Buchanan et al., 1999; Buchanan et al., 2002). Major elements supported by petrographic observations suggest magma that underwent fractional crystallization. Additionally, the REE and trace elements suggest the magma with origin consistent with partial melting of the crust. A combination of depletion of LREEs and enrichment of HREEs is associated with upper crust (c.f., White, 1999). Further, enrichment of incompatible trace elements is normally associated with continental volcanic rocks formed from partial melting of enriched source or assimilation continental crust (Buchanan, et al., 1993; Thompson et al., 1984). The manuscript by Jolayemi et al. (in preparation) presents the model that suggests partial melting as a dominant contribution that resulted in the Rooiberg Group volcanics. The ascending of these crustal melts to the surface caused major thermal doming and rapid uplift of the strata of the uppermost Pretoria Group (c.f., Eriksson et al. 1998). The abundant felsic rocks formed as a

result of seemingly continuous volcanism producing voluminous lavas. This extensive lava outflows can be attributed to the combination of intensive and extensive parameters (c.f., Manley, 1992). These parameters include large voluminous magma chamber, low viscosities, high eruptive temperatures and the ability of felsic lavas to retain heat due to thick outer insulating layers. The thickness and voluminous nature of these lavas is attributed to the voluminous magma chamber, high eruptive temperatures (up to 1200 ºC) and high viscosities (up to $\log_{10} \eta$ 857 Pa s) (Lenhardt and Eriksson, 2012).

Xu et al. (2008), suggest the subdivision of crustal melting triggered by mantle plume to be either conductive heating from underlying mantle and/or advective heating from basaltic magma that underplates at the crust-mantle boundary. The author suggest that the mantle plume head wedged on the base of thick lithosphere, inducing the partial melting of enriched components in lithosphreric mantle; and due to density contrast, part of this mantle may pond near the crust-mantle boundary (c.f., Sparks et al., 1980). In the case of Rooiberg Group, the partially melted enriched components in lithosphreric mantle are thought to be represented by the Rustenburg layered suite inducing the partial melting and emplacement of the basaltic-andesitic (Dullstroom Formation; Buchanan et al., 2000) and voluminous felsic magma (Damwal, Kwaggasnek and Schrikkloof Fromations). However, the emplacement might have occurred concurrently. Similar cases were crustal melting induced by under-plating basaltic magma can be found in the Tarim Large Igneous Province, were flood basalts erupted simultenously with the low Nb-Ta rhyolites (Liu et al., 2014).

10. Conclusions

Geochemistry, petrography and physical volcanology (i.e. lithofacies analysis) can be used to construct the geodynamic settings of a sLIP. The Palaeoproterozoic Rooiberg Group volcanics present a substantial yet challenging task of mapping, textural interpretation and facies analysis. The thickness of the volcano-sedimentary sequence reaches up to more than 5 km in the Loskop dam area. Three formations, namely from bottom-up Damwal, Kwaggasnek and Schrikkloof, have been encountered within the study area. The tectonic situation within the Kaapvaal Craton and the predominance of lava flows is seen as evidence for a majority of fissure eruptions in the Rooiberg Group. Although most of the described sLIPs are known to exhibit more explosive eruption style and producing voluminous and laterally extensive ignimbrites, the Rooiberg Group in the study area exhibit less explosive character yet voluminous.

Properly constrained and detailed set of lithofacies type were analysed. In this regard, a total of nine lithofacies were encountered, ranging from coherent lava flows and massive tuffs to cross-bedded sandstones and conglomerates. The lithofacies types can be grouped into syn-to inter-eruptive lithofacies associations, thus, illustrating changes in time and space as shown by intercalated products of effusive eruptions and clastic sedimentation, characterising times of relative quiescence. The lithofacies successions and associations found in the Loskop dam suggest that the Rooiberg Group represents a dynamic environment, where large volumes of silicic lavas were effusively erupted through fissure vents. The intercalation of continuous and discontinuous sandstones, pebbly sandstone and conglomerate depicts active braided river systems concomitant with the volcanic eruption of the Rooiberg Group. These sediments are not associated with erosion of Rooiberg Group volcanics. Active fluvial systems during the eruption are depicted by the presence of peperitic rocks. The bedded chert facies in close association with volcanic rocks and sandstone depicts a probable small lake environment.

11. Outlook

The here presented detailed lithofacies analysis in the northeast of Loskop Dam is a first attempt initiative of physical volcanology study of the Rooiberg Group. Similar studies have to be taken especially in the Modimolle area (Limpopo Province), Dullstroom, Middleburg and Stoffberg areas (Mpumalanga Province). This study recommends geochronological investigation of the successions of the Rooiberg Group in order to support and verify its age

relationship of all the formations with the mafic rocks of Rustenburg Layered Suite, especially with Kwaggasnek and Schrikkloof. Only a combination of both precise dating, and large scale lithofacies analysis will provide a knowledge of accurate estimates of lateral extend and duration of the deposition which is necessary for the correct interpretation of Geotectonic setting of the Bushveld large igneous province as a whole. Although the genetic linkage between the mafic-andesitic Dullstroom and the upper dacitic-rhyolitic Formations (Damwal, Kwaggasnek and Schrikkloof Formations) is pronounced their eruptive timing is not yet concluded.

References

Agangi, A., Kamentesky, V.S., McPhie, J., 2012. Evolution and emplacement of high fluorine rhyolites in the Mesoproterozoic Gawler silicic large igneous province, South Australia. Precambrian. Research. 208: 124-144.

Allen, S.R., McPhie, J., 2002. The Eucarro Rhyolite, Gawler Range Volcanics, South Australia: a >675 km3 compositionally zoned felsic lava of Mesoproterozoic age. Geol. Soc. American. Bulletin. 114: 1592-1609.

Allen, S.R., McPhie, J., Ferris, G., Simpson, C., 2008. Evolution and architecture of a large felsic Igneous Province in western Laurentia: the 1.6 Ga Gawler Range Volcanics, South Australia. Journal Volcanology and Geothermal. Research. 172: 132-147.

Altermann, W., Lenhardt, N., 2012. The volcano-sedimentary succession of the Archean Sodium Group, Ventersdorp Supergroup, South Africa: Volcanology, sedimentology and geochemistry. Precambrian Research. 214-215: 60-81

Armstrong, R.A., Compston, W., Retief E.A., Williams I.S., Welke, H.j., 1991. Zircon ion microprobe studies bearing on the age and evolution of the Witwatersrand Triad. Precambrian Research. 53: 243-266.

Asvesta, A., Dimitriadis, S., 2010 Facies architecture of a Triassic rift-related Silicic Volcano-Sedimentary succession in the Tethyan realm, Peonias subzone, Vardar (Axios) Zone, northern Greece; Regional implications. Journal. Volcanol. Geothermal. Research. 193 (3-4): 245 – 269.

Aubele, J.C., Crumpler, L.S., Elston, W.E., 1988. Vesicle zonation and vertical structure of basalt flows. Journal of Volcanology and Geothermal Research. 35 (4): 349-374.

Barley, M.E., Pickard, A.L., Sylvester, P.J., 1997. Emplacement of a Large Igneous Province as a possible cause of banded iron formation 2.45 billion years ago. Nature. 385: 55-58.

Barrett, A.S., Brown, L.R., Barrett, L., Henzi, P., 2010. A Floristic Description and utilization of Two Home Ranges by Vervet Monkeys in Loskop Dam Nature Reserve, South Africa. Koedoe. 52 (1): 1-12.

Blatt, H., Middleton, G., Murray, R., 1980. Origin of sedimentary rocks. (2nd Editon). Prentice-Hall. Englewood Cliffs. 571 – 582.

Bolstad, P., 2008. GIS Fundamentals: A First Text on Geographic Information Systems. 3rd Ed. Eider Press, Minnesota. 502.

Bonnichsen, B., Kauffmann, D.F., 1987. Physical features of rhyolite lava flows in the Snake River Plain volcanic province, South-western Idaho. In; Fink, J.H., (ed), The emplacement of silicic domes and lava flows. Geological Society of America Special Paper. 212: 119-145.

Boynton, W.V. 1984. Geochemistry of the rare earth elements: meteorite studies. In: Henderson, P. (ed), Rare Earth Element Geochemistry, Elsevier. 63-114.

Breitkreuz, C., 2013. Spherulites and Lithophysae – 200 years of investigation on high-temperature crystallisation domains in silica-rich volcanic rocks. Bulletin of Volcanology. 75: 1-16

Bryan, S.E. and Ferrari, L., 2013. Large igneous provinces and silicic large igneous provinces: Progress in our understanding over the last 25 years. Geological Society of America Bulletin: Published online 25 April 2013; doi:10.1130/B30820.1

Buchanan, P.C. and Reimold, W.U., 1998. Studies of the Rooiberg Group, Bushveld Complex, South Africa: No evidence for an impact origin. Earth and Planetary Science Letters. 155: 149-165.

Buchanan, P.C., Reimold, W.U., Koeberl, C. and Kruger F.J. (2004). Rb–Sr and Sm–Nd isotopic compositions of the Rooiberg Group, South Africa: early Bushveld-related volcanism. Lithos. 29: 373 – 388.

Buchanan, PC., Reimold, W.U., Koeberl, C. and Kruger F.J. (2002). Geochemistry of intermediate to siliceous volcanic rocks of the Rooiberg Group, Bushveld Magmatic Province, South Africa. Contributions Mineralogy. Petrology. 144: 131-143.

Buick, I.S., Maas, R., Gibson., R. (2001). Precise, U-PB titanite age constraints on the emplacement of the Bushveld Complex, South Africa. J. Geological Society of London. 158: 3-6.

Bumby A.J., Eriksson P.G., Catuneanu O., Nelson D.R., Rigby M.J. (2012). Meso-Archaean and Palaeo-Proterozoic sedimentary sequence stratigraphy of the Kaapvaal Craton. Marine and Petroleum Geology. 33 (1): 92-116.

Burger, AJ., Coertze, F.J., 1975. Age determinations-April 1972 to March 1974. Ann. Geol. Surv. S. Afr. 10: 135-141.

Button, A., 1986. The Transvaal sub-basin of the Transvaal sequence. In: Anhaeusser, C.R., Maske, S. (Eds), Mineral Deposits of Southern Africa Geol. Soc, S. Afr. Johannesburg. 811-817.

Cas, R.A.F., Wright, J.V., 1987. Volcanic Successions: modern and ancient. Allen and Unwin Publishers Ltd. London

Catuneanu, O. and Biddulph, M.N., 2001. Sequence stratigraphy of the Vaal reef facies associations in the Witwatersrand foredeep, South Africa. Sedmentary Geology. 141 – 142 (201): 113-130.

Catuneanu, O., 2001. Flexural partitioning of the Late Archaean Witwatersrand foreland system, South Africa. Sedimentary Geology. 141-142: 95-112.

Cawthorn, R.G., 2013. The Residual or Roof Zone of the Bushveld Complex, South Africa. J Petrology, 54(9): 1875-1900.

Cawthorn, R.G., Walraven, F., 1997. The Bushveld Complex: A Time to Fill and a Time to Cool. Economic Geology Research Unit Information Circular, University of Witwatersrand. 307.

Cheney, E.S. and Twist, D., 1991. The conformable emplacement of the Bushveld mafic rocks along a regional unconformity in the Transvaal succession of South Africa. Precambrian Research. 74: 203-223.

Chough, S.K., Sohn, Y.K., 1990. Depositional mechanics and sequences of base surges, Songaksan tuff ring, Cheju Island, Korea. Sedimentology. 37: 1115-1135.

Clubley-Armstrong, A. R., 1977. The Geology of the Selons River Area, North of Middelburg, Transvaal, with Special Reference to the Structure of the Regions Southeast of the Dennilton Dome. MSc thesis (Unpublished), University of Pretoria.

Coertze, F.J., Burger, A.J., Walraven, F., Marlow, A.G., MacCaskie, D.R., 1978. Field relations and age determinations in the Bushveld Complex. Trans. Geol. Soc. S. Afr. 81: 1-11.

Coffin, M.F., Eldolm, O., 1994. Large igneous provinces: crustal structure, dimensions and external consequences. Reviews of Geophysics. 32: 1-36.

Collinson J.D., 1996. Sedimentary Environments: Processes, Facies and Stratigraphy. In Alluvial sediments (3rd Edition by Reading H.G). Blackwell Scientific Publishers. 31-81.

Creaser, R.A., 1995. Neodymium isotopic constraints for the origin of Mesoproterozoic silicic magmatism, Gawler Craton, South Australia. Can. Journal of Earth Science. 32: 469-471.

Creaser, R.A., White, A.J.R., 1991. Yardea Dacite, large-volume, high-temperature felsic volcanism from the Middle Proterozoic of South Australia. Journal of Geology. 19, 48-51.

Davies B. and McPhie J., 1996. Spherulites, quenched fractures and relict perlite in a Late Devonian rhyolote dyke. Queensland, Australia. Journal of Volcanology and Geothermal. Research. 71: 1-11.

De Wit, M..J., Roering, C., Hart, R.J., Armstrong, R.A., De Ronde, C.E.J., Green, R.W.E., Tredoux, M., Perdeby, E., Hart, R.A., 1992. Formation of an Archean continent. Nature. 357: 553-562.

Els, B.G., 1998. The auriferous late Arhaean sedimentation system of SouthAfrica: unique palaeoenvironmental conditions? Sedimentary Geology. 120: 205-224.

Elston, W. E., 2012. Daly and Molengraaff (19240 vindicated: the huge Bushveld Igneous Complex, South Africa (2.055 Ma, A=67 000 km^2, V=106 km^3) is a surficial open system. Annual meeting of Geological Society of America; history and philosophy of Geology division.

Elston, W.E., 1992. Does the Bushveld-Vredefort system (South Africa) record the largest known terrestrial impact catastrophe? Lunar and Planetary Institute Contribution. 790: 23-24.

Eriksson P.G., Catuneanu, O., Els, B.G., Bumby, A.J., van Rooy, J.L., Popa M., 2005. Kaapvaal Craton: changing first- and second-order controls on sea level from c. 3.0 Ga to 2.0 Ga. Sedimentary Geology. 176: 121-148.

Eriksson P.G., Mazumder R., Sarkar S., Bose P.K., Altermann W., van der Merwe R., 1999. The 2.7 – 2.0 Ga volcano – sedimentary record of Africa, India, and Australia: evidence for global and local changes in sea level and continental freeboard. Precambrian Research. 97: 269-302.

Eriksson P.G., Reczko, B.F.F., Corner, B., Jenkins, S.L., 1996. The Kanye axis, Kaapvaal Craton, southern Africa: a postulated Archaean crustal architecrural elements inferred from three-dimensional basin modelling of the lower Transvaal Supergroup. Journal of African Earth Sciences. 22: 223-233.

Eriksson P.G., Schreiber, U.M., van dr Nuit, M., 1991. A review of the sedimentology of the early Proterozoic Pretoria Group, Transvaal Sequence. South Africa: implication for tectonic setting. Journal of African Earth Sciences. 13: 107 – 119.

Eriksson, P. G., Hattingh, P. J. and Altermann, W., 1995. An Overview of the Geology of the Transvaal Sequence and Bushveld Complex, South Africa. Mineral Deposita. 30: 98-111.

Eriksson, P. G., Reczko, B.F.F., 1995. The sedimentary and tectonic setting of the Transvaal Supergroup floor rocks to the Bushveld Complex. Journal of African Earth Sciences. 21: 487 -504.

Eriksson, P. G., van der Merwe, R.., Bumby, A.J., 1998. The Palaeoproterozoic Woodlands Formation of eastern Botswana – northwestern South Africa: litostratigraphy and relationship with Transvval basin inversion structures. Journal of African Earth Sciences. 27: 349-358.

Eriksson, P.G, Shreiber, U.M., Reczko, B.F.F., and Snyman, C.P., 1994. Petrography and Geochemistry of Sandstone interbedded with the Rooiberg Felsite Group (Transvaal sequence, South Africa): Implications for provenance and tectonics. Journal of Sedimentary Research, Windhoek. A64 (no. 4): 836-846.

Ernst, R.E., Bell, K., 2010. Large Igneous Provinces (LIPs) and carbonatites. Mineralogy and Petrolology. 98: 55-76.

Ezz El Din Abdel Hakim Khalaf., 2010. Stratigraphy, facies architecture and palaeoenvironment of Neoproterozoic volcanic and volcaniclastic deposits in Fatira area Central Eastern Desert, Egypt. Journal of African Earth Sciences. 58: 405-426.

Filmater, N., 2010. A Vegetation Classification and Management Plan for the Hondekraal Section of the Loskop Dam Nature Reserve. Magister Technologiae Dissertation (unpublished), University of South Africa, Pretoria, South Africa. 227.

Friedman, I., Long, W., 1984. Volcanic glasses their origins and alteration processes. J. Non-Cryst. 67: 127-133.

Gábor Kereszturi and Károly Németh, (2012). Monogenetic Basaltic Volcanoes: Genetic Classification, Growth, Geomorphology and Degradation, Updates in Volcanology - New Advances in Understanding Volcanic Systems, Dr. Karoly Nemeth (Ed.), ISBN: 978-953-51-0915-0,: In Tech, DOI: 10.5772/51387. Available: http://www.intechopen.com/books/updates-in-volcanology-new-advances-in-understanding-volcanic-systems/monogenetic-basaltic-volcanoes-genetic-classification-growth-geomorphology-and-degradation

Galerne, C., Caroff, M., Rolet, J., Le Gall, B., 2006. Magma-sediment mingling in an Ordovian rift basin: The Plouézec-Plourivo half-graben, Armorican Massif, France. Journal of Volcanology and Geothermal Research. 155: 164-178.

Gast, P.W., 1972. The chemical composition of the earth, the moon and chondritic meteorites. In: The nature of the solid earth (ed. Robertson, E.C.). McGraw-Hill.

Ghazi, S., Mountney, N.P., 2009. Facies and architectural element analysis of a meandering fluvial succession: The Permian Warchha Sandstone, Salt Range, Pakistan. Sedimentary Geology. 221: 99-126.

Goto, Y., McPhie, J., 1996. A Miocene basanite pepperitic dyke at Stanley, northwestern Tasmania, Australia. Journal of Volcanology and Geothermal Research. 74: 111-120.

Goto, Y., McPhie, J., 1998. Endogenous growth of a Miocene submarine dacite cryptodome, Rebun Island Hokkaido, Japan. Journal of Volcanology and Geothermal Research. 84: 273-286.

Green, J.C., Fitz, T.J., 1993. Extensive felsic lavas and rheoignimbrites in the Keweenawan Midcontinent Rift plateau volcanics, Minnesota: petrographic and field recognition. Journal of Volcanology and Geothermal Research. 54: 177-196.

Hanson, R.E., Hargrove, U.S., 1999. Processes of magma/wet sediment interaction in a large-scale Jurassic andesite peperite complex. Northern Sierra Nevada, California. Bulletin of Volcanology. 60: 610 – 626.

Harmer, R.E., Armstrong, R.A., 2000. New precise dates on the acid phase of the Bushveld and their implications. In: Abstract. Workshop on the Bushveld Complex, 18 – 21 November 2000, Burgersfort. University of Witwatersrand.

Hatton, C. J., 1995. Mantle Plume Origin for the Bushveld and Ventersdorp Magmatic Provinces. Journal of African Earth Sciences. 21: 571-577.

Hatton, C.J and Schweitzer, J.K., 1995. Evidence for synchronous extrusive and intrusive Bushveld magmatism. Journal of African Earth Sciences. 21: 579-594.

Hickman, A.H., 1983. Geology of the Pilbara Block and its environs. Western Australia Geological Survey Bulletin. 127: 268

Hunns, S.R., McPhie, J., 1999. Pumiceous peperite in a submarine volcanic succession at Mount Chalmers, Queensland, Australia. Journal Volcanology and Geothermal Research. 88: 239-254.

Ingram, R.L., 1952. Terminology for the thicknesses of stratification and parting units in sedimentary rocks. Geological Society of America, Bulletin. 65: 937-938.

Jolayemi, O.O., Lenhardt, N., Roberts, J., Masango, S.M., Eriksson, P.G., (in preparation) Chemical evolution of the Paleoproterozoic Rooiberg Group, Kaapvaal Craton, South Africa: new insights into the formation of silicic large igneous provinces (SLIPs).

Jones B.F., Eugster, H.P., Rettig., 1977. Hydrochemistry of the Lake Magadi Basin, Kenya. Geochimica et Cosmochimica Acta. 41: 53-72

Kamber, B., Blenkinsop, T.G., Villa, I. M., Dahl, P.S., 1995. Proterozoic transpressive deformation in the Northern Marginal Zone, Limpopo Belt, Zimbabwe. Journal of Geology. 103: 493-508.

Kamber, B., Kramers, J.D., Napier, R., Cliff, R.A., Rollinson, H. R., 1995. The Triangle Shear Zone, Zimbabwe, revisited: new data document an important event at 2.0 Ga in the Limpopo Belt. Precambrian Research. 70: 191-213.

Keszthelyi, L., Thordarson, T., 2000. Rubbly pahoehoe: a previously undescribed but widespread lava type transitional between aa and pahoehoe. Geological Society of America. Abstract with programs. 32: 7

Kinnaird, J. A., 2005. The Bushveld Large Igneous Province. Internet; Place unknown). Large igneous provinces. Available from: http://www.largeigneousprovinces.org/LOM.html (23 September 2013)

Kokelaar, B. P., 1982. Fluidisation of wet sediments during the emplacement and cooling of various igneous bodies. Journal of Geological Society. 139: 21-33

Kshirsager. P.V., Sheth H.C., Seaman S.J., Shaik B., Mohite P., Gurav T., and Chandraseharam D., 2012. Spherulites and thundereggs from pitchstones of the Deccan Traps: geology petrochemistry and emplacement environments. Bulletin of Volcanology. 74: 559-577.

Lenhardt, N., Eriksson, P.G., 2012. Volcanism of the Palaeoproterozoic Bushveld Large Igneous Province: the Rooiberg Group, Kaapvaal Craton, South Africa. Precambrian Research. 214-215: 82-94.

Lenhardt, N., Eriksson, P.G., Catuneanu, O., Bumby, A.J., 2012. Nature of and controls on volcanism in the ca. 2.32–2.06 Ga Pretoria Group, Transvaal Supergroup, Kaapvaal Craton, South Africa. Precambrian Research. 214-215: 106-123.

Letts, S., Torsvik, T.H., Webb, S.J., Ashwal, L.D., 2009. Palaeomagnetism of the 2054 Ma Bushveld Complex (South Africa): implications for emplacement and cooling. Geophysical Journal International. 179: 850-872.

Liu, H.-Q., Xu, Y.-G., Tian, W., Zhong, Y.-T., Mundil, R., Li, X.-H., Yang, Y.-H., Lou, Z.-Y., Shang-Guan, S.-M. Origin of two types of rhyolites in the Tarim Large Igneous Province: Consequences of incubation and melting of a mantle plume. Lithos (2014). http://dx.doi.org/10.1016/j.lithos.2014.02.007

Loubser, M. and Verryn, S., 2008. Combining XRF and XRD analyses and sample preparation to solve mineralogical problems. South African Journal of Geology. 111: 229-238.

Low, A.B., Rebelo, A.G., 1998. Vegetation of South Africa, Lesotho and Swaziland (2nd Ed). Department of Environmental Affairs and Tourism. Pretoria.

Luchetti, A.C.F., Nardy, A.J.R., Machado, F.B., Madeira, J E.O., Arnosio, J.M., 2014. New insights on the occurrence of peperites and sedimentary deposits within the silicic volcanic sequences of the Paraná Magmatic Province, Brazil. Solid Earth. 5: 121-130.

Maddock, R.H., 1983. Melt origin of pseudotachylytes demonstrated by textures. Geology. 11: 105-108.

Manley, C.R., 1992. Extended cooling and viscous flow of large, hot rhyolite lavas: implications of numerical modelling results. Journal Volcanolology and Geothermal Research. 53: 27-46.

Marshall, R.R., 1961. Devitrification of natural glass. Geological Society of America. 72: 1493-1520.

Martini, J.E.J., 1998. The Loskop Formation and its relationship to Bushveld, South Africa. Journal of African Earth Sciences. 27 (2): 193-222.

Mathez, E.A., Van Tonngeren, J.A., Schweitzer, J., 2013. On the relationship between the Bushveld Complex and its felsic roof rocks, part 1. Petrogenesis of Rooiberg and related Felsites. Contributions to Mineralogy and Petrology. 166: 435-449.

McDowell, F.W., Keizer, R.P., 1977. Timing of mid Tertiary volcanism in the Sierra Madre Occidental between Durango City and Mazatlán, Mexico. Geological Society of America. 88: 1479-1487.

McPhie, J., Doyle, M., Allen, R., 1993. Volcanic textures: a guide to the interpretation of textures in volcanic rocks. In: Centre for Ore Deposit and Exploration studies. University of Tasmania.

Miall, A.D., (ed) 1978. Fluvial sedimentology. Cannadian Society of Petroleum Geology. 5.

Miall, A.D., 1977. A review of the braided river depositional environment..Earth Science Reviews. 13: 1-62.

Miall, A.D., 1985. Architectural-element analysis: a new method of facies analysis applied to fluvial deposits. Earth Science Reviews. 22: 261-308.

Miall, A.D., 1996. The geology of fluvial deposits: sedimentary facies, basin analysis, and petroleum geology. Springer-Verlag Berlin Heidelberg.

Milner, S.C., Duncan, A.R., Ewart, A., 1992. Quartz latite rheoignimbrite flows of the Etendeka Formation, north western Namibia. Bulletin of Volcanology. 54: 200-219.

Mucina, L., Rutherford, M.C., 2006. Vegetation of South Africa, Lesotho and Swaziland. Strelitzia 19. Souh African National Biodiversity Institute. Pretoria. 807.

Nemec W. and Postma G., 1993. Quaternary alluvial fans in southwestern Crete: sedimentation processes and geomorphic evolution. In: Alluvial Sedimentation (Ed. M. Marzo and C. Puigdefabregas). 235-276.

Németh, K., and Martin, U., 2007. Practical volcanology- lecturer notes for understanding volcanic rocks from field based studies. Occasional Papers of the Geological Institute of Hungary. 207-221.

Nesbitt, HW., Young., GM., 1982. Early Proterozoic climates and plates motion inferred from major elements chemistry of Lutites. Nature. 299: 715 - 717.

O'Neill, J.R., and Hay, R.L., 1973. O^{18}/O^{16} ratios in cherts associated with the saline lake deposits of East Africa. Earth and Planetary Science Letters. 19: 257-266.

Óskarsson, B.V., Riishuus, M.S., 2013. The mode of emplacement of Neogene flood basalts in Eastern Iceland: Facies architecture and structure of the Hólmar and Grjótá olivine basalt groups. Journal of Volcanology and Geothermal Research. 267: 92-118.

Palinkaš, L.A., Bermanec, V., Šoštarić, S.B., Kolar-Jurkovšek, T., Palinkaš, S.S., Molnar, F., Kniewald, G., 2008. Volcanic facies analysis of subaqueous basalt lava-flow complex at Hruškovec, NW Croatia – Evidence of advanced rifting in the Tethyan domain. Journal of Volcanology and Geothermal Research. 178: 644-656.

Pankhurst, M.J., Scheaefer, B.F., Betts, P.G., 2011. Geodynamics of rapid voluminous felsic magmatism through time. Lithos. 123: 92-101.

Parker, D.F., White, J.C., 2008. Large –scale silicic alkali magmatism associated with the Buckhorn Caldera, Trans-Pecos Taxes, U.S.A: A comparison with Pantelleria, Italy. Bulletin of Volcanology. 70: 403-415.

Pearce, J.A., Harris, N.B.W., Tindle, A.G., 1984. Trace element discrimination diagrams for the tectonic interpretation of granitic rocks. Journal Petrolology. 25: 956-983.

Pilote, C., Corcorana, P.L., Mueller W.U., 2012. A Neoproterozoic continental rift succession: The volcano-sedimentary Koivib Mountains deposits of Namibia. Precambrian Research. 214: 172-184.

Rajesh, H.M., Chisonga, B.C., Shindo, K., Beukes, N.J., Armstrong, R.A., 2013. Petrographic, geochemical and SHRIMP U-Pb titanite age characterisation of the Thabazimbi mafic sills: Extended time frame and a unifying petrogenetic model for the Bushveld Large Igneous Province. Precamrian Research. 203: 79-102.

Rhodes, R. C., 1975. New evidence for impact origin of the Bushveld Complex, South Africa. Geology. 3: 549-554.

Roache, M.W., Allen, S.R., McPhie, J., 2000. Surface and subsurface facies architecture of a small hydroexplosive, rhyolititc centre in the Mesoproterozoic Gawler Range Volcanics, South Australia. Journal of Volcanology and Geothermal Research. 104: 237-259.

Rowland, S. M., 1986. Structural Analysis and Synthesis: A Laborotary Course in Structural Geology. 1st Edition. Blackwell Scientific Publishers. 208.

Rust, B. R., 1978. Aclassification of alluvial channel systems. In: Miall, A.D., (ed) Fluvial sedimentology. Cannadian Society of Petroleum Geology. 5: 187-198.

Santos Barreto, C.J., de Lima, E.F., Scherer, C.M., de Magalhães May Rossetti, L., 2014. Lithofacies analysis of basic lava flows of the Paraná igneous province in the south hinge of Torres Syncline, Southern Brazil. Journal of Volcanology and Geothermal Research. 285: 81-99.

Schmincke, H.-U., 1967. Fused tuff and peperites in south central Washington. Geolological. Society. America. 78: 319-330.

Schreiber, U.M., Eriksson, P.G., 1992. The sedimentology of post – Magaliesberg formations of the Pretoria Group, Transvaal Sequence, in the eastern Transvaal. South African Journal of Geology. 95: 1-16.

Schweitzer J.K., Hatton C.J., and de Waal S.A., 1995. Regional lithochemical Stratigraphy of the Rooiberg Group, upper Transvaal Supergroup: A proposed new subdivision. South African Journal of Geology. 98 (3): 245-255.

Schweitzer, J.K., 1987. The transition from the Dullstroom Basalt Formation to the Rooiberg Felsite Group, Transvaal Supergroup: a volcanological, geochemical and petrological investigation. Ph.D. thesis (Unpublished), University of Pretoria.

Shellnutt, J.G., Bhat, G.M., Wang, K,-L., Brookfield, M.E., Dostal, J., Jahn, B.-M., 2012. Origin of silicic igneous volcanic rocks of the Early Permian Panjal Traps, Kashmir, India. Chemical Geology. 334: 154-170.

Sheth H.C., 2007. 'Large igneous pronvinces': definition, recommended terminology and hierarchial classification. Earth Science Letters. 289: 509-519.

Silva Simões, M., Esteves Almeida, M., Honorato de Souza, A.G., Balieiro da Silva, D.P., Rocha, P.G., 2014. Characterization of the volcanic and hypabissal rocks of the Paleoproterozoic Iricoumé Group in the Pitinga region and Balbina Lake area, Amazonian Craton, Brazil: Petrographic distinguishing features and emplacement conditions. Journal of Volcanology and Geothermal Research. 286: 138-147.

Skilling, I.P., White, J.D.L., McPhie, J., 2002. Peperite: a review of magma-sediment mingling. Journal of Volcanology and Geothermal Research. 114: 1-17.

Song, S.R., Lo, H.J., 2002. Lithofacies of volcanic rocks in the central Coastal Range, eastern Taiwan: Implications for island arc evolution. Journal of Asian Earth Sciences. 21: 23-38.

Soueka, T., Lee, I.K., Huramatsu, M., Imamura, S., 1985. Geochemical properties and engineering classification for decomposed granites soils in Kaduna district, Nigeria. First International Conference of Geomachenics in tropical lateritic and saproliticsolis, Brasilia, Publication. 1: 175-186.

South African Committee for Stratigraphy (SACS), 1980. Stratigraphy of South Africa Part 1: Lithostratigraphy of the republic of South Africa, South West Africa / Namibia and the republics of Bophuthatswana, Transkei and Venda. Handbook Geological Survey of South Africa. 8: 690. Pretoria, South Africa.

Sparks R.S.J., Meyer, P., Sigurdsson, H., 1980. Density variation amongst mid-oceanic ridge basalts: implication for magma mixing and the scarcity of primitive lavas. Earth and Planetary Science Letters. 46: 419-430.

Sun, S.S., Bailey, D.K., Tarney, J., Dunham, K., 1980. Lead isotopic study of young volcanic rocks from mid-oceanic ridges, ocean islands and island arc. Philosophical Transactions of the Royal Society. London A. 297: 409-445.

Sutton R.R., 1993. Volcaniclastic rocks of the Orton-Bradley Formation, Banks Peninsula, New Zealand: A Thesis Submitted in Fulfilment of the Requirements of the Degree of Masters of Science (Unpublished), University of Canterbury.

Theron, G.K., 1973. n Ecologiese studie van die plantegroei van die Loskopdamnatuur-reservaat. DSc. Thesis (Unpublished), University of Pretoria.

Trendall, A.F., 1995. The Woongarra Rhyolite: A Giant Lava like Felsic Sheet in the Hamersley Basin. Geological Survey. W. Aust. Rep. 42.

Tuffen H., and Castro J.M., 2009. The emplacement of an obsidian dyke through thin ice: Hrafntinnuhryggur, Krafla, Iceland. Journal of Volcanology and Geothermal Research. 185: 352-366.

Twist, D., 1985. Geochemical evolution of the Rooiberg Silicic Lavas in the Loskop Dam Area Southern Bushveld. Economic Geology. 80: 1153-1165.

Twist, D., French, B.M., 1983. Voluminous acid volcanism in the Bushveld Complex: A review of the Rooiberg Felsite. Bulletin of Volcanology. 46 (3): 225-242.

Van der Westhuizen, W.A., De Bruiyn, H., Meintjies, P.G., 2006. The Ventersdorp Supergroup. In: Johnson, M.R., Anhaeusser, C.R., Thomas, R.J., (Eds) The Geology of South Africa. Geological Society of South Africa. 187-209.

Van Tongeren, J.A., Mathez, E.A., Kelemen, P.B., 2010. A felsic end to Bushveld differentiation. Journal of Petrology. 51, Issue 9: 1891-1912.

Wager, L.R., Brown, G.M., 1968. Layered Igneous Rocks. London, Oliver & Boyd. 572.

Walraven, F. J., 1985. Genetic aspects of the granophyric rocks of the Bushveld Complex. Economic Geology. 80, 1166-1180.

Walraven, F., 1997. Geochronology of the Rooiberg Group, Transvaal Supergroup, South Africa. Information Circular, Economic Geology Research Unit, University of the Witwatersrand, Johannesburg, South Africa. 97: 316.

Walraven, F., Hattngh, E., 1993. Geocronology of the Nebo Granite Bushveld Complex. South African Journal of Geology. 96: 31-41.

White, J.C., Holt, G.S., Parker, D.F., Ren, M.H., 2003. Trace-element partitioning between alkali feldspar and peralkalic quartz trachyte to rhyolite magma. Part I: systematics of trace-element partitioning. American Mineralogist. 88: 316-329.

Winchester, J.A., Floyd, P.A., 1977. Geochemical discrimination of different magma series and their differentiation products using immobile elements. Chem. Geol. 20: 325-343.

Xu, Y.G., Luo, Z.Y., Huang, X.L., He, B., Xiao, L., Xie, L.W., Shi, Y.R., 2008. Zircon U-Pb and Hf isotope constraints on partial melting associated with Emeishan mantle plume. Geochimica et Cosmochimica Acta. 72: 3084-3104.

Zhu, B., Guo, Z., Liu, R., Liu, D., Du, W., 2014. No pre-eruptive uplift in the Emeishan large igneous province: New evidences from its 'inner zone', Dali area, Southwest China. Journal of Volcanology and Geothermal Research. 269: 57-67.
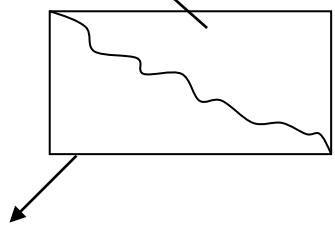
Appendix A

Table 10 A: Depicts field data as write from the field, and later modified after analysis (for SM samples).

Stop	Co-ordinates	Sample	Picture date time	Description
1	S 25°23'38,5" E 29°30'17,7"	BG1	**12 May** 08h39	Red (mostly) with black crystals (fresh), fine-med. Grained, k-feldspars, quartz, unknown black minerals
2	S 25°23'48,8" E 29°30'17,7"	BG2	09h47	Granophyre
4	S 25°23'43,4" E 29°30'39,4"	BG3	11h52	Granophyre
5	S 25°23'44,0" E 29°30'30,5"	RL1	12h47	Brown-Black fine grained lava
6	S 25°23'43,0" E 29°30'37,0"	RL2	12h53	Brown-Black fine grained lava
7	S 25°23'43,5" E 29°30'38,2"			**Contact** (Bushveld Granophyres)
8	S 25°23'42,9" E 29°30'40,6"			Bushveld Granophyres
9	S 25°23'42,5" E 29°30'47,3"			Bushveld Granophyres
10	S 25°23'43,5" E 29°30'52,1"			Rooiberg Lava
11	S 25°23'42,2" E 29°30'52,0"	RL3	14h19	Rooiberg Lava
12	S 25°23'24,2" E 29°30'17,3"	BGX		
13	S 25°24'08,8" E 29°29'57,2"	SS1	**13 May** 07h50	
14	S 25°24'11,2" E 29°29'58,8"		08h00	Damwal Formation

116

15	S 25°24'13,0" E 29°30'02,6"	SM1		Pyroclastic, k-feldspar, quartz, courser grained than stop 14, plagioclase phenocrysts
16	S 25°24'12,8" E 29°30'04,9"	SM2		Flow banding, spherulitic texture, vesicles therefore it is top of lava flow, devitrification
17	S 25°24'13,1" E 29°30'06,7"	SM3 (SM4 – pyro?)		Greenschist facies-metamorphism (sm3)
18	S 25°24'12,9" E 29°30'09,7"	KM1	08h52	Confirm. Conglomerate or larger breccias particles in matrix. Pyroclastic flow – boundary. Enriched vesicles zone at the top. Difference in particle fragments in zones.
19	S 25°24'13,0" E 29°30'10,7"	SS2		
20	S 25°24'12,4" E 29°30'12,0"	SM5		Lava
21	S 25°24'12,8" E 29°30'12,6"	KM2	09h16	Pyroclastic/conglomerate 302°/35°N Pipe vesicles (stretched bubble), could lead to flow banding
22	S 25°24'13,0" E 29°30'13,9"	SM6		Lava
23	S 25°24'12,3" E 29°30'14,6"	KM3	09h43	
24	S 25°24'12,6" E 29°30'16,7"	SM7		Lava
25	S 25°24'12,8" E 29°30'17,3"		09h59	Pyroclastic
26	S 25°24'12,2" E 29°30'19,2"	NL1	10h06	
27	S 25°24'12,2" E 29°30'19,2"	SS3		Lava, Glassy, lithofied±chert - part of a pyroclastic fall, fine ash setting on surface
28	S 25°24'18,0" E 29°30'24,1"	SM8	10h27	**Start of an outcrop**, lava
29	S 25°24'19,8"	SM9	10h49	

	E 29°30'24,7"			
30			10h50	
31	S 25°24'20,7" E 29°30'25,6"	SM10		
	S 25°24'22,8" E 29°30'25,9"			**End of outcrop**
32	S 25°24'23,2" E 29°30'26,0"			
33	S 25°24'42,2" E 29°30'31,5"		11h54	Pyroclastic particles in fine matrix
34	S 25°24'42,2" E 29°30'31,5"	SM11 + KM4		Lava + Pyroclastic? Hydrothermal evidence: veins
35	S 25°24'48,8" E 29°30'39,0"	SM12 + SM14	12h21	Gas bubbles, by quartz, variolitic, SM14 has a spherulitic texture, lava empties first then inclusion of dyke with metamorphic aureole
36	S 25°24'50,8" E 29°30'37,1"	SM13	12h30	Lava
			12h35	Quartz veins
			12h36	Flow banding
37	S 25°24'48,7" E 29°30'39,4"	SM15	12h44	**Start of outcrop**
38	S 25°24'48,7" E 29°30'40,2"		12h49	Spherulitic texture, clay minerals (washed out) Lava
	S 25°24'50,0" E 29°30'42,7"			**End of outcrop**
39	S 25°24'53,3" E 29°30'55,3"	SM16		
40	S 25°24'53,8" E 29°30'58,6"	SM17		

118

41	S 25°24'58,5" E 29°31'07,9"	SS4	01h39 01h40 01h41 ©	- Conglomerate, rounded with cornered stones - Particles of different sizes, silty to fine grained sandy matrix Clasts: well-rounded to angular - Composition: lava, possibly quartz of ±2cm, dense lava of ±7cm ×±5cm - However, thisis not the normal make-up/matrix of conglomerate (vesicular texture, infilling of vesicles) - The lavas close to the vent (volcano opening) remains in a liquid phase when it falls to the ground, gathering particles that stick together (Lava fountaining) - This forms cinder/spatter cones. Erupts once, then empties. Thereafter, fisher eruptions occur. Lava, lots of fields, smaller magma chambers form. - Braided rivers. streams, funnels
42	S 25°24'58,5" E 29°31'07,9"		02h02	
			02h07	Quartzite pebbles
43	S 25°25'01,8" E 29°31'15,0"	SS5	**14 May**	Quartz
44	S 25°26'00,0" E 29°31'44,8"	SM18	08h57 (×4)	Flow banding, reddish lava (Hand specimen)
45	S 25°25'59,3" E 29°31'43,8"	SM19	09h26 (×2) 09h35	Same as Stop #44
46	S 25°25'58,2" E 29°31'36,4"			Too weathered
47	S 25°25'54,6" E 29°31'34,1"	SM20		Laminar (red and black) Quarts and K-feldspar
48	S 25°25'58,1" E 29°31'36,5"	SM21	10h08 (×2) 10h17	Flow banding

			(×2)	
49	S 25°25'19,7" E 29°31'39,8"	SM22	11h35 (×3)	K-feldspar, Quartz, Black minerals?
50	S 25°25'17,8" E 29°31'39,0"	SM23		K-feldspar, Quartz, Black minerals?
51	S 25°25'17,5" E 29°31'38,4"	SM23		Little K-feldspar, Quartz, Black minerals?
52	S 25°25'17,3" E 29°31'38,3"			**Contact:** Mostly K-feld. Rhy.← **4m** → Black, K-feld., Quartz
53	S 25°25'16,1" E 29°31'38,1"	SM24	12h01	Mostly feldspars
54	S 25°25'16,1" E 29°31'37,5"	SM25		Same as above, possible different in chemistry
55	S 25°25'14,6" E 29°31'36,5"	SM26		
56	S 25°25'12,7" E 29°31'35,8"	SM27		Green mineral introduced
57	S 25°25'07,0" E 29°31'32,1"	SM28	01h41	Matrix is redder than before
58	S 25°25'06,0" E 29°31'29,2"	SM29		Large green grains in matrix
59	S 25°25'06,0" E 29°31'26,8"			Red matrix → black matrix with minor k-feldspar
60	S 25°25'05,6" E 29°31'25,5"	SM30		Black matrix
61	S 25°25'04,9" E 29°31'22,8"			**Contact estimation**
62	S 25°24'14,0" E 29°30'27,3"	SM31	**15 May** 10h58	Soil sample, black bag
63	S 25°23'22,3" E 29°30'00,8"	SM32		**Start of outcrop**
64	S 25°23'22,3"			**Contact**

120

	E 29°30'01,3"			
65	S 25°23'16,1" E 29°30'09,7"	SM33	**16 May** 08h26	
66	S 25°23'17,4" E 29°30'12,5"	SM34	08h55	Red Granophyre
68	S 25°23'19,7" E 29°30'11,7"	SM26	09h29 (×2)	Finer grained granophyres Course GB Conglomerate Fine BG
69	S 25°24'13,0" E 29°30'25,8"	SM37	12h56 *08h59* *17 May*	Pyroclastic/Extensive hydrothermal activity **Srike/Dip: 072°/E-W**
70	S 25°24'10,7" E 29°30'27,8"	SM38		(After pyroclastic) Granophyre Found quartz-rich + quartz veined rocks (×2)
71	S 25°24'10,2" E 29°30'27,2"		11h23 (×3)	Flow of lava Also quartzite rocks from Stop #70 **Strike/Dip: 276°/50°S**
72	S 25°23'14,0" E 29°30'09,2"	SM39		
73	S 25°23'10,1" E 29°30'14,7"	SM40		
74	S 25°24'10,5" E 29°30'26,6"		**17 May** 09h20 (×3) 09h25	Sedimentary, quartz, sandstone No cross-bedding, only slight horizontal evidence **Strike/Dip: 270°/47°S**
75	S 25°24'10,5" E 29°30'26,6"			**Strike/Dip: 257°/42°S**
76	S 25°24'09,9" E 29°30'27,1"			**Contact** Border between Granophyres and SS N ⟵ | Grano. | SS | Pyro. |

				Aerial View Sandstone (SS) has quartz/chert veins, Pyro?= Pyroclastic(Analysis reveal that its actually hydrothermally altered lava)(perlitic fractures)
77	S 25°24'10,7" E 29°30'25,8"	SM41 (SS) SM42	09h50 (SS)	**Contact** Pyroclastic(Not Pyro but hydrothermally altered lava), Sandstone border
78	S 25°24'10,4" E 29°30'26,5"			Pyroclastic?
79	S 25°24'14,7" E 29°30'28,7"	SM43 SM44		- Lava - Further upwards is green phenocrysts in the lava, but only weathered samples were found - Vesicles are also found/ amygdales with quartz - d = 3mm - ½ cm
80	S 25°24'13,8" E 29°30'31,5"	SM45 (lava)	10h59	**Contact** (Pyro) Lava is in-situ Big ±7cm quartz amygdales N ← [**Lava** | **Pyroclastic**] Aerial View Lava has green phenocrysts
81	S 25°24'14,1" E 29°30'38,6"			
82	S 25°24'15,3" E 29°30'38,6"	SM46		Lava outcrop
83	S 25°24'14,6" E 29°30'42,3"	SM47 (Qtzite) SM48 (Lava)		**Contact** N ← [**Lava** | **Quartzite**] Aerial View Lava first deposited, surface was eroded, SS deposited over the eroded surface. Thereafter, tilting occurred millions of years later.

122

84	S 25°24'12,8" E 29°30'48,0"	SM49		Lava, olivine?
85	S 25°24'13,7" E 29°30'48,4"	SM50		Lava with black and white crystals
86	S 25°24'12,0" E 29°30'53,0"	SM51		Lava, phenocrysts
87	S 25°24'11,9" E 29°30'59,3"	SM52		Brown-Black Lava (Peak), porphyric, euhedral phenocryst
88	S 25°24'12,8" E 29°30'04,1"	SM53	02h16 (×2)	- Further down, quartzite amygdales are found - Top of the lava flow, full of vesicles (concentrated) therefore amygdales formed
89	S 25°24'15,2" E 29°30'05,3"	SM54	02h24 (×4)	Magma + wet sediment = pepperitic texture
90	S 25°24'26,2" E 29°30'37,9"	SM55		Granophyre
91	S 25°24'01,1" E 29°30'56,0"	SM56		
92	S 25°24'49,7" E 29°30'54,1"	SM57		Thick weathering skin brown red lava

Table 10 B: Depicts field data as write from the field, and later modified after analysis (for LD samples).

Stop	Co-ordinates	Sample	Picture	Elevation/Description
1	S 25°25'22,1" E 29°23'00,6"			
2	S 25°25'19,5" E 29°22'59,8"			
3	S 25°25'17," E 29°23'00,7"			
4	S 25°25'16,6" E 29°22'59,9"	LD002	10:57	El: 1134 m, Brown-red lava Lava, flow bands
5	S 25°25'15,2" E 29°22'59,9"	PLD003		El: 1135 m, Breacciated lava. Top of LD002
6	S 25°25'14,0" E 29°22'59,9"	LD005 part of LD004	11:43	El: 1140 m, Red lava, Micro-spherulites
7	S 25°25'11,9" E 29°22'59,1"	LD006		El: 1173 m, Red lava with visible quartz crystals
8	S 25°25'11,9" E 29°22'59,1"	LD007		EL: 1173 m, Red lava with small visicles
9	S 25°25'17,5" E 29°22'57,0"	No sample		El: 1144 m, carapace
10	S 25°25'19,9" E 29°22'58,0"	No sample		El: 1086 m, red lava
11	S 25°25'15,7" E 29°22'28,6"	LD008	14th /09 start	El: 1063 m, Red lava
12	S 25°25'14,2" E 29°22'28,5"	LD009		El: 1089 m, grey-red lava
13	S 25°25'13,1" E 29°22'29,1"	LD010	9:26 9:29	El:1101 m, red lava, flow bands
14	S 25°25'12,3" E 29°22'29,8"	LD011		El: 1101 m, red lava with cooling bands,
15	S 25°25'12,6" E 29°22'19,3"	LD012		El: 1058 m, red lava
16	S 25°25'10,7" E 29°22'19,4"	LD013		El: 1066 m, brown-red lava

17	S 25°25'00,6" E 29°22'21,9"	LD014		El: 1127 m, Highly vesiculated red-brown lava of same size (0.5-1 cm). Few large amygdales (7.9 cm)
18	S 25°25'07,9" E 29°22'19,9"	Rock C		El: 1081 m. Same as LD014 but less % of vesicles
19	S 25°25'12,3" E 29°22'04,1"	LD015	15th /09	El: 1061 m, fine aphyric red lava
20	S 25°25'09,8" E 29°22'04,6"	LD016		El: 1092 m, aphyric red lava (core)
21	S 25°25'08,4" E 29°22'02,7"	LD017		Core of lava flow grey-brown
22	S 25°25'06,0" E 29°22'01,0"	LD018		El: 1141 m, red lava with minor flow foliation
23	S 25°25'04,6" E 29°22'02,4"			Not in situ green rock
24	S 25°25'02,1" E 29°22'03,1"	LD019	10:53	El: 1142 m, grey lava with green mineralised amygdales
25	S 25°24'58,4" E 29°22'05,8"	LD020		El: 1144 m, red lava (fine texture)
26	S 25°24'55,1" E 29°22'09,4"	LD021		El: 1156 m, same as LD020
27	S 25°24'52,1" E 29°22'11,5"	LD022	(12:22 -LD022) (pic 103-3783 sandstone)	El: 1226 m, red lava, probable near southern contact to conglomerate(horizontally bedded, matrix supported- sandy matrix, clasts - 8.5 Cross bedding sandstone
28	S 25°24'51,2" E 29°22'11,5"	LD023		El: 1235 m, vesicular red lava, northern contact with horizontally bedded fine-grained sandstone
29	S 25°24'51,4" E 29°22'09,8"			sandstone
30	S 25°24'51,8"			sandstone

	E 29°22'11,6"			
31	S 25°25'12,1" E 29°22'32,7"	LD024		El: 1138 m, red lava with white phenocrysts (probable plagioclase
32	S 25°25'08,8" E 29°22'41,4"	LD025		El: 1206 m, red lava in contact with white bedded chert (striking 262 E-W
33	S 25°25'09,2" E 29°22'42,8"	X		WHITE BEDDED CHERT
34	S 25°25'08,2" E 29°22'44,7"	LD026		El: 1234 m, red lava with sparsely distributed vesicles
35	S 25°25'00,3" E 29°22'51,3"	LD027		El: 1264 m, red lava
36	S 25°25'07,9" E 29°22'19,9"	LD028		Grey-red lava, less vesiculated but bigger cavities (1-5 cm)

Appendix B

Table 11: Analysed samples (Note the coordinates of these samples are found in appendix A)

No.	Sample name	rock type	Chemical composition	Formation
1	SM-23	lava	Dacite	Damwal
2	SM-25	lava	Rhyolite	Schrikkloof
3	SM-28.2	lava	Rhyodacite	Schrikkloof
4	SM-38.1	lava	Dacite	Damwal
5	SM-44.1	lava	Dacite	Damwal
6	SM-45.1	lava	Dacite	Damwal
7	SM-48	lava	Dacite	Kwaggasnek
8	SM-50	lava	Dacite	Damwal
9	SM-51.1	lava	Dacite	Damwal
10	SM-4.1	lava	Dacite	Kwaggasnek
11	SM-RL1	lava	Dacite	Damwal
12	SM-3	lava	Dacite	Damwal
13	SM-5.1	lava	Dacite	Damwal
14	SM-5.2	lava	Rhyolite	Schrikkloof
15	SM-6	lava	Dacite	Damwal
16	SM-10	lava	Dacite	Damwal
17	SM-13	lava	Dacite	Damwal
18	SM-14	lava	Dacite	Damwal
19	SM-18.1	lava	Rhyolite	Schrikkloof
20	SM-19	lava	Rhyolite	Schrikkloof
21	SM-22	lava	Rhyodacite	Schrikkloof
22	LD016	lava	Rhyodacite	Kwaggasnek
23	LD07	lava	Rhyodacite	Kwaggasnek
24	LD018	lava	Rhyodacite	Kwaggasnek
25	LD04	lava	Rhyodacite	Kwaggasnek
26	LD02	lava	Rhyodacite	Kwaggasnek
27	LD015	lava	Rhyodacite	Kwaggasnek
28	LD012A	lava	Rhyodacite	Kwaggasnek
29	LD012B	lava	Rhyodacite	Kwaggasnek
30	LD028	lava	Dacite	Damwal
31	LD026	lava	Dacite	Damwal
32	LD09	lava	Rhyodacite	Kwaggasnek
33	LD019	lava	Dacite	Damwal
34	LD017	lava	Rhyodacite	Kwaggasnek
35	LD08	lava	Rhyodacite	Kwaggasnek
36	LD010	lava	Rhyodacite	Kwaggasnek
37	LD011	lava	Rhyodacite	Kwaggasnek
38	LD013	lava	Rhyodacite	Kwaggasnek
39	LD014	lava	Dacite	Damwal
40	LD020	lava	Dacite	Damwal
41	LD021	lava	Dacite	Damwal

Appendix C

Petrography: Other analysed lava textures
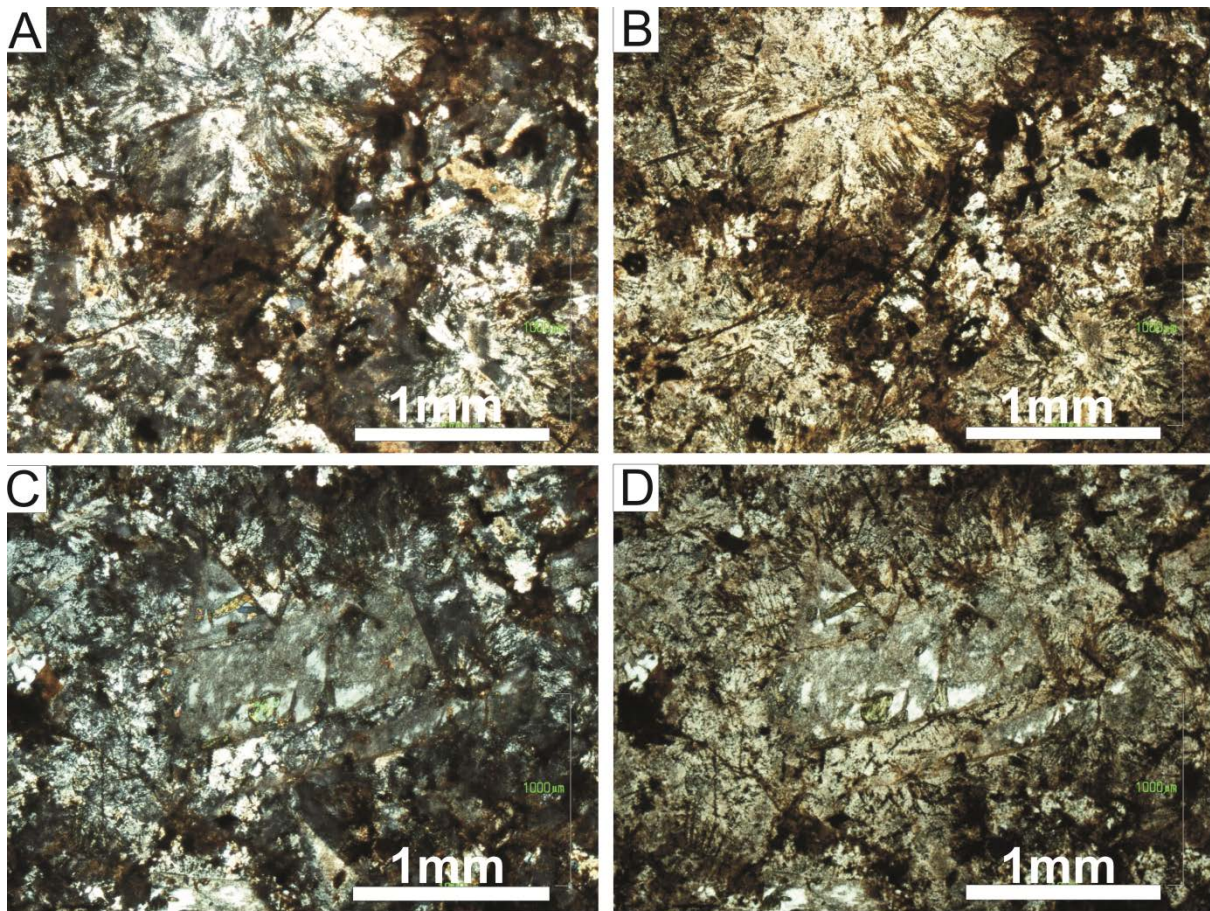
Photomicrographs of dacitic lava (sample SM 51 Damwal Formation). This rock is dominated by the micro-spherulitic texture (pictures A-D). Like LD028, some spherulites completely engulf plagioclase crystals (C and D). The spherulites have the size range from 1 mm to 5 mm. Rare plagioclase crystals are <2 mm. Pictures A and C are taken in cross polar while B and D in non-polar light.
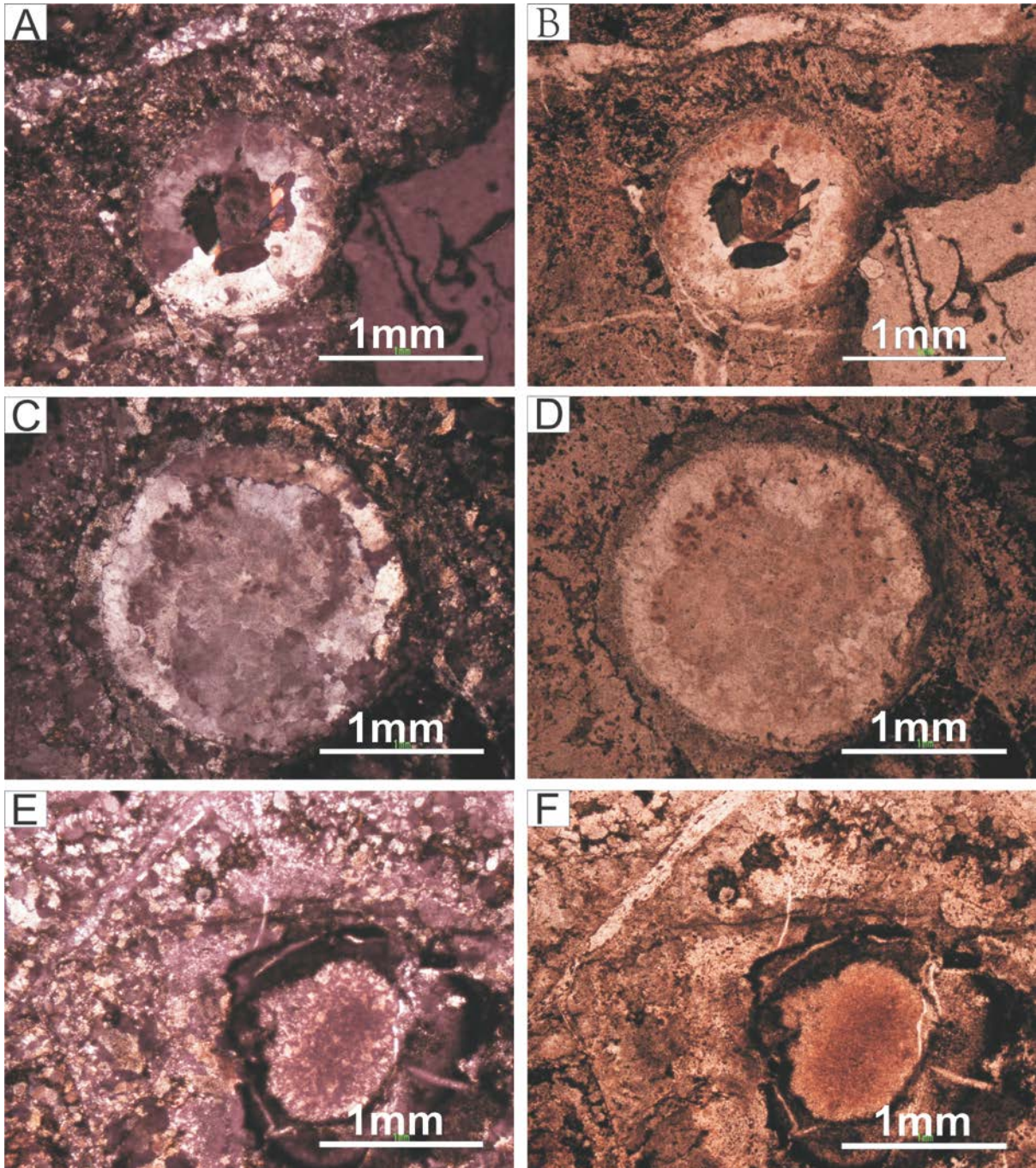
Photomicrographs of rhyodacitic lava (sample SM17 Damwal Formation). This rock consists of recrystallized glass with minor quartz filled veins. It consists of 5% amygdales (1-3 mm diameter) which appear to be well rounded. The amygdales are either filled with concentric quartz layers (C and D) or concentric layers of quartz (outer layer) and quartz, amphibole and biotite (inner layer) (A and B). The spherical characteristic of vesicles is normally associated with pahoehoe lava flows and indicates that gasses were still exsolved when the lava solidified. A, C and E are taken in polarised light while B, D and F are in non-polar.

129
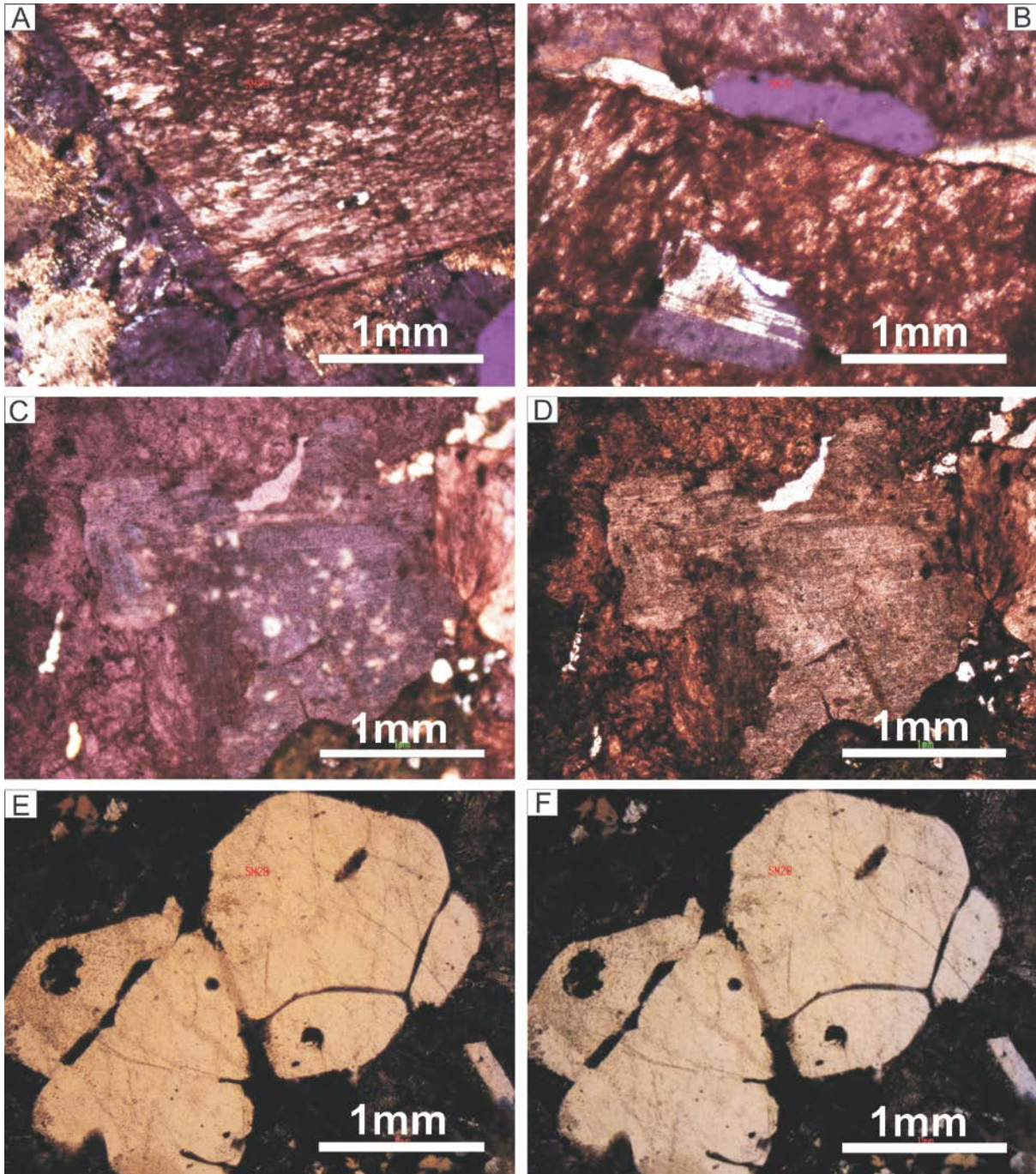
Photomicrographs of rhyodacitic lava (sample SM28; Schrikloof Formation). A-B show huge (~1 cm) feldspar crystals. B shows the inclusion of plagioclase in k- feldspar. C and D show unhedral plagioclase being corroded by amphibole (bottom left). Note the granophyric material surrounding the embayed and resorbed quartz crystals (pictures E and F) and euhedral plagioclase picture A). A, B, C and E are taken in polarised light while D and E are in non-polar.
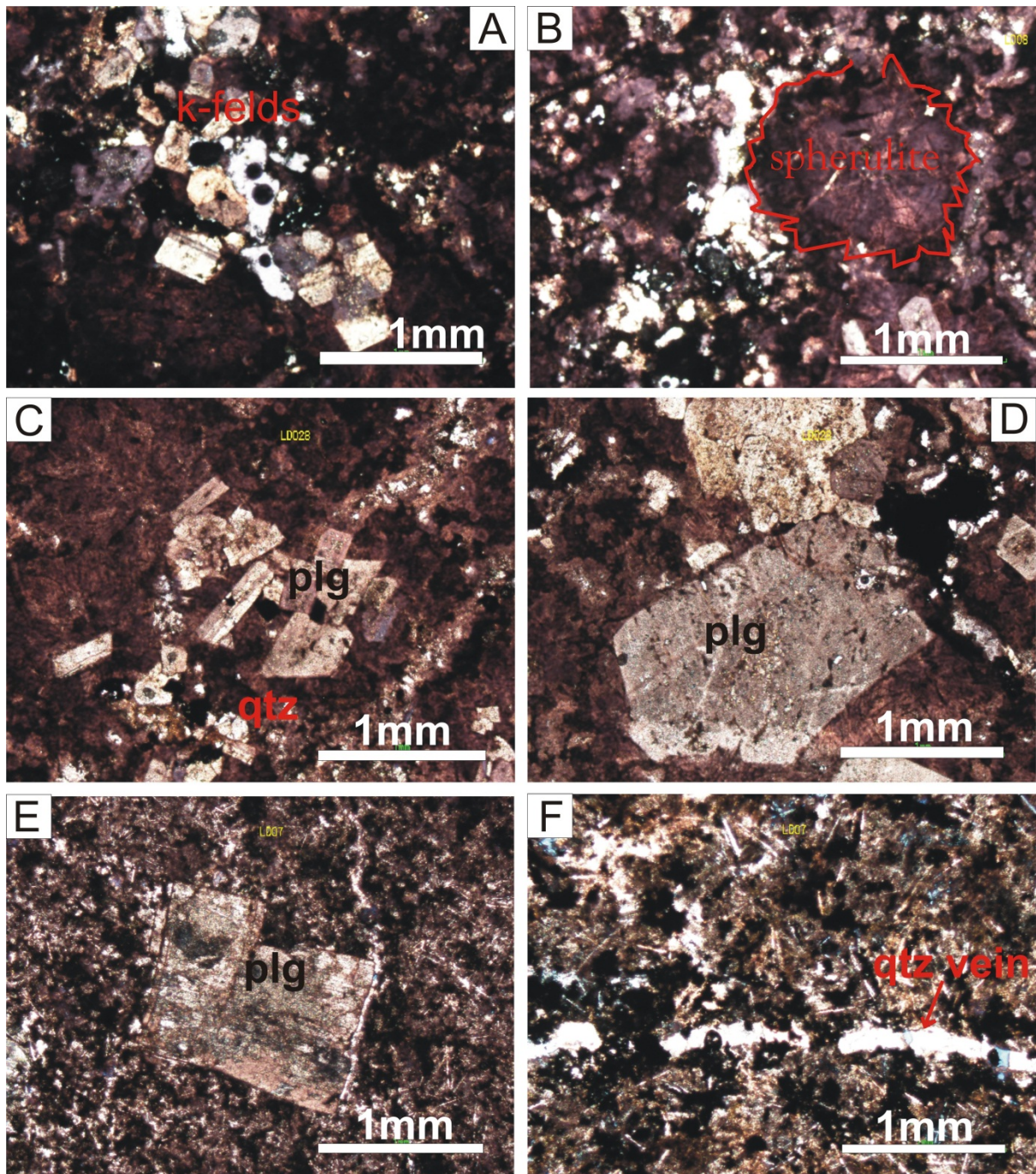
Photomicrographs of rocks from Damwal Formation (sample LD028, pictures C and D) and Kwaggasnek Formation [samples LD08 (pictures A and B) and LD07 (pictures E and F)]. A-B and C-D show similar textures clusters of feldspar crystals and micro spherulites (picture B, in red highlight). These spherulites are oftenly seen with engulfed plagioclase. The feldspars are mainly euhedral plagioclase and minor k- feldspar. Rare rounded quartz is also observed. E shows at least 1 % porphyritic texture. Plagioclase phenocrysts are set in a recrystallised groundmass consisting of elongate microlites of quartz as replacement mineral

131

after plagioclase and devitrified glass with quartz filled veins (F). A, B and F are taken in polarised light while C, D and E are in non- polar.
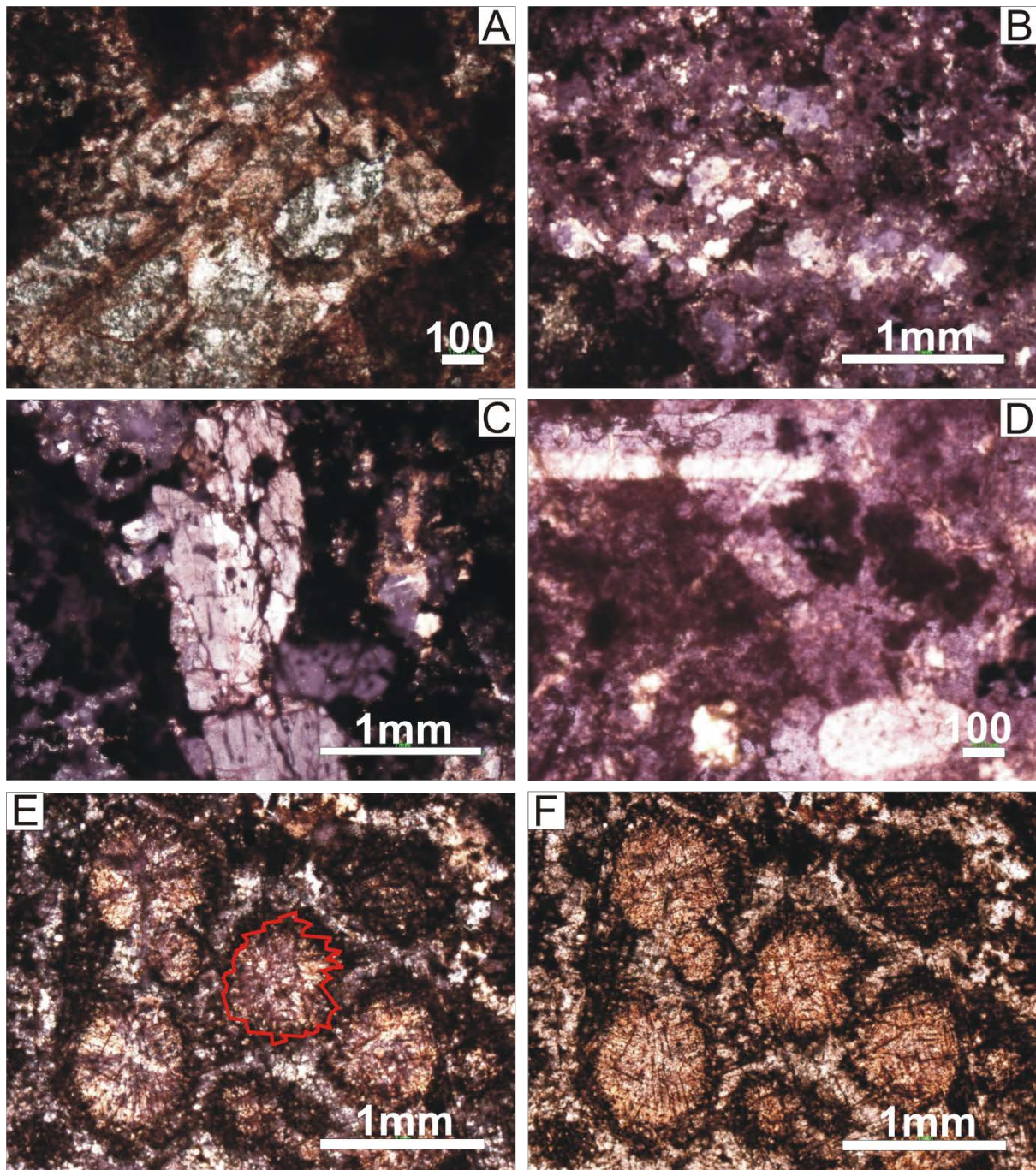
Photomicrographs of rocks from Kwaggasnek Formation (LD011, pictures A-D) and Damwal Formation (RL1, pictures E and F). LD011 consist of 2 % euhedral (A and D) and corroded (C) plagioclase phenocrysts. B shows the recrystallized texture of the groundmass consisting of plagioclase quartz and k-feldspar. E and F shows apredominately micro spherulitic texture set in a devitrified material. Pictures A and D have a white line

representing 100 micrometer scale. B, C and E are taken in polarised light while A, D and F are in non-polar.
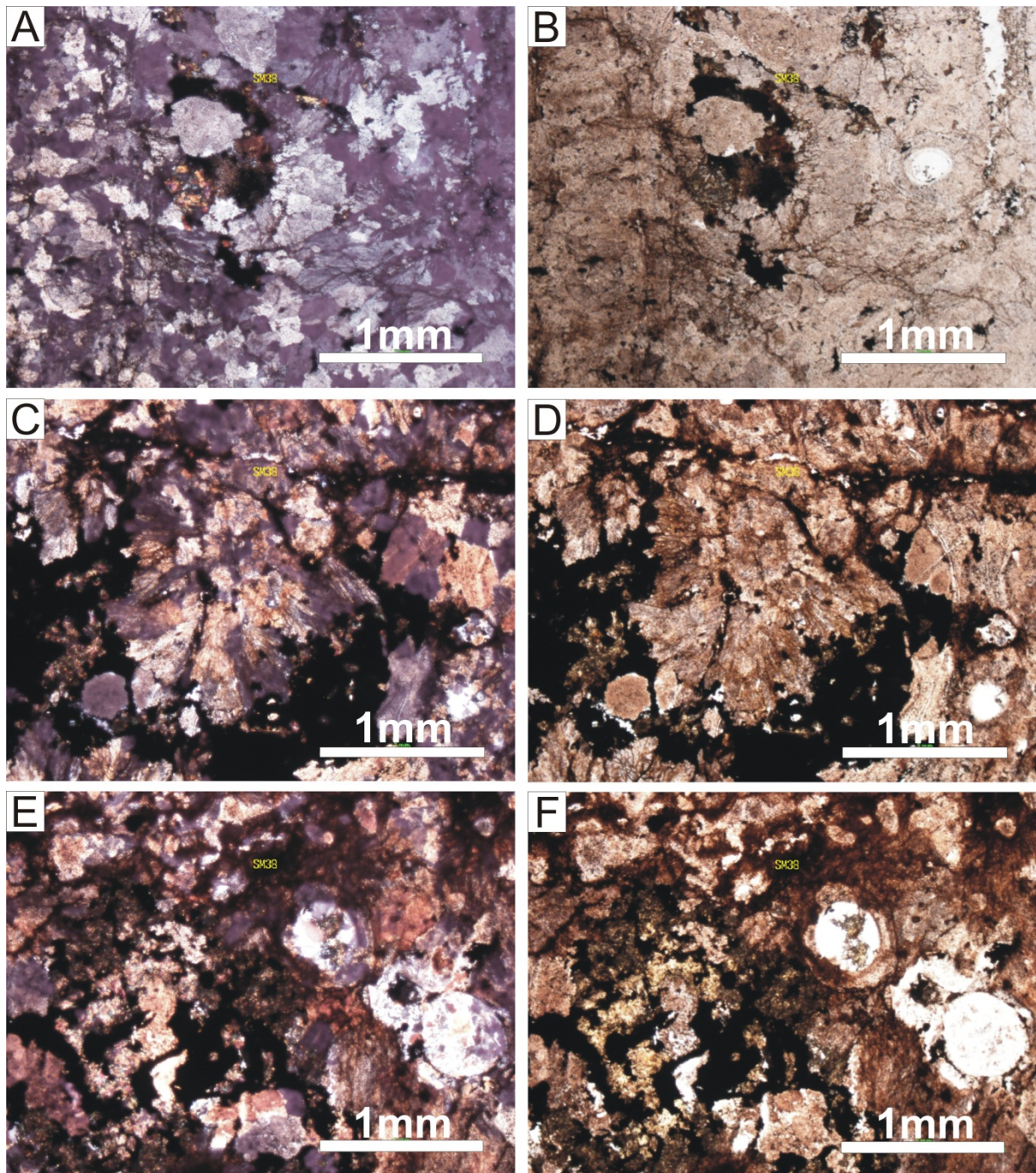
Photomicrographs of dacitic glass from Damwal Formation (sample SM38.1). The texture is dominated by perlitic fractures set in a devitrified glass. The glass has completely recrystallized (picture A-B). Pseudospherulites (centre of pictures C-D) and well-rounded zoned amygdales (middle left of pictures E-F) are also observed.
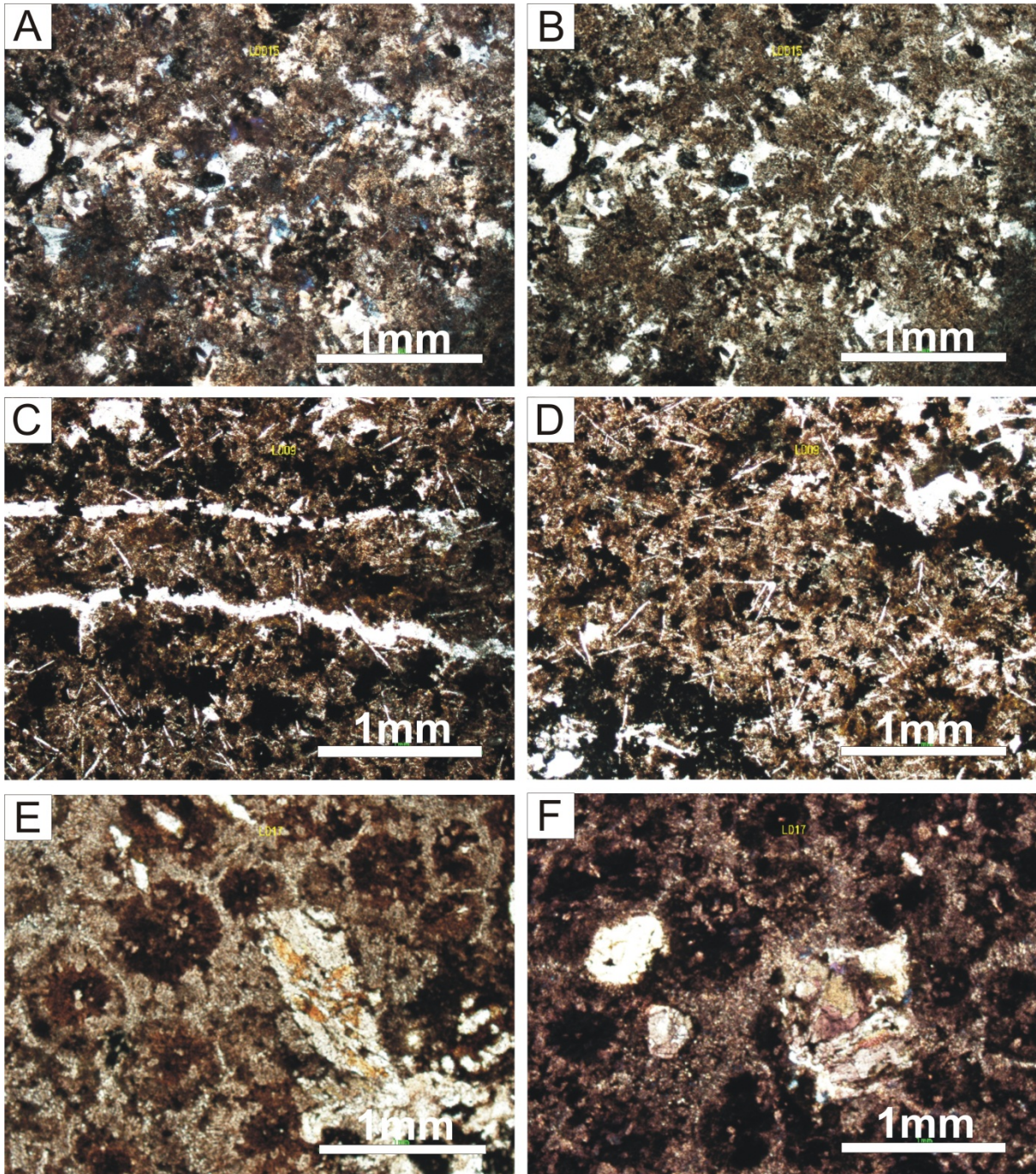
Photomicrographs of rocks found in Kwaggasnek Formation. Pictures A-B (sample LD015) show minor small (0.3 mm) euhedral plagioclase crystals with anhedral quartz patchily distributed in a recrystallized groundmass. C-D (sample LD09) show elongated microlites of quartz (as a replacement mineral of plagioclase) in a groundmass of devitrified glass. Minor quartz veins are also common (C). E-F (sample LD017) show textures similar to sample RL1 but with additional plagioclase phenocrysts that edge and cleavage altered by orange-yellow alteration products. A, C and F are in cross polarised light while B, D and E are in non-polar.
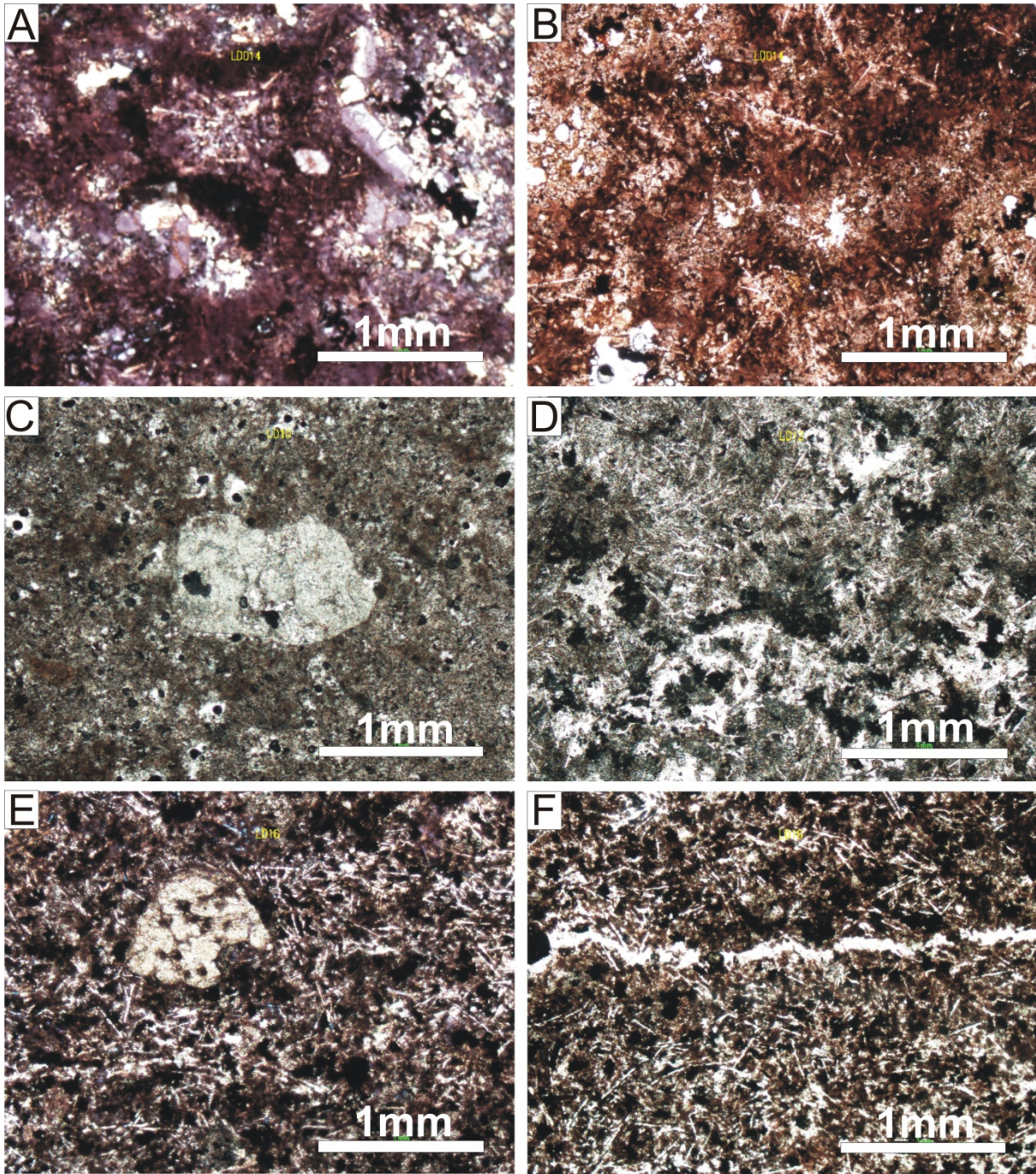
Photomicrographs of rocks found in Damwal Formation (sample LD014) and Kwaggasnek Formation (samples LD010 and LD016). All this rocks have similar texture dominated by devitrified glass with a randomly arranged elonagate microlites and 1-2 % phenocrysts content. The microlite minerals are more concentrated in LD016. However, A shows lath shaped plagioclase while C and E show resorbed plagioclase.
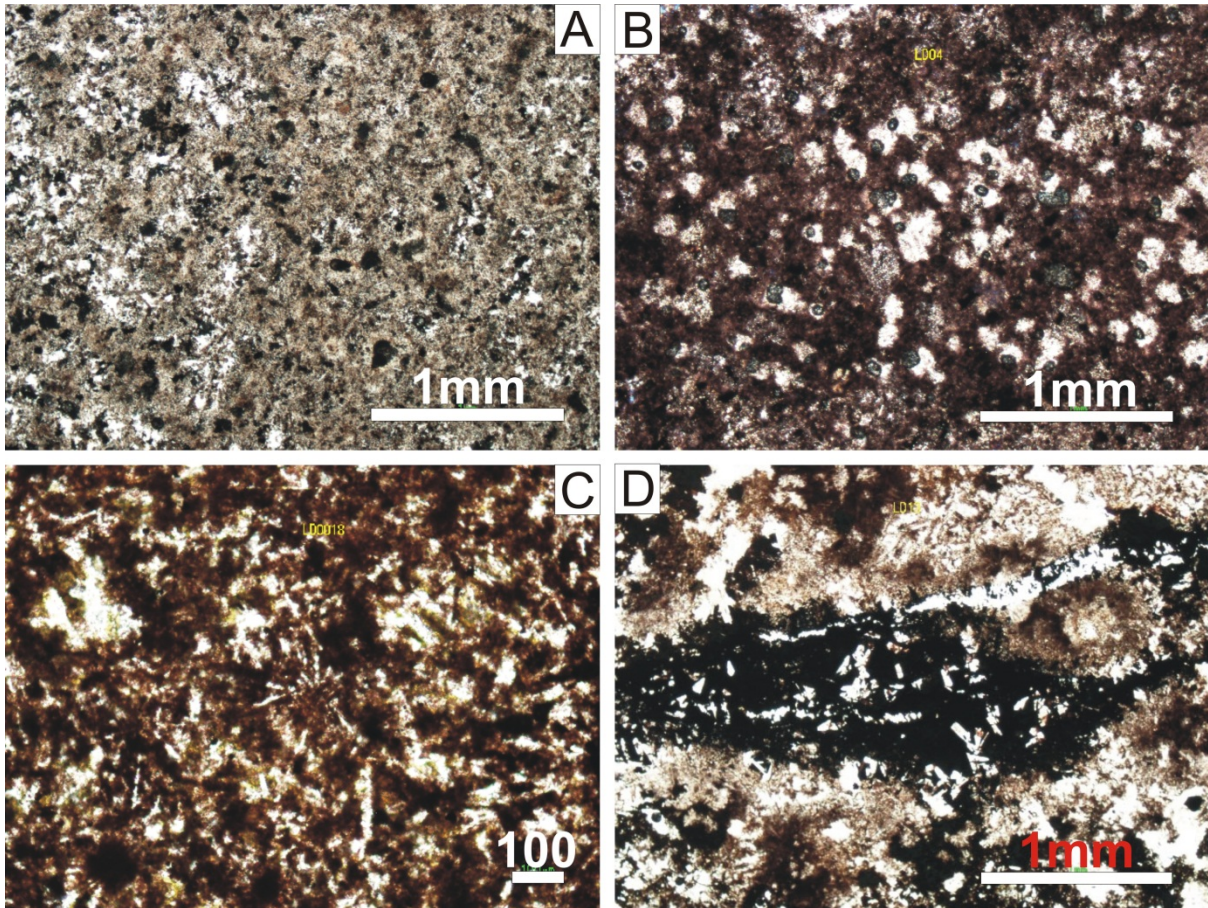
Micrographs of samples from Kwaggasnek Formation. A and B (samples LD002 and LD004 respectively) shows recrystallized glass with patches of microcrystalline plagioclase and quartz. C (sample LD018) shows elongated dendritic microlites of plagioclase. This is a common texture suggesting rapid growth. D (sample LD013) shows devitrified glass surrounding euhedral microcrystalline plagioclase. All pictures are taken in non-polarised light.
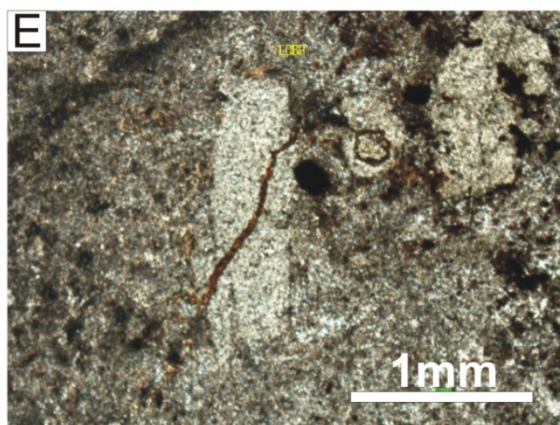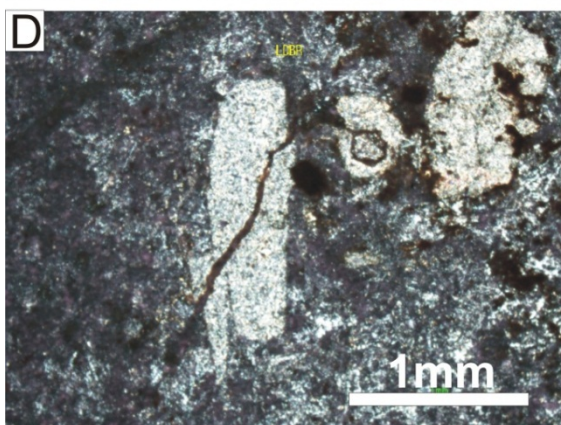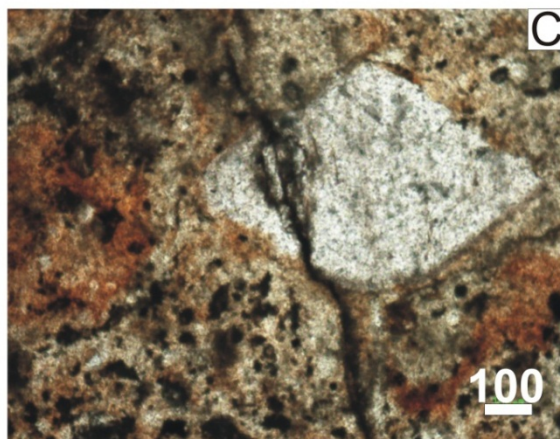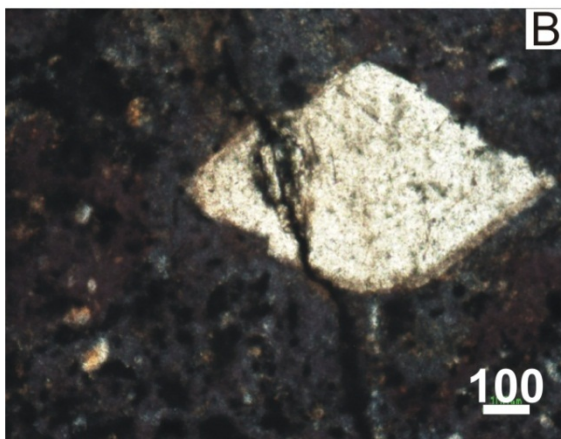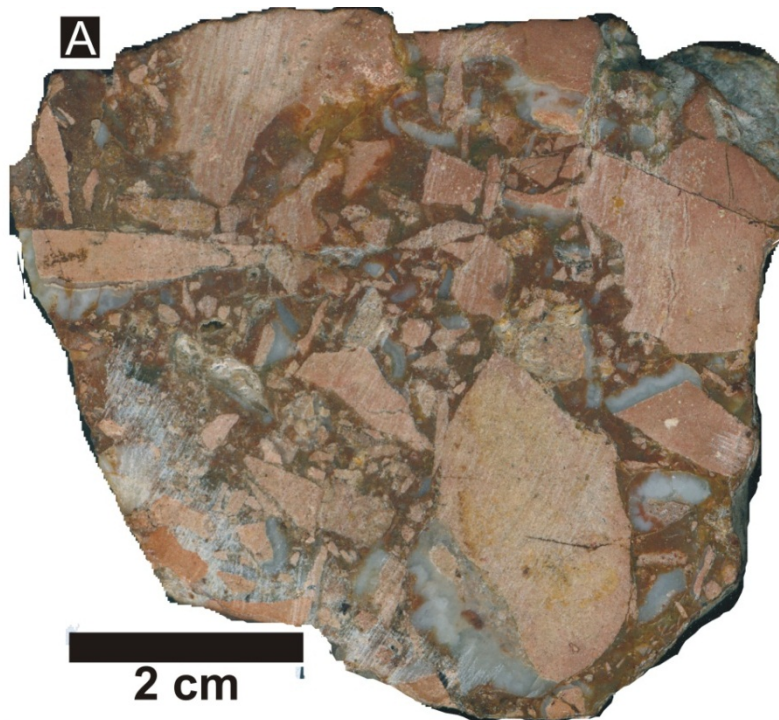
Picture A represent the polished slap of the carapace. The clast sizes range from 5 mm to 20 cm. The brecciated rock show probable strain fractures produced during slow movement of the carapace. The fractures are seen from both macro (clasts) and micro (plagioclase) scale. A-B and C-D show diapyramid and elongate subhedral feldspar phenocrysts in a quenched glass.

137

Appendix D

Table 12: Major element oxide's data of the Rooiberg Group samples. Chemical Index of Alteration (CIA) is calculated using Nesbitt and Young, (1982)

Sample	Formation*	SiO2	Al$_2$O$_3$	Fe$_2$O$_3$	MgO	CaO	MnO	Na$_2$O	K$_2$O	TiO$_2$	P$_2$O$_5$	LOI	CIA
SM-23	DW	69.11	11.62	7.14	0.26	2.62	0.14	2.23	4.60	0.58	0.12	1.60	55.15
SM-38.1	DW	70.12	11.43	7.33	0.07	3.63	0.07	3.34	1.23	0.56	0.13	1.81	58.23
SM-44.1	DW	67.08	12.04	7.80	0.68	2.10	0.14	3.59	3.05	0.66	0.17	1.73	57.94
SM-45.1	DW	68.27	12.38	7.52	0.40	2.56	0.11	3.59	3.47	0.65	0.17	1.65	56.27
SM-50	DW	69.06	11.83	7.39	0.17	1.19	0.12	2.74	4.97	0.53	0.11	1.80	57.07
SM-51.1	DW	69.67	12.09	7.37	0.19	0.89	0.13	2.95	4.69	0.57	0.12	1.75	58.63
SM-RL1	DW	68.78	12.17	8.26	0.32	0.09	0.10	2.92	3.69	0.64	0.13	2.39	64.49
SM-3	DW	67.40	12.94	7.94	0.48	2.18	0.12	2.54	5.31	0.69	0.17	0.84	56.33
SM-5.1	DW	66.07	11.94	9.77	0.44	2.55	0.16	2.82	3.75	0.65	0.23	1.29	56.70
SM-6	DW	67.63	12.03	9.03	0.32	1.74	0.13	2.92	4.16	0.60	0.17	1.08	57.70
SM-13	DW	72.86	11.22	6.21	0.91	0.59	0.12	2.44	2.73	0.64	0.13	1.86	66.08
SM-14	DW	66.96	11.96	9.10	0.03	1.91	0.14	2.93	4.08	0.61	0.18	1.66	57.28
LD028	DW	68.93	11.83	7.74	0.67	1.02	0.10	2.44	4.12	0.59	0.15	2.13	60.95
LD026	DW	65.65	11.42	8.05	0.25	2.80	0.12	1.86	4.56	0.05	0.10	3.43	55.33
LD019	DW	69.03	12.20	9.98	0.03	0.63	0.06	2.50	5.04	0.66	0.21	1.34	59.89
LD014	DW	67.19	11.77	9.87	0.03	0.61	0.06	2.41	4.93	0.61	0.21	2.06	59.69
LD020	DW	68.64	11.59	7.77	0.25	1.71	0.11	1.99	1.71	0.56	0.16	3.02	59.68
LD021	DW	68.27	11.74	7.25	0.49	1.74	0.13	2.03	4.00	0.61	0.18	3.13	60.17
SM-48	KG	70.11	11.59	6.78	0.12	1.04	0.14	2.47	4.58	0.41	0.05	1.91	58.89
SM-4.1	KG	80.84	7.13	5.35	0.13	00.0	0.05	0.01	3.61	0.40	0.07	1.94	66.33
SM-10	KG	71.89	11.40	5.85	0.11	0.91	0.06	2.33	4.99	0.44	0.07	1.81	58.08
LD016	KG	69.44	11.12	5.64	<0.01	2.07	0.09	1.96	5.00	0.37	0.03	2.97	55.19
LD007	KG	69.86	12.40	6.61	0.07	0.59	0.06	2.00	4.01	0.40	0.08	2.46	65.26
LD018	KG	70.74	11.75	6.57	0.06	0.14	0.09	2.58	4.22	0.41	0.04	1.85	62.87
LD004	KG	74.19	12.21	5.75	0.04	<0.01	0.03	1.54	5.24	0.39	0.03	1.85	00.00
LD002	KG	71.24	11.32	7.37	<0.01	<0.01	0.12	2.76	4.10	0.37	0.03	1.61	00.00
LD015	KG	77.08	11.41	1.49	<0.01	<0.01	<0.01	1.68	5.30	0.36	0.02	1.55	00.00
LD012A	KG	69.80	11.47	5.94	0.10	2.49	0.11	1.23	5.10	0.38	0.03	4.93	56.53
LD012B	KG	68.94	11.14	5.76	0.02	2.08	0.13	1.83	5.07	0.37	0.03	3.05	55.37
LD009	KG	69.34	12.58	6.15	0.05	2.01	0.10	2.40	5.05	0.39	0.03	3.06	57.08
LD017	KG	70.88	13.21	5.18	0.10	<0.01	0.01	2.99	4.69	0.39	0.05	1.90	00.00
LD008	KG	76.18	13.28	1.11	0.01	<0.01	0.01	0.42	6.21	0.37	0.02	1.91	00.00
LD010	KG	71.91	11.79	5.96	0.02	<0.01	0.04	1.57	4.81	0.39	0.06	2.04	00.00
LD011	KG	71.97	11.26	6.17	<0.01	<0.01	0.03	2.38	4.90	0.42	0.03	1.48	00.00
LD013	KG	73.81	11.27	3.65	<0.01	1.56	0.05	2.41	4.31	0.39	0.04	2.33	57.65
SM-25	SC	73.93	11.73	3.50	0.05	0.00	0.06	3.24	4.52	0.25	0.01	1.58	60.18
SM-28.2	SC	74.28	12.13	3.94	0.30	0.00	0.08	3.39	4.54	0.29	0.02	1.08	60.47
SM-5.2	SC	73.47	12.90	3.48	0.03	0.00	0.02	2.99	5.35	0.21	0.03	1.57	60.73
SM-18.1	SC	76.37	10.92	3.37	0.04	0.12	0.04	2.33	5.19	0.24	0.01	0.86	58.84
SM-19	SC	73.72	12.08	3.70	0.02	0.06	0.03	2.54	5.73	0.27	0.01	1.21	59.19
SM-22	SC	79.54	7.70	4.38	0.08	0.74	0.07	1.98	2.97	0.26	0.05	1.31	57.51

*(SC = Schrikloof Formation, KG = Kwagganek Formation, DW = Damwaal Formation)

138

Appendix E

Table 13: Trace elements data of the Rooiberg Group samples. The values are in parts per million (ppm). <d.l. = below detection limits

Sample	Formation	Li	Sc	V	Cr	Co	Ni	Cu	Zn	Rb	Sr	Y	Zr	Nb	Ba	La	Ce	Pr	Nd	Sm	Eu	Tb	Gd	Dy	Ho	Er	Tm	Yb	Lu	Hf	Ta	Pb	Th	U
SM-23	DW	24.6	11.6	1.77	0.57	113	< d.l.	34.9	149	132	114	49.5	313	16.2	869	62.3	123	13.7	52.6	10	2.01	1.48	9.68	9.33	1.88	5.46	0.8	5.23	0.78	8.11	1.1	25	19	4.72
SM-25	SC	7.22	< d.l.	1.15	1.38	303	3.35	11.8	133	158	55	74.2	312	23.1	877	107	156	22.5	87.3	15.8	2.54	2.26	14.6	14.1	2.84	8.17	1.19	7.75	1.15	8.99	1.67	11	26	6.26
SM-28.2	SC	13.5	< d.l.	1.54	2.78	107	1.74	9.23	126	158	62	87.2	328	24.2	963	117	181	22.9	88.7	16.3	2.88	2.63	17.6	16.3	3.27	9.25	1.31	8.36	1.22	9.33	1.6	12	25	5.17
SM-38.1	DW	11.2	8.99	15.1	2.53	128	< d.l.	61.2	73.9	54.2	353	40.4	269	13.8	198	61.4	107	12.2	45.3	8.16	1.85	1.27	8.31	7.8	1.55	4.38	0.62	4	0.59	6.97	1.03	57	16	3.78
SM-44.1	DW	13.5	10.6	20.4	0.96	101	< d.l.	19.3	119	91	125	39.6	290	14.3	737	57	111	12.6	47.3	8.77	1.57	1.18	7.71	7.26	1.47	4.22	0.62	4.07	0.61	7.64	1.05	19	18	4.62
SM-45.1	DW	5.24	9.88	14.4	2.57	182	< d.l.	7.22	100	103	253	41.6	287	14.4	512	59.9	118	13.2	50.4	9.43	1.76	1.23	8.14	7.62	1.52	4.31	0.62	4.12	0.61	7.55	1.32	137	18	4.7
SM-48	KG	16.1	4.27	0.3	0.7	240	0.64	15.4	164	154	81	57.7	368	18	971	72.1	138	15.5	60.6	11.3	1.94	1.59	10.2	10.2	2.09	6.11	0.9	5.93	0.89	9.53	1.27	34	22	5.59
SM-50	DW	8.28	7.12	2.12	0.54	120	< d.l.	28.1	165	167	105	44.9	323	16	985	62.4	121	13.5	52.5	9.75	1.6	1.28	8.35	8.02	1.62	4.69	0.69	4.6	0.69	8.42	1.13	46	21	5.31
SM-51.1	DW	7.06	7.39	2.42	0.64	153	0.11	25.8	216	146	104	45.6	316	15.8	997	63.4	138	14.1	53.8	10.1	1.62	1.29	8.32	8.17	1.65	4.77	0.7	4.68	0.69	8.29	1.21	71	21	5.21
SM-4.1	KG	59.2	3.96	29.1	57.9	99	23.5	10.9	28	140	58	12.6	170	5.38	900	43.6	40.6	7.74	25.4	4.28	0.73	0.44	3.04	2.53	0.47	1.31	0.19	1.31	0.2	4.56	0.45	21	9.7	2.17
SM-RL1	DW	9.05	7.28	7.09	1.06	107	1.44	39.4	162	116	60	45.4	328	15.9	814	61.2	124	14.4	54.8	10.4	1.63	1.29	8.41	8.1	1.64	4.72	0.69	4.6	0.69	8.7	1.18	27	20	4.55
SM-3	DW	12.4	9.29	13.7	1.64	88.7	< d.l.	24.4	160	144	138	44.8	322	16.4	1216	58.9	116	12.9	48.9	8.9	1.61	1.31	8.58	8.01	1.62	4.77	0.69	4.49	0.67	8.38	1.12	56	20	5.05
SM-5.1	DW	20.4	13.8	2.18	0.92	55.3	< d.l.	35.7	149	122	154	51	296	16.5	852	60.1	120	13	49.5	9.08	2.25	1.54	10.1	9.36	1.89	5.48	0.77	5.08	0.75	7.52	1.03	23	17	4.24
SM-5.2	SC	9.05	0.78	8.91	3.4	135	5.48	21.2	62.7	184	101	34.9	226	20.8	571	22.1	54.8	6.63	25.9	5.27	1.04	0.92	5.64	5.94	1.25	3.93	0.61	4.17	0.61	6.69	1.86	53	35	7
SM-6	DW	21.3	11.1	1.7	0.39	54.1	< d.l.	36.1	145	136	117	53.2	319	17	897	62.3	124	13.3	50.4	9.27	2.22	1.58	10.6	9.83	1.97	5.7	0.81	5.35	0.79	8.11	1.11	21	18	4.48
SM-10	DW	5.33	4.48	0.38	0.75	532	1.81	25.3	73.9	186	91	69	355	18.2	997	82.5	150	17.7	66.3	12.3	2.22	1.84	12	11.6	2.38	6.96	0.99	6.46	0.98	9.25	1.59	13	20	5.18
SM-13	DW	74.7	4.9	46.2	60.7	135	16	25.7	206	107	110	32.1	385	12.9	1063	61.9	121	13	48	8.08	1.19	1.02	7.12	5.91	1.18	3.52	0.51	3.43	0.52	10.1	0.94	56	23	4.76
SM-14	DW	18.2	8.28	3.65	4.43	145	< d.l.	26.2	99.8	180	116	52.7	341	17.5	1088	64.3	125	13.5	51.4	9.55	1.95	1.48	9.62	9.22	1.89	5.62	0.81	5.35	0.79	8.84	1.18	20	21	5.17
SM-18.1	SC	11.1	< d.l.	0.19	0.61	128	0.6	22.8	68.2	184	69	71	427	20.1	1149	80.7	155	17.6	66.1	12.2	1.8	1.93	12.1	12.5	2.56	7.67	1.11	7.21	1.07	10.9	1.36	37	23	4.15
SM-19	SC	17.6		0.62	0.93	322	2.13	21.3	104	207	83	62.2	480	23.7	1269	78.3	140	17	63.7	11.7	1.99	1.77	11.4	11.2	2.31	6.93	1.02	6.81	1.02	12.1	1.73	27	26	4.17
SM-22	SC	6.51	1.63	0.58	2.38	131	0.7	42	111	103	53	46.2	268	13.5	679	49.2	90.9	10.5	39.9	7.72	1.5	1.25	7.96	7.95	1.62	4.83	0.7	4.51	0.66	6.83	0.88	35	15	3.47

Table 13 continue…

Sample	Formation	Li	Sc	V	Cr	Co	Ni	Cu	Zn	Rb	Sr	Y	Zr	Nb	Ba	La	Ce	Pr	Nd	Sm	Eu	Tb	Gd	Dy	Ho	Er	Tm	Yb	Lu	Hf	Ta	Pb	Th	U
LD016	KG	7.79	2.47	0.28	0.17	103	< d.l.	5.67	87	189	69	60.7	352	16.5	1953	82.7	138	16.8	62.7	11.9	2.06	1.67	11.3	10	2.04	6.12	0.88	5.8	0.86	9.27	1.14	50	22	5.73
LD07	KG	26.3	3.56	0.75	1.77	107	0.86	19.8	146	147	62	67.6	372	18	1197	91.4	144	18.2	68.9	12.9	2.39	1.89	13	11.3	2.31	6.85	0.97	6.46	0.96	9.77	1.25	36	21	5.73
LD018	KG	27.3	1.89	0.24	0.72	91	0.81	17.2	179	134	32	60.3	369	17.2	1197	84.2	146	17.6	66.7	12.6	2.17	1.72	11.9	10.3	2.09	6.2	0.87	5.87	0.88	9.71	1.2	18	21	5.51
LD04	KG	7.15	1.59	1.1	0.38	100	2.54	12.7	130	192	16	42.6	373	17.2	861	60.3	140	14	52.3	10.2	1.68	1.36	9.09	8.31	1.67	4.98	0.73	4.88	0.73	9.78	1.19	16	22	5.97
LD02	KG	5.75	2.85	0.84	1.35	123	1.44	11.7	180	147	28	55.3	360	16.9	811	67	129	14.9	56	11	1.84	1.58	9.96	9.85	2.01	5.99	0.86	5.78	0.86	9.51	1.17	13	23	6.06
LD015	KG	5.93	1.88	1.7	0.28	120	1.65	31.1	34.6	172	20	50.9	347	15.8	639	85	157	21.7	80.7	15.3	2.33	1.78	13.3	9.8	1.88	5.45	0.76	5.06	0.77	9.25	1.15	60	20	5.11
LD012A	KG	7.98	1.75	0.38	0.37	138	< d.l.	19.8	126	199	48	54.2	354	17	724	68.8	134	14.9	55.6	10.7	1.87	1.61	10.2	9.85	2.05	6.06	0.89	5.82	0.88	9.28	1.24	14	22	5.34
LD012B	KG	8.04	2.75	0.31	0.24	83.6	< d.l.	10.6	80.5	201	69	62	348	16.7	2077	91.8	143	17.7	65.8	12.2	2.1	1.73	11.8	10.4	2.1	6.27	0.9	5.89	0.89	9.12	1.18	36	22	5.59
LD028	DW	27.7	9.11	9.67	13.8	91.2	1.27	27.6	114	126	103	41.1	282	13.1	1016	53.9	107	11.7	43.9	8.38	1.62	1.23	7.99	7.5	1.53	4.5	0.66	4.29	0.65	7.4	0.95	34	18	4.41
LD026	DW	37.5	8.08	0.88	0.27	72.2	< d.l.	27.4	144	162	111	52.1	307	14.9	1006	61.5	121	13.4	50.7	9.8	1.91	1.46	9.41	9.13	1.86	5.56	0.79	5.31	0.79	8.09	1.05	15	19	4.82
LD09	KG	10.1	2.47	0.24	0.25	125	< d.l.	10.1	115	175	66	56.3	349	16.5	1158	78.8	135	16.1	60.5	11.5	1.98	1.62	10.9	9.92	2.02	6	0.87	5.76	0.85	9.2	1.17	19	22	5.33
LD019	DW	4.76	9.78	3.02	0.96	92.4	0.26	11	59.2	172	58	43	288	14.6	1353	51.5	109	12.2	46.9	9.32	1.84	1.29	8.65	8.01	1.63	4.79	0.69	4.6	0.69	7.48	1.02	19	17	4.78
LD017	KG	15.9	2.19	0.45	0.42	102	1.02	27.3	111	140	31	46	352	16.4	978	79.2	191	19.1	74.3	14.5	2.41	1.64	12.8	9.28	1.84	5.56	0.82	5.65	0.85	9.07	1.15	12	17	5.3
LD08	KG	6.68	1.87	1.03	1.44	159	2.18	7.91	46.6	212	23	54.6	358	16.3	2370	99.3	186	23.2	87.4	15.6	2.56	1.77	13.2	10.1	1.97	5.72	0.79	5.2	0.75	9.36	1.17	46	22	4.84
LD010	KG	6.91	1.62	0.76	0.71	122	1.57	16.5	149	175	25	63.9	378	17.6	1054	98.4	143	21.7	81	14.8	2.55	1.97	14.1	11.7	2.3	6.86	0.98	6.38	0.94	9.82	1.24	17	22	5.4
LD011	KG	6.28	2.42	0.48	0.65	152	1.92	7.43	150	171	30	57.2	378	18.4	875	72	144	15.9	59.4	11.4	2.13	1.69	11.2	10.3	2.15	6.67	0.97	6.42	0.97	9.84	1.34	20	21	5.79
LD013	KG	4.6	2.51	0.27	0.66	119	< d.l.	8	119	164	55	60.1	343	15.3	728	70.6	133	15.2	56.5	10.7	2.05	1.66	10.8	10.1	2.05	6.05	0.87	5.66	0.84	8.93	1.12	21	20	4.54
LD014	DW	32.6	10.7	24.1	14.3	69.5	3.67	37.8	155	137	124	41.7	276	12.3	1289	49.9	97.5	12.5	49.4	9.86	2.04	1.34	9.54	7.94	1.56	4.52	0.63	4.2	0.62	7.13	0.84	20	13	3.4
LD020	DW	6.09	8.01	10.6	12.2	93.3	< d.l.	9.11	144	158	51	39.5	272	12.6	651	54.4	108	12.2	45.4	8.72	1.74	1.23	8.4	7.37	1.46	4.36	0.63	4.19	0.62	7.12	0.87	67	16	4.03
LD021	DW	28.3	9.32	9.98	11	114	0.37	37.3	149	138	88	45.8	269	12.4	1798	56.1	108	12.8	48.7	9.65	2.01	1.39	9.56	8.3	1.64	4.89	0.67	4.38	0.65	7.03	0.86	17	16	3.89

Appendix F

Descriptive names of coherent lavas and intrusions (after McPhie, 1993)

Coherent lavas can be described based on four properties that characterise the rock. The four properties are further elaborated (below) and they include the mineral composition, lithofacies, texture and the degree of alteration based on alteration minerals as summarised by tables 14 – 17.

Table 14: Descriptive classification of rocks based on the phenocryst assemblage and the not so reliable colour classification; hence the question mark is used after the name (after Mcphie 1993).

AA	Based on Phenocrysts (Slow cooling; big grains)	Rhyolitic	K-feldspar ± Quartz (±Ca poor plagioclase ±ferromagnesian phase: Biotite, Amphibole, Pyroxene, Fayalite)
AB		Dacite	Plagioclase ±ferromagnesian phase: Biotite, Amphibole, Pyroxene ± Quartz (± K-feldspar)
AC	Based on Phenocrysts (Slow cooling; big grains)	Andesite	Plagioclase ±ferromagnesian phase: Biotite, Amphibole, Pyroxene (± Olivine)
AD	Based on Phenocrysts (Slow cooling; big grains)	Basalt	Pyroxene + Ca rich plagioclase ± Olivine
AE	Based on Phenocrysts (Slow cooling; big grains)	Rhyolite? Dacite?	Pale grey, pink, cream, pale green
AF	Aphanitic Samples (minerals can't be seen with the naked eye or hand lense) Aphanitic Samples (minerlscan't be seen with the naked eye or hand lense)	Andesite? Basalt?	Dark grey, dark blue, dark green, dark purple

Mineral assemblages of phenocrysts and colour of the rock are used to suggest a descriptive name. For instance, if the rock is comprised of K-feldspar ± Quartz (±Ca poor plagioclase ±ferromagnesian phase: Biotite, Amphibole, Pyroxene, Fayalite in minor quantities) it can be assumed to be a rhyolite. Textural description is subdivided into crystallinityclass, subclass and the specific type. Table 7.2.3 divides porphyritic classes which may possibly be subdivided into both phenocryst and groundmass subclasses and furthermore quantify crystals by percentage abundancefocusing on the nature of groundmass (i.e. holocrystalline (90-100%), hypocrystalline (50-90%), hypohyaline (10-50%), and hyaline (0-10%); and grain sizein millimetres (i.e., coarse (≥ 5 mm), medium (1-5 mm) and fine (≤ 1 mm). Percentage abundance of vesicles is also applied in order to describe vesicle content of handsamples as depicted on Table 7.2.3. Altaration minerals and their distribution behaviour are used to determine the degree of alteration. Further, the degree of alteration is also specified (i.e.unaltered (<2%), slight (2-10%), moderate (10-40%), high (40-80%), very high (80-95%), complete (95-100%)) as seen from table 16.

Table 15: Descriptive classification of rocks based on the lithofacies (after McPhie 1993).

BA	Flow	Massive
BC	Flow	Flow-foliated
BD	Flow	Flow-banded
BE	Flow	Flow-laminated
BF	Jointing	Columnar
BG	Jointing	Radial-columnar
BH	Jointing	Concentric
BI	Jointing	Tortoise shell
BJ	Jointing	Blocky
BK	Jointing	Prismatic
BL	Jointing	Platy
BM	Pillows	Pillows
BN	Pillows	Pseudo-pillows

Table 16: Descriptive classification of rocks based on the texture assemblage and the not so reliable colour classification hence the question mark is used after the name (after McPhie 1993).

CA	Porphyrictic	Phenocryst	Type (specify)
CB	Porphyrictic	Phenocryst	Poorly abundant (hypohyaline)(10-50%)
CC	Porphyrictic	Phenocryst	Moderately abundant (hypocrystalline) (50-90%)
CD	Porphyrictic	Phenocryst	Highly abundant (holocrystalline) (90-100%)
CE	Porphyrictic	Phenocryst	Fine ≤ 2 mm
CF	Porphyrictic	Phenocryst	Medium 2-5 mm
CG	Porphyrictic	Phenocryst	Coarse ≥ 5 mm
CH	Porphyrictic	Groundmass	Glassy (hyaline) (0-10%)
CI	Porphyrictic	Groundmass	Cryptocrystalline (not visible, light microscope
CJ	Porphyrictic	Groundmass	Microcrystalline (< 0.5 mm)
CK	Porphyrictic	Groundmass	Very fine grained(hyaline) (0-10%)
CL	Aphanitic	-	Uniformly microcrystalline (<1 mm)
CM	Aphyric	-	No phenocrysts (<1%)
CN	Glassy	-	Composed of volcanic glass
CO	Vesicular	(or amygdaloidal)	Sparsely (1-5%)
CP	Vesicular	(or amygdaloidal)	Moderately (5-20%)
CQ	Vesicular	(or amygdaloidal)	Highly (>20%)
CR	Vesicular	(or amygdaloidal)	Pumiceous
CS	Vesicular	(or amygdaloidal)	Scoriaceous
CT	Spherulites	-	Spherulitic
CU	Spherulites	-	Micro-spherulitic
CV	Spherulites	-	Lithophysae bearing

Table 18: Description based on mineral composition (after McPhie 1993).

DA	Mineralogy	Chlorite
DB	Mineralogy	Sericite
DC	Mineralogy	Silica
DE	Mineralogy	Pyrite
DF	Mineralogy	Carbonate
DG	Mineralogy	Feldspar
DH	Mineralogy	Haematite
DI	Distribution	Disseminated
DJ	Distribution	Nodular
DK	Distribution	Spotted
DL	Distribution	Pervasive
DM	Distribution	Patchy